# Hypersonic Technology Developments with EU Co-Funded Projects

**J. Steelant**
Section of Aerothermodynamics and Propulsion Analysis
ESA-ESTEC
Keplerlaan 1, 2200 AG Noordwijk, The Netherlands

Johan.Steelant@esa.int

## *ABSTRACT*

*Through the well-known framework contracts, the EU is continuously supporting innovative technologies that might facilitate a step change required for air transport in the second half of this century and beyond. One of these goals is assessing high-speed flight transportation and its related technologies which are explored in LAPCAT and ATLLAS both being co-funded by the EC. Recently, they have been successfully extended towards a 2nd phase within the 7th Framework Programme. Whereas LAPCAT focuses on high-speed propulsion and aerothermodynamics, ATLLAS addresses rather the need for light-weight and high-temperature resistant materials.*
*The present paper summarizes the objectives and the achievements for each of these projects. The definitions and requirements for the different technologies enabling the design, construction and manufacturing of these vehicles and their sub-systems are driven by new conceptual designs which are carried out in each of them. This assures testing and evaluations at realistic conditions.*

## 1.0 INTRODUCTION

Tendencies in aeronautics clearly show a continuous increase in air traffic (Figure 1). Based on IATA statistics of November 2006 [1], "*the international passenger traffic growth increased with 6.4% in November 2006 over 2005. Premium traffic growth on international routes increased to 5.6% in November and continued to grow strongly on routes from the Middle East but also grew strongly on routes within North America and on routes from the Far East to Australia. Of the five main premium traffic routes by volume (together accounting for 75% of total premium traffic), Europe to the Far East continues to grow at the strongest rate, with growth of 10.9% in November and 11% for the year-to-date. Growth on this route has been boosted by strong Asian economic growth and liberalisation on some routes*".


**Figure 1 International passenger Growth by Route [1]**

# Report Documentation Page

*Form Approved*
*OMB No. 0704-0188*



| 1. REPORT DATE | 2. REPORT TYPE | 3. DATES COVERED |
|---|---|---|
| **SEP 2010** | **N/A** | **-** |

| 4. TITLE AND SUBTITLE | 5a. CONTRACT NUMBER |
|---|---|
| **Hypersonic Technology Developments with EU Co-Funded Projects** | 5b. GRANT NUMBER |
| | 5c. PROGRAM ELEMENT NUMBER |
| 6. AUTHOR(S) | 5d. PROJECT NUMBER |
| | 5e. TASK NUMBER |
| | 5f. WORK UNIT NUMBER |
| 7. PERFORMING ORGANIZATION NAME(S) AND ADDRESS(ES) **Section of Aerothermodynamics and Propulsion Analysis ESA-ESTEC** | 8. PERFORMING ORGANIZATION REPORT NUMBER |
| 9. SPONSORING/MONITORING AGENCY NAME(S) AND ADDRESS(ES) | 10. SPONSOR/MONITOR'S ACRONYM(S) |
| | 11. SPONSOR/MONITOR'S REPORT NUMBER(S) |

12. DISTRIBUTION/AVAILABILITY STATEMENT
**Approved for public release, distribution unlimited**

13. SUPPLEMENTARY NOTES
**See also ADA564620. High Speed Propulsion: Engine Design - Integration and Thermal Management (Propulsion a vitesse elevee : Conception du moteur - integration et gestion thermique)**

14. ABSTRACT
**Through the well-known framework contracts, the EU is continuously supporting innovative technologies that might facilitate a step change required for air transport in the second half of this century and beyond. One of these goals is assessing high-speed flight transportation and its related technologies which are explored in LAPCAT and ATLLAS both being co-funded by the EC. Recently, they have been successfully extended towards a 2nd phase within the 7th Framework Programme. Whereas LAPCAT focuses on high-speed propulsion and aerothermodynamics, ATLLAS addresses rather the need for light-weight and high-temperature resistant materials. The present paper summarizes the objectives and the achievements for each of these projects. The definitions and requirements for the different technologies enabling the design, construction and manufacturing of these vehicles and their sub-systems are driven by new conceptual designs which are carried out in each of them. This assures testing and evaluations at realistic conditions**

15. SUBJECT TERMS

| 16. SECURITY CLASSIFICATION OF: | | | 17. LIMITATION OF ABSTRACT | 18. NUMBER OF PAGES | 19a. NAME OF RESPONSIBLE PERSON |
|---|---|---|---|---|---|
| a. REPORT | b. ABSTRACT | c. THIS PAGE | | | |
| **unclassified** | **unclassified** | **unclassified** | **SAR** | **68** | |

These long-distance flight taking easily flight times of 16 hours or more to connect two major intercontinental cities, would become more attractive when travel-time would be reduced drastically such that a final destination can be reached within 4 hours or less.
However, with present aircraft and propulsion designs, we're getting close to the optimal design and margins for further improvement are getting smaller. Only drastic changes in aircraft configuration, propulsion concepts and flight velocities are able to achieve these goals.

New aircraft configurations and related propulsion engines presently studied for classical flight Mach numbers around M=0.9 look into e.g. blended wing-body configuration for aerodynamic performance and multiple engines mounted on top of the wings close to its trailing edges to improve propulsion efficiency. These interesting developments will decrease further fuel consumption up to 30% but will not enable the shortening of travel times.

New aircraft development seems to be stalled with respect to flight speed, despite the proven technical possibility shown by the supersonic Concorde, the experience gained in military aircraft design up to Mach 3 (e.g. SR-71) and finally experimental vehicles (e.g. X-15 at Mach 6). Opponents to supersonic transport development always point to the large specific fuel consumption of Concorde which undeniable is roughly twice the value of present commercial aircraft. However, one should not forget that the specific fuel consumption, sfc, obtained for the first turbojet driven aircraft, e.g. Comet in 1951 were only 20% lower. Since then fuel consumption reduction for aero-engines has been drastically driven throughout time by technology e.g. cooling techniques, new alloys, improved thermodynamic cycles by increased pressure ratios and TIT, etc… As the Olympus 593 engine was based on the Olympus design of 1950 for the Canberra and later for the Avro Vulcan in 1956, it is hence impossible to compare its sfc with e.g. the latest Trent's of R&R or the GE90-family when half a century of technology development has not been implemented in these Olympus engines.

Before given an overview of LAPCAT and ATLLAS, some basic considerations about supersonic vs. subsonic flight and its potential for evolution will be discussed. As the present paper served as a lecture note giving an overview on EU research programs related to advanced on propulsion technology for high-speed aircraft, it's primarily constructed around a collection of recent publications [2][3],[4],[5] along with some upgrades made during the execution of the projects.

## Nomenclature

| | |
|---|---|
| ATR | Air Turbo Reactor |
| CG | Centre of Gravity |
| CP | Centre of Pressure |
| EoS | Equation of State |
| ER | Equivalence Ratio |
| HHV | Higher Heating Value [MJ/kg] |
| HSCT | High Speed Civil Transport |
| $I_{sp}$ | Specific Impulse [s] |
| LHV | Lower Heating Value [MJ/kg] |
| m' | air mass flow [kg/s] |
| $m_f$' | fuel mass flow [kg/s] |
| MTF | Mid Tandem Fan |
| OPR | Overall Pressure Ratio |
| RBCC | Rocket Based Combined Cycle |
| RTA | Revolutionary Turbine Accelerator |
| RTD | Research and Technology Development |
| sfc | Specific Fuel Consumption [kg/s/daN] |

| | |
|---|---|
| SST | Supersonic Transport |
| TIT | Turbine Inlet Temperature [K] |
| TBCC | Turbine Based Combined Cycle |
| VCE | Variable Cycle Engine |

Subscripts

| | |
|---|---|
| a | ambient |
| cc | combustion chamber |
| j | jet condition |
| ∞ | cruise flight point |

## 2.0 MOTIVATION AND ASSESSMENT

Reducing travel times by going supersonic has only sense on long-distance flights. Range is hence an important figure of merit to evaluate high-speed aircraft concepts. It is strongly dependent on total available fuel mass and its consumption throughout the itinerary, i.e. from taxiing, speed-up cruise and final descent manoeuvres. Among these different parts, cruise represents a major portion of the needed fuel. The range achieved during cruise can be easily derived from the Bréguet range equation:

$$R = \frac{H}{g}\eta\frac{L}{D}\ln\left[\frac{1}{1-W_F/W}\right] = \frac{V_\infty}{g\,sfc}\frac{L}{D}\ln\left[\frac{1}{1-W_F/W}\right] \qquad (1)$$

where:

| | |
|---|---|
| $R$ | Range [m] |
| $H$ | the fuel energy content [J/kg]: 120 (LHV) and 142 (HHV) MJ/kg for $H_2$, 43.5 (LHV) and 47MJ/kg (HHV) for kerosene, 50.0 (LHV) and 55.5MJ/kg (HHV) for Methane |
| $g$ | gravity constant [m/s$^2$] |
| $\eta$ | the overall installed engine efficiency |
| $sfc$ | specific fuel consumption [kg/s/N] |
| $V$ | flight velocity [m/s] |
| $W$ | total take-off mass [kg] |
| $W_F$ | fuel mass [kg] |

The range depends linearly on the energy content $H$ in the fuel which can be increased with a factor of 2.7 by switching e.g. from kerosene to hydrogen.

The aerodynamic performance given by $L/D$ in eq. (1) depends primarily on the Mach number and was analyzed by Küchemann [6] who formulated a general empirical relationship referred to as the "L/D barrier":

$$\left(\frac{L}{D}\right)_{\max} = \frac{4(M_\infty + 3)}{M_\infty} \qquad (2)$$

Further studies optimized waverider designs taken into account viscous effects resulted in better $L/D$ ratio resulting in a shifted $L/D$ barrier (Anderson [7]).

$$\left(\frac{L}{D}\right)_{\max,viscous} = \frac{6(M_\infty + 2)}{M_\infty} \qquad (3)$$

For an increasing Mach range the values are decreasing asymptotically to a value of 4 or 6:

| $M_\infty$ | 0.9 | 2 | 4 | 6 | 8 | 10 |
|---|---|---|---|---|---|---|
| $L/D_{max,euler}$ | 17.3 | 10 | 7 | 6 | 5.5 | 5.2 |
| $L/D_{max,viscous}$ | 19.2 | 12 | 9 | 8 | 7.5 | 7.2 |
| $\eta$ | 0.25 | 0.4 | 0.57 | 0.67 | 0.73 | 0.77 |

**Table 1 Aerodynamic *L/D* barrier and overall installed engine efficiency in function of flight Mach number**

This decrease of aerodynamic performance with increasing Mach number would inherently exclude long-range supersonic flight as it would be economically not viable. However, the overall propulsion efficiency, defined as

$$\eta = \frac{T \cdot V_\infty}{m_f' H} = \frac{V_\infty}{sfc\, H} \tag{4}$$

increases with Mach number for turbojets and ramjets as will be explained further. A first approach, suggested by R.G. Thorne according to [1], is given by:

$$\eta = \frac{M_0}{M_0 + 3} \tag{5}$$

To better understand the increase of the overall efficiency $\eta$ of an aircraft engine, one can split the term thermodynamically into a thermal and propulsion efficiency $\eta = \eta_t \eta_p$. given approximately for a single jet by:

$$\eta_t = \frac{m'(V_j^2 - V_\infty^2)}{2m_f' H} \qquad \eta_p = \frac{2V_\infty}{V_j + V_\infty}$$

The thermal efficiency of either compressor or ram-based engines can be approached as a Brayton cycle and hence its efficiency is mainly driven by the combustor temperature $T_{cc}$ to intake temperature $T_a$ ratio. This ratio would be at its optimal point when operating the combustor close to the stochiometric value. However, for turbojets or turbofans, the rotary turbine components limit this ratio due to material yield strengths to a value of about $T_{cc}/T_a$=6 or $\eta_t$ = 47%.

Typical values for propulsion efficiency of a modern engine at $M_\infty$=0.85 is 48% for a turbojet and 77% for a turbofan with a bypass ratio of 6. The overall efficiency in cruise results into values of 20% to 37% and increases above 40% for larger bypass ratios [8].

For ram- and scramjets, the combustion temperature is not limited by rotary components. Hence higher equivalence ratios are easier to reach and ER=1 is presently used in scramjet flight experiments. Hence, the thermal efficiency can reach values as high as $\eta_t$ = 60-70%. The propulsion efficiency is clearly better as the jet/flight velocity difference is rather small resulting into a ηp = 70-90% leading to an overall efficiency of $\eta$ = 42-63%. This large $\eta_p$ implies that a massive intake needs to be foreseen, which can occupy the complete frontal section of the aircraft in order to provide the necessary thrust given by $T = m'(V_j - U_\infty)$.

As shown above, both factors $\eta$ and $L/D$ have reverse dependencies on flight Mach number and for a first assessment the cruise efficiency $\eta L/D$ can be considered in first order to be constant, i.e. a value of about 3 to 4, at worst only 40% smaller for careful designs. This means that the range is more or less independent of the flight speed and is then only determined by the relative fuel fraction $W_F/W$ and the fuel type.

Though anticipating on the results obtained by GDL during the ATLLAS project [9], an optimization analysis integrating both the aerodynamics and the propulsion unit on a two-dimensional conceptual design (Figure 2), showed a potential to a cruise efficiency factor $\eta L/D$ beyond 4 for flight Mach numbers above 3.5 (Figure 3). This could only be achieved by combining a lifting flow on the windward side with a propulsive-lifting leeward flow. The latter is possible by providing an expansion on the leeward side (Figure 2). This potential is only feasible in an ideal situation where the exhaust can expand fully in the base of the vehicle. However, it clearly indicates the critical points to be respected guaranteeing a minimal cruise efficiency required for high-speed long-range vehicles.

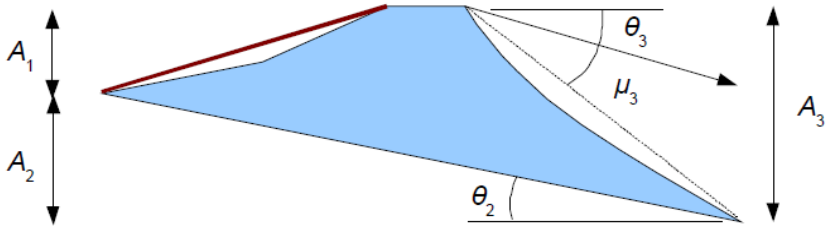


**Figure 2 The two stream solution in a dorsal configuration [9]**

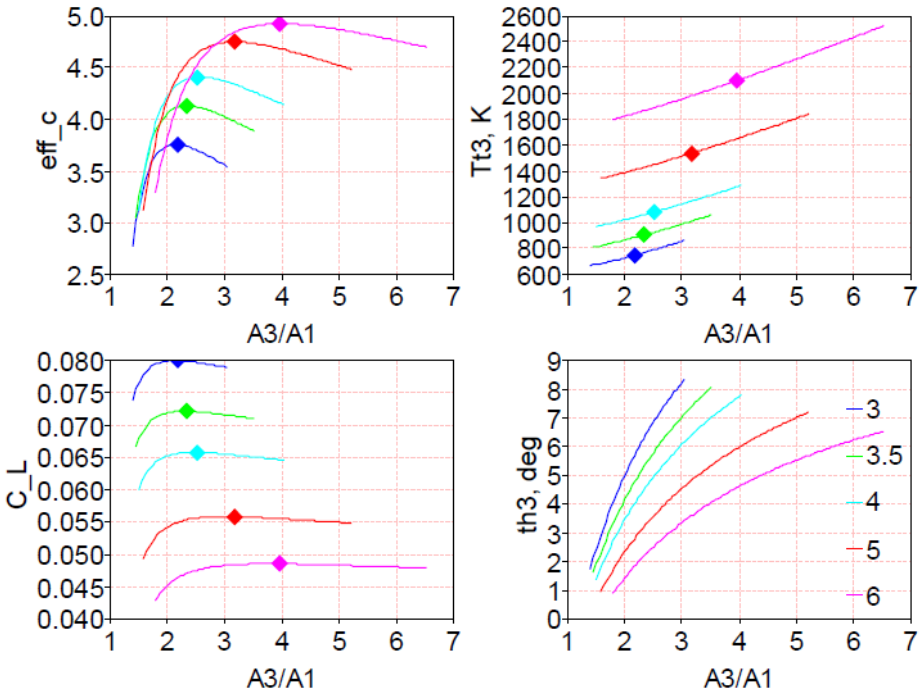


**Figure 3 Top left: cruise efficiency; top right: exhaust total temperature Tt3, Bottom left: lift coefficient (based on $A2/\tan(\theta_2)$) and bottom right exhaust / lee deflection as a function of $A3/A1$ for Mach numbers between 3 to 6 for the two stream dorsal engine aircraft [9].**

However, one point of caution should be raised. This general analysis is purely based on the Bréguet range, i.e. cruise flight. However, aircraft's operation and handling largely depends on this performance at

take-off and during acceleration. In particular the latter is increasingly more dominant for higher Mach number flights. For example, a practical flight at Mach 5, such as the LAPCAT A2 vehicle, reveals that the acceleration and deceleration entails about 50 minutes each compared to a 2.8h flight. At higher Mach numbers, these phases are becoming even more dominant in the propulsion optimization process not only due to the longer speed-up and slow-down phases, but also to the relatively shorter cruise phase.

Another important point, also highlighted by Cain and Walton [10], is how far one can extend or extrapolate parameters for subsonic transport to supersonic or even hypersonic transport. So far, this first order approximation does not include the effect of changes in structural mass fractions that may be required to cope with the high heating loads during flight. Also the requirement that the plane needs to operate over a wide range of flight Mach numbers, i.e. from take-off to cruise, will demand for a largely flexible engine, most likely as a variable cycle engine, which sequentially will penalize the concept by a larger engine mass fraction. Related to this is the need for fully integrated design of engine and airframe to obtain a global maximum in efficiency whereas up to now engine and airframe can and are being designed and optimized quite separately.

Despite these concerns, it is worthwhile to assess the performance of a wide range of existing aircraft in the light of the above described logic. Data were mainly obtained from websites of a/c manufacturers, manuals or other sources. Hence, these might not necessarily represent the true values but should rather be taken as indicative.

The specific fuel consumption (sfc) is plotted versus a non-dimensional range defined as $R/R_g$ in Figure 4. $R_g$ is the ultimate anti-nodal point for a final destination, i.e. 20,000km. The Concorde is very competitive in range compared to the aircraft designed in the same period (60's and 70's) e.g. Comet, DC-9,… despite a larger sfc. Ranges for subsonic aircraft designed in the 90's have almost doubled, e.g. MD-11, B767,... This is of course related to the improved aerodynamics, availability of light-weight and high-temperature materials, lower sfc due to higher bypass ratios, higher TIT, etc. Similar improvements can be applied to a successor of the Concorde to improve its sfc or range for the same flight speed: implementation of a bypass ratio of 0.5 to 1 or higher instead of presently none, application of more advanced cooling concepts for turbine blades, use of light-weight heat resistant materials, use of a Variable Cycle Engine rather than using an afterburner or reheat, etc…

The positive effect of the cruise speed on the overall propulsion efficiency is clearly depicted on Figure 5. Equation (5), represented as a full line, clearly fit the efficiencies of the first designs of their kind for subsonic, e.g. Comet-4 and supersonic commercial vehicles, e.g. Concorde.

.

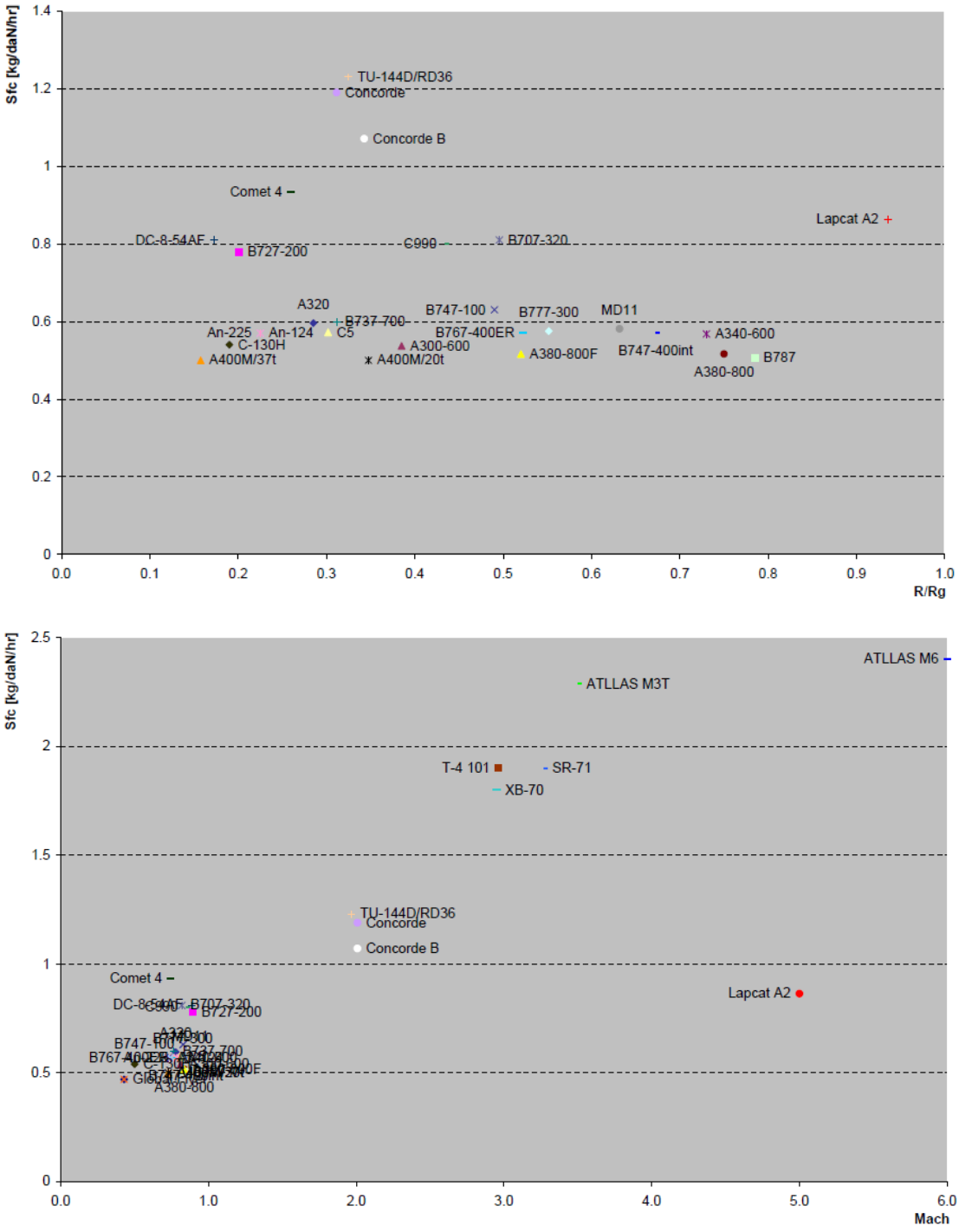


**Figure 4: Indicative specific fuel consumption values for various sub- and supersonic aircraft in function of non-dimensional range and Mach number. A400M is given for two different payloads.**

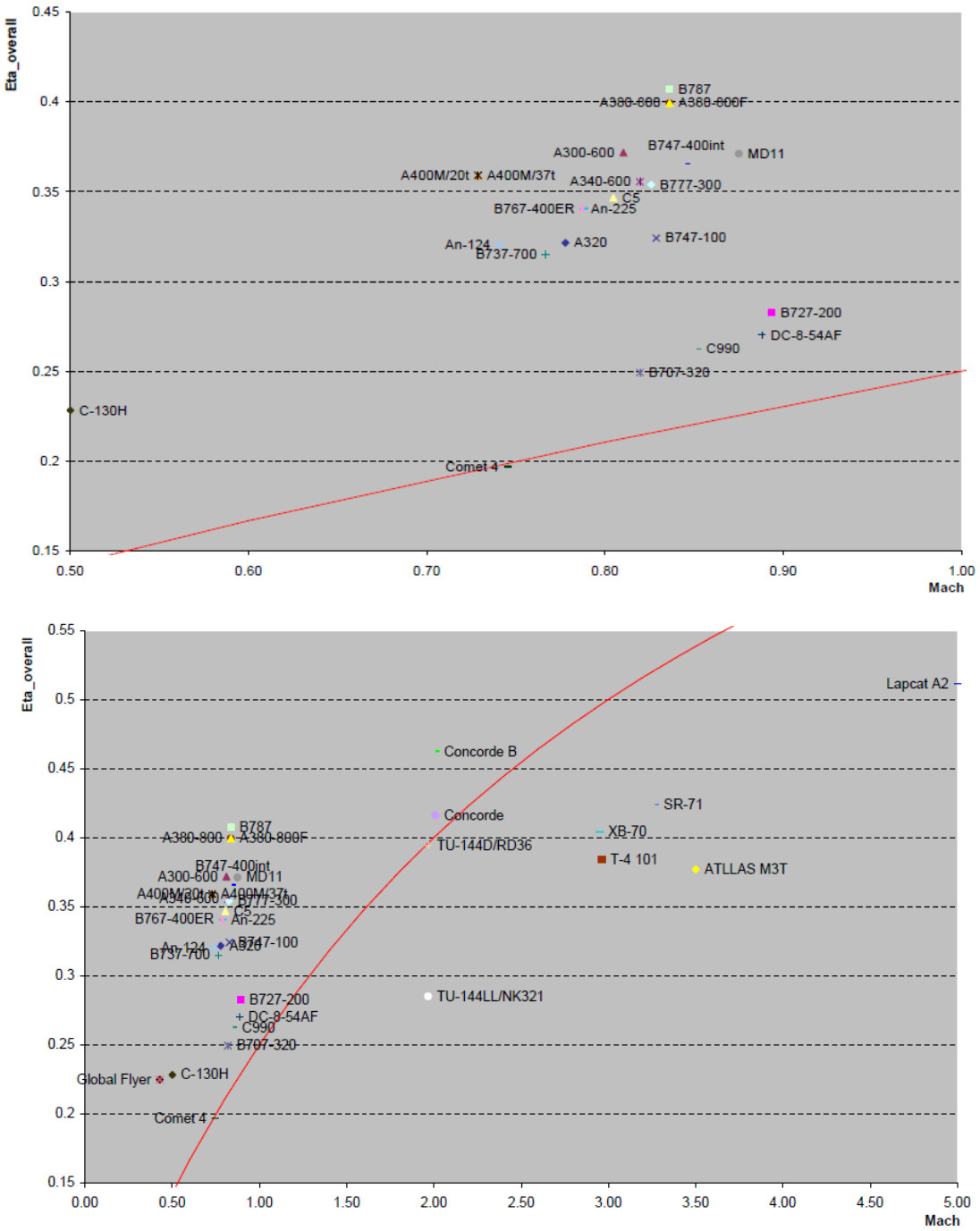


**Figure 5: Indicative overall engine efficiencies for various subsonic aircraft in function of flight Mach number. Eq. (5) is given by full line.**

The formula (5) seems to provide a lower limit. The earlier mentioned 20% efficiency for turbojet and its evolution towards values above 40% for large bypass turbofans seems to be confirmed by the trend observed for commercial aircraft. With respect to fig. 1, this efficiency doubling results inherently in a doubling of the range. Not surprisingly, efficiencies have in particular improved for the heavily used subsonic aircraft. This is entirely due to massive resources made available to improve this range of aircraft in their aerodynamics' design and engine fuel consumption and not due to intrinsic physical limitations for

supersonic transport vehicles.

The aircraft indicated below this line are all supersonic transport vehicles. In order to sustain supersonic flight, these aircraft are equipped with engines which require to be run with afterburning, which is of course thermodynamically inefficient (low $\eta_t$). Concorde and TU-144D are however equipped with high thrust engines enabling to sustain supersonic flight without afterburner.

Further improvements were in the planning which would have led to a further efficiency increase away from the lower limit given by eq. 4. Indeed, less know to the public is the start of studies to improve the performance of the Concorde four months after the start of scheduled services in 1976. This project should lead to the Concorde B model. Among modifications on aerodynamics, systems, weight, fuel tanks, the modification on the propulsion unit consisted of replacing the low-pressure compressor by a compressor with increased diameter and the low pressure turbine assembly by a two-stage turbine (Figure 7). The installation of a discharge system to increase the margin of air flow through the engine would result in an increase in air flow which reaches 25 % on takeoff and 35 % during approach. The thrust gains obtained at takeoff and at transonic speeds also make it possible to remove the reheat (afterburner) system with its very heavy fuel consumption and significant addition to the noise generated by the powerplant.

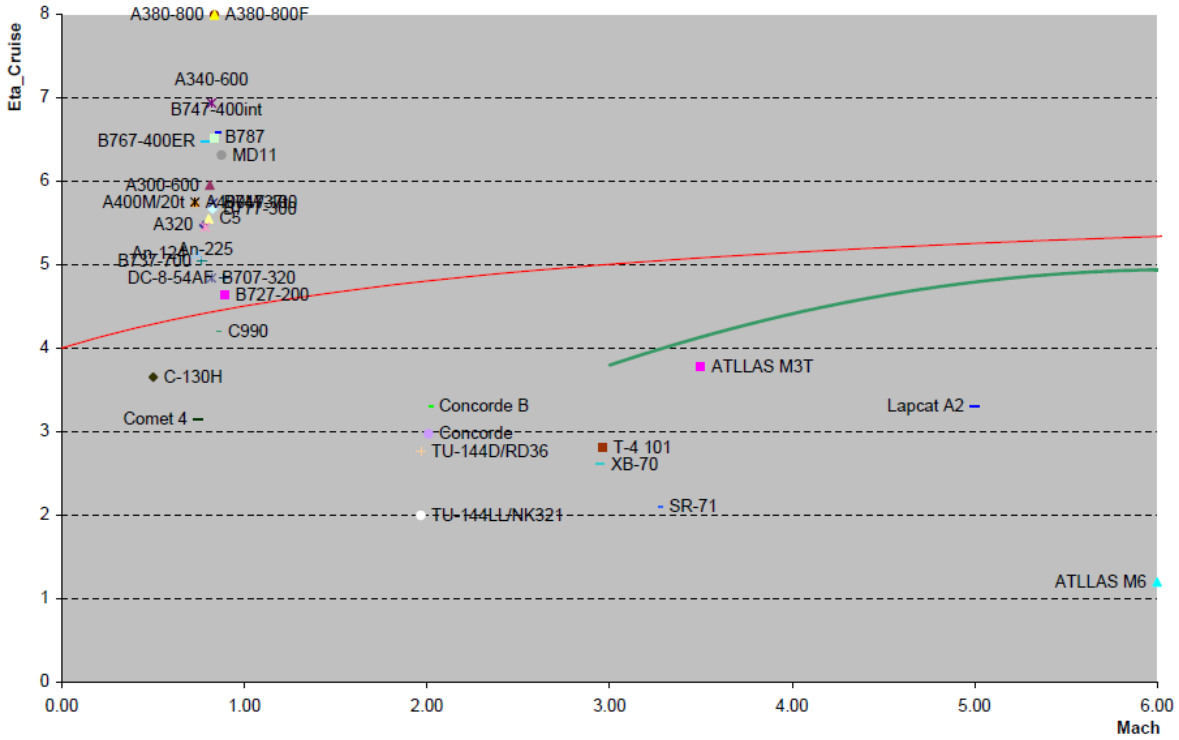


**Figure 6: Indicative cruise efficiency in function of flight Mach number for existing subsonic and supersonic vehicles along with the ATLLAS M3T (new concept) and the ATLLAS M6 (Optimized by means of MDO from the existing Hycat configuration of Lockheed). Green line denotes maxima retrieved from Figure 3. Red line is product of eq. 3 x eq. 5.**

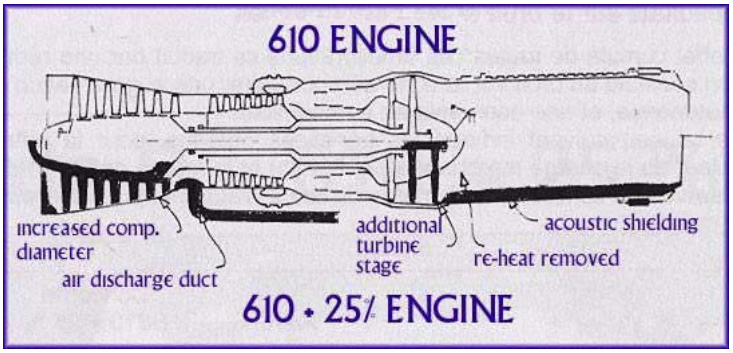


**Figure 7: Suggested improvements (lower part) to the original Olympus (upper part) engine shortly after the Concorde introduction with higher thrust and lower sfc, avoiding the use of an afterburner [11].**

Presently, within the military aircraft development, there is an objective to equip their fighters with high-thrust engines to avoid the use of afterburner not only for sustained supersonic flight but also to accelerate through the high-drag transonic flight regime. Examples are the Eurofighter Typhoon and The F-22 raptor. The latter incorporates a pair of new, higher thrust-to-weight turbofan engines, the Pratt & Whitney F119-PW-100, which is designed for efficient supersonic operation without afterburner (called supercruise). The F119 engine develops more than twice the thrust of current engines under supersonic conditions, and more thrust without afterburner than conventional engines with afterburner. Of course, limited data is available related to sfc, bypass ratio, TET, OPR … to plot them relatively to the other data.

In [1], a weight breakdown analysis is described for which the total take-off weight $W$ is split into different parts. Items including wings, undercarriage, services and equipment are proportional to the overall weight, i.e. $c_1W$. Other items are proportional to payload $c_2W_p$ including fuselage weight, furnishings and the payload itself, hence $c_2 > 1$. Finally we have the engine and fuel weight $W_E$ and $W_F$. This results into:

$$W = c_1 W + c_2 W_p + W_E + W_F$$

Combined with eq. (1) one can obtain:

$$\frac{W_P}{W} = \frac{1}{c_2}\left[\exp\left(-R\frac{H}{g}\eta\frac{L}{D}\right) - c_1 - \frac{W_E}{W}\right] \qquad (6)$$

Evaluating $W_E/W$ from a large range of data (Figure 8), setting this value to 0.05 seems to be a good average. The factors $c_1$ and $c_2$ largely depend on the use of state-of-the-art structural materials and are retained here as variable parameters. In Figure 9, the payload fraction $W_p/W$, i.e. passengers or cargo, for multiple existing aircraft is plotted against the non-dimensional range. These data have been fitted by adapting the structural parameters $c_1$ and $c_2$, along with the propulsion and aerodynamic performance parameter $\eta L/D$ of eq. (6) according to the values given in Table 2.

| | $\eta L/D$ | $c_1$ | $c_2$ |
|---|---|---|---|
| A | 4 | 0.3 | 2.25 |
| B | 5 | 0.25 | 2.00 |
| C | 5.5 | 0.2 | 1.90 |
| D | 6 | 0.15 | 1.75 |
| E | 3 | 0.35 | 2.75 |

**Table 2: Parameter sets used for evaluation of future trends**

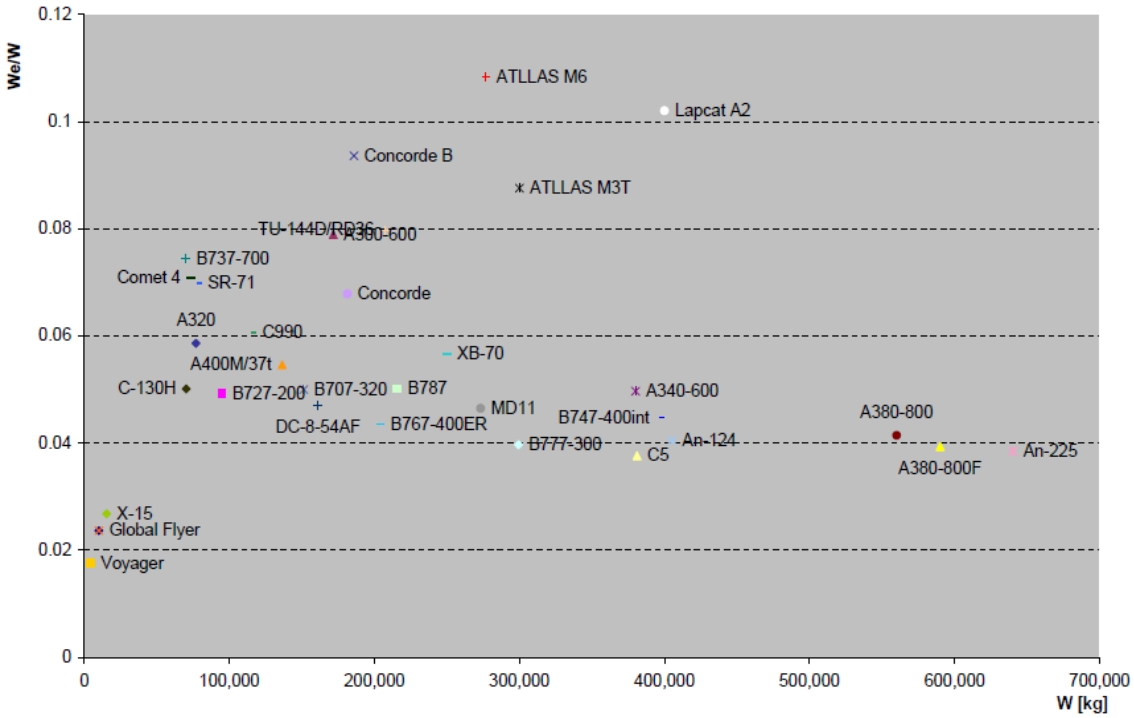


**Figure 8: Indicative engine fraction for various aircraft**

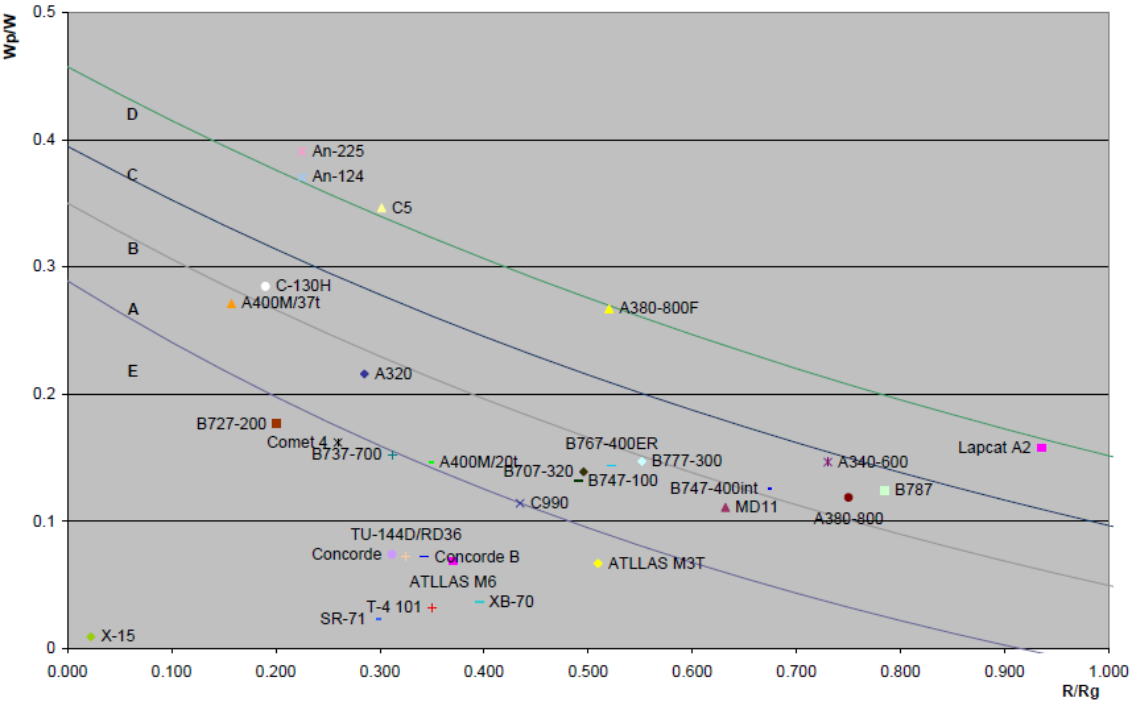


**Figure 9: Indicative payload fraction in function of non-dimensional range for various aircraft. Full lines A to E are based on eq. (6) for structural, propulsion & aerodynamic parameter variation.**

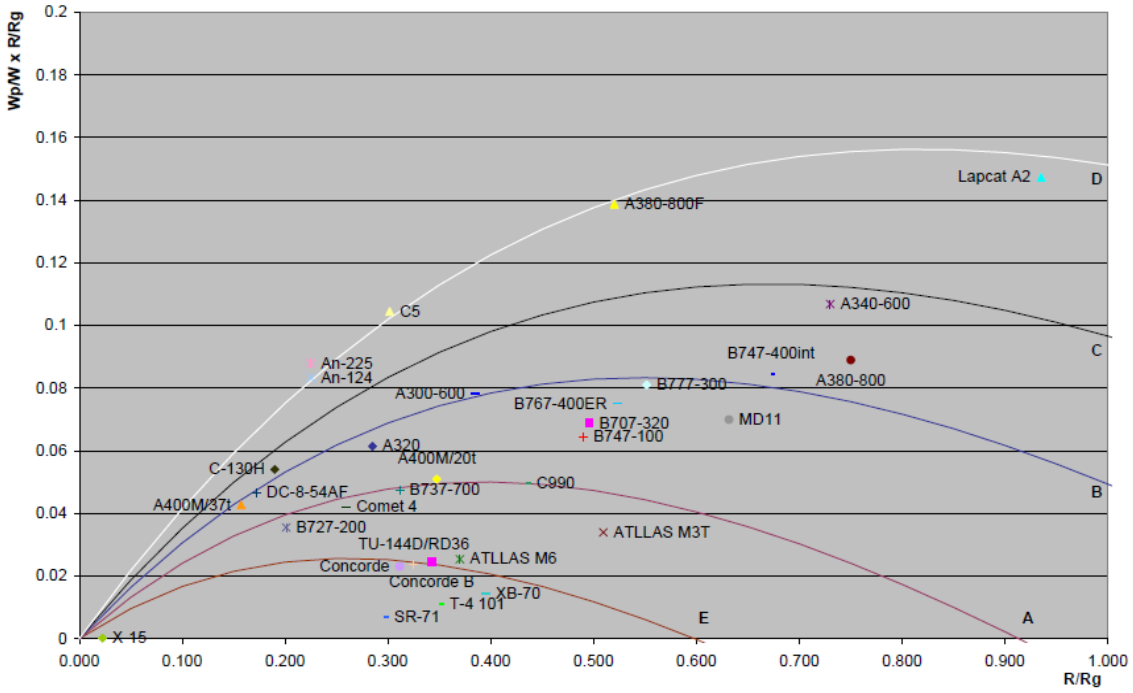


**Figure 10: Indicative seat-km: figure of merit comprising both payload and range for various aircraft**

Generally speaking, the payload fraction increases from A to D due to the improved structural and propulsive parameters and demonstrate the technological evolution introduced into the newer airplanes. The line E is definitely lower for the supersonic aircraft which is due to the lower $\eta L/D=3$ versus *4* for the subsonic ones achieved in the same era. Small changes on the aerodynamics, as proposed for Concorde B in 1976, combined with efficiencies of recent engines developed for supersonic fighters, indicate that a recent SST might achieve a performance which lies in between lines A and B.

Another important figure of merit for aircraft is seat-kilometre produced which can be expressed as $W_g$/W x $R/R_g$. This is shown in Figure 10 along with the fittings discussed previously. Also here the tendencies are well represented by the equations with higher values for the more recent airplanes and the lowest for the obsolete commercial SST.

The still remaining parameter to be discussed is the use of hydrogen as fuel. Studies have been performed in Europe (e.g. Cryoplane) and Russia, but little information is available on the aircraft performance. However, making use of the suggested correlations, the influence of hydrogen as a fuel can be easily assessed. In Figure 11 and Figure 12 , the previous parameter settings A, D and E have been applied for a hydrogen aircraft, denoted respectively AH2, DH2, EH2. This is a first approximation as the larger required volume for hydrogen storage will induce a higher drag which is not accounted for. The dashed lines clearly indicate that aircraft have a larger potential in range with still an interesting payload capacity, including SST. Aircraft of lower performance, according to A, have now a potential equivalent for the ultimate range to aircraft of type D by switching to hydrogen. This opens up the potential to reach anti-nodal destination with optimum seat-km already for conservatively designed aircraft.

These observations were the main drivers of the ATLLAS and LAPCAT projects to tackle the final technological challenge within aviation: can man travel over long distance at a high speed within a relatively short time of about four hours?

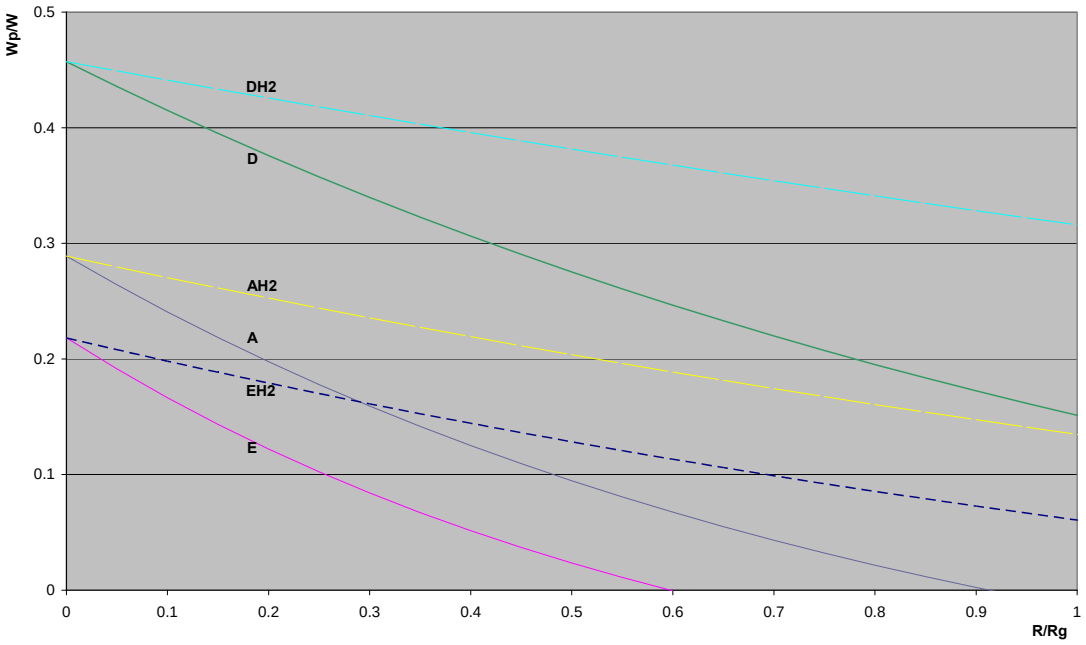


**Figure 11: Payload fraction dependence on fuel type: Kerosene (full), hydrogen (dashed).**

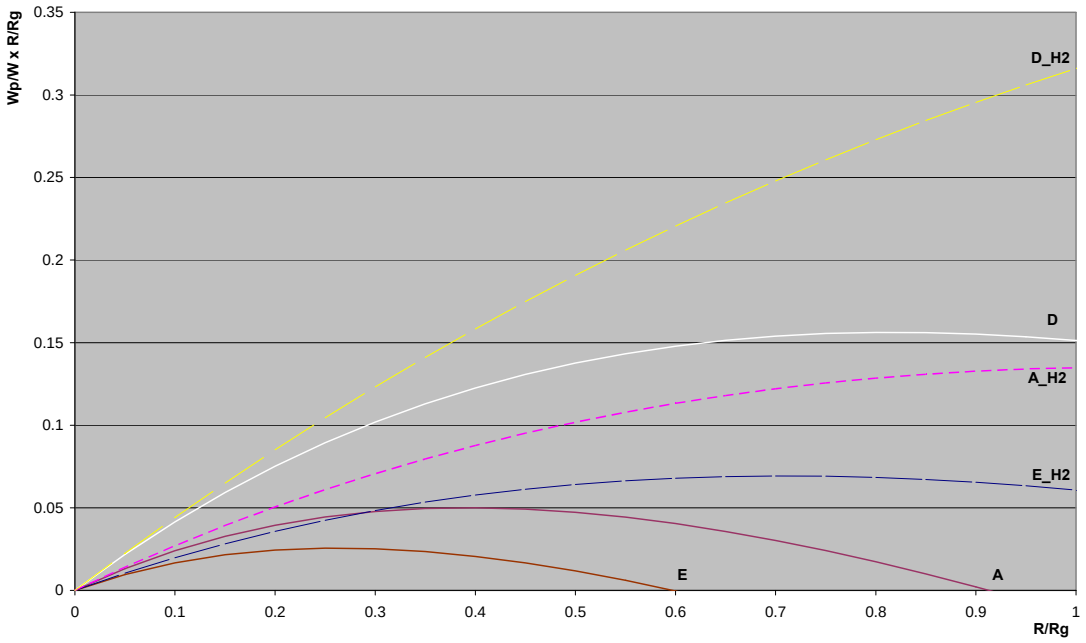


**Figure 12: Seat-km dependence on fuel type: kerosene (full), hydrogen (dashed)**

## 3.0 LAPCAT-I PROJECT AND ITS ACHIEVEMENTS

In Europe, continuous effort for basic high-speed airbreathing propulsion research has been made at many institutions. However, these efforts are scattered or strongly specialized. The LAPCAT project offers the opportunity to practice the indispensable cooperation on European level and to integrate specialized findings into a system to assess the overall relevance and benefits. During the project, system design tools are developed as well as rules and guidelines for conceptual development of system which have not been in place before. The capability to systematically guide a system development process through interface management and to assess its output will be enhanced.

The baseline mission requirement is to reduce travelling time of long-distance flights, e.g. Brussels to Sydney, in about 4 hours. This requires a new flight regime with Mach numbers ranging from 4 to 8. At these high speeds, classical turbo-jet engines need to be replaced by advanced airbreathing propulsion concepts and hence related technologies need to be developed. As objectives, two major directions at conceptual and technological level are considered: ram-compression and active compression. The latter has an upper Mach number limitation but can accelerate a vehicle up to its cruise speed. Ram-compression engines need an additional propulsion system to achieve their minimum working speed. Key objectives are the definition and evaluation of:

- different propulsion cycles and concepts for high-speed flight at Mach 4 to 8 in terms of turbine-based (TBCC) and rocket-based combined cycles (RBCC)
- critical technologies for integrated engine/aircraft performance, mass-efficient turbines and heat exchangers, high-pressure & supersonic combustion experiments and modelling.

The most critical RTD-building blocks were identified employing analytical, numerical and experimental tools to address issues of the following road-map:

- two airbreathing engines for selected reference vehicle(s) and trajectory point(s),
- dedicated combustion experiments for supersonic and high-pressure combustion,
- modelling and validation of combustion physics,
- aerodynamic experiments for major engine components and for inter-action of vehicle and propulsion aerodynamics.
- evaluation and validation of advanced turbulence and transition modelling for unsteady and separated flow regimes,
- performance prediction of contra-rotating turbines and light cryogenic fuel heat exchangers.

The team consisted of 12 partners out of 6 European countries and was coordinated by the European Space Research and Technology Centre ESTEC-ESA in the Netherlands. This involved four industries EADS-Astrium (D), Reaction Engines (UK), Snecma (F) and Cenaero (B); four research institutions being ESA-ESTEC (NL), DLR (D), CIRA (I) and VKI (B) and finally the universities of Stuttgart (D), Southampton (UK), Rome (I) and Oxford (UK).

### 3.1 Turbine Based Combined Cycles

The project objective is to examine two turbine based cycle (TBCC) engine concepts for high Mach number (4 – 5) flight in the context of future civilian transportation. The experience accumulated from turbojet design and operation is huge and this should obviously form the basis of the next generation of engines if at all possible.

#### 3.1.1 Hydrogen Mach 5 Cruiser

The LAPCAT A2 vehicle flying at Mach 5 was carried out by Reaction Engines. The preliminary results of this analysis are encouraging. The vehicle study is complete at initial project study level and indicates that a 400ton, 300 passenger vehicle could achieve antipodal range without marginality. The concept is particularly interesting for this mission requirements as a trajectory optimization allowed to fly almost continuously over sea and avoiding sonic boom impact when flying over land.

The proposed aircraft configuration A2 is shown in Figure 13. The vehicle consists of a slender fuselage with a delta wing carrying 4 engine nacelles positioned at roughly mid length. The vehicle is controlled by active foreplanes in pitch, an all moving fin in yaw and ailerons in roll. This configuration is designed to have good supersonic and subsonic lift/drag ratio and acceptable low speed handling qualities for takeoff and landing.

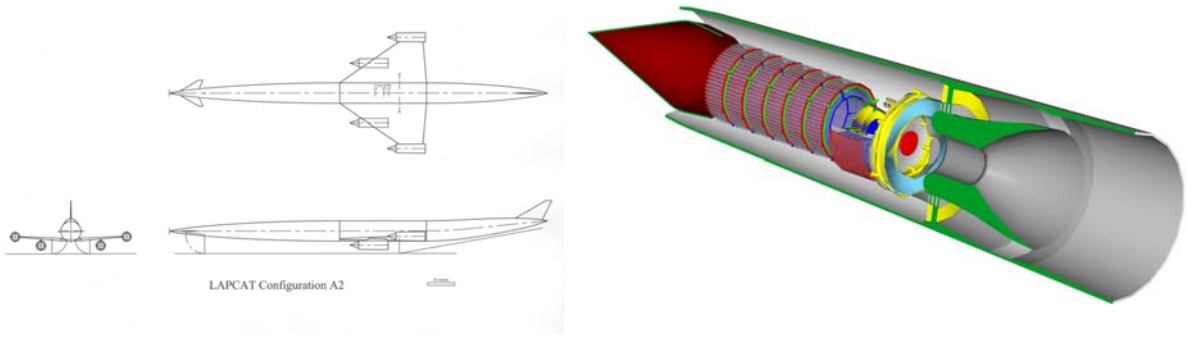


**Figure 13: LAPCAT A2: Mach 5 hydrogen based vehicle (left) with precooled turbofan-ramjet Scimitar engine**

The first study focused on a precooled Mach 5 engine, named Scimitar, employing a cycle based on the Reaction Engines SABRE spaceplane engine and fuelled by liquid hydrogen. The Scimitar engine must have good subsonic and supersonic performance if it is to be a practical engine for a new generation of hypersonic aircraft. This would allow it to operate from normal airports and over-fly inhabited regions without the nuisance and political problems which limited Concorde's effectiveness. These characteristics have been successfully incorporated into the Scimitar design (Figure 13) by incorporating a high bypass fan into the bypass duct which encloses the core engine and is otherwise needed to match the intake air capture flow to the engine demanded flow over the supersonic Mach number range. The bypass fan is driven by a hub turbine using flow diverted from the core engine nozzle. The flow then discharges into the bypass and mixes with the bypass flow. More details on the engine and its thermodynamic cycle are given by A. Bond [12].

Due to their central role to the concept of the precooled engine two technologies are being addressed at experimental level: a lightweight heat exchanger and contra-rotating turbine.

Two precooler modules have been built for this program (Figure 14). They are the correct flow length and tube dimensions, but shorter than a full engine module. They were used to demonstrate the manufacturing technology for these items. This demonstration consisted of tube surface preparation, support of the matrix in the brazing fixture and brazing of the tubes to the headers. This program reinforced the conclusion that precooler manufacture by this technique is practical, although some refinement of the industrial process is still needed.

The SiC technology program became hard going quite early in the project. Although straight SiC tubes made by sintering are available and can undoubtedly be refined, other surface shapes proved very daunting to manufacturers. The manufacture of multi-channelled plates by green state extrusion followed by siliconising showed much greater promise. Extrusion of rectangular strips of 600mm long was successful with relatively good control of channel dimensions and wall thickness Figure 15.

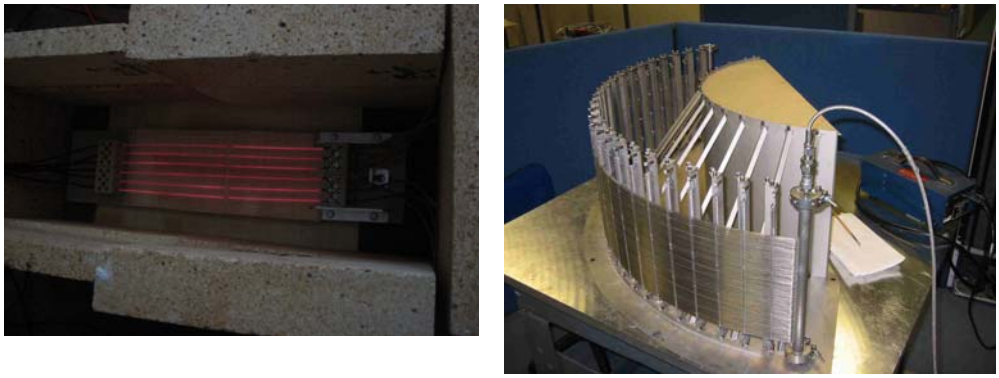

**Figure 14 Left: Oxidation testing of Inconel 718 tubes, right: completed precooler module in assembly fixture during pressure testing.**

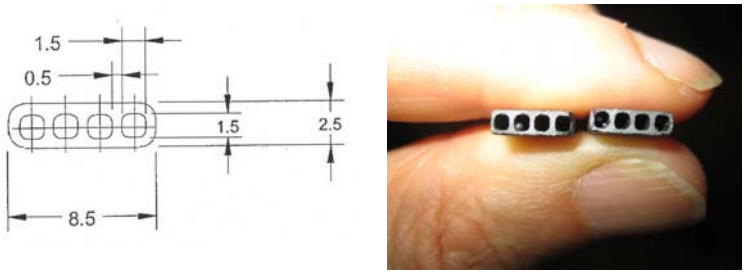


**Figure 15: Trial heat exchanger strip extrusion**

The design, building and testing of a stator-less contra-rotating model turbine is aerodynamically similar to the real turbine for the engine concept (Figure 16). This was run on a low pressure high molecular weight gas which can simulate the high pressure helium used in the engine. REL prepared an initial scoping design for the real engine for which VKI has optimised the aerodynamics [21]. CENAERO scaled and optimised the helium aerodynamic design to the model.

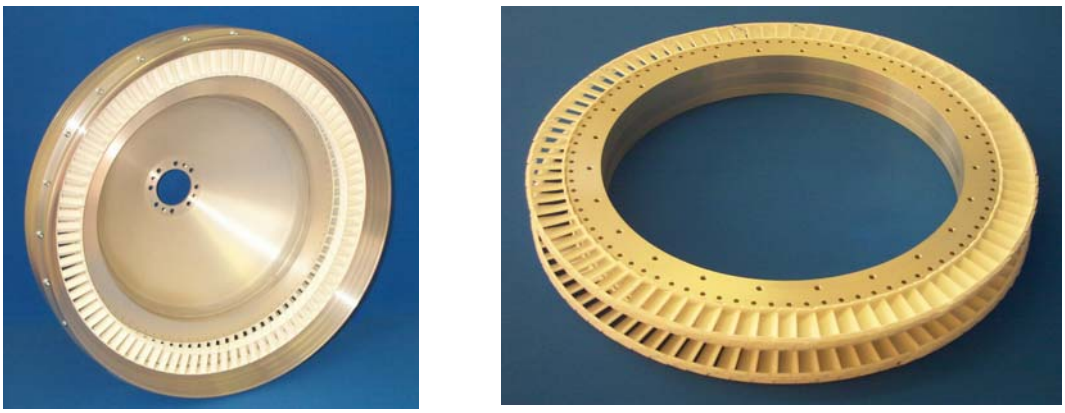

**Figure 16: Contra-rotating stages of the Scimitar engine: left: rotors 1 and 3, right: rotors 2 and 4**

The Scimitar engine analysis suggests that it can produce efficient supersonic and subsonic flight and meet

the anticipated noise regulations for normal airport operation. An important side result is the critical role of environmental impacts, specifically NOx, contrails and Ozone damage. Future studies need to include these problems.

To address the relatively high technical risk of this project it is proposed that the development program proceed in a step by step basis in 3 phases, namely Concept Validation (2 years), Technology Demonstration (3 years) and System Development (8 years). At the end of each program stage the project would be reviewed before deciding whether to proceed with the next stage. An arbitrary start date of 2010 has been assumed which implies an Entry Into Service date at the beginning of 2023. The predicted engine development cost in 2006 prices is 8,147M€ and vehicle development cost 14,454M€ to give a total development cost of 22,601M€. The first vehicle production cost is 979M€. Assuming an 85% learning factor and a total production run of 100 vehicles implies an average vehicle sale price of 639M€ (including full development cost recovery). The estimated annual operating cost per vehicle is 553,8M€ of which the liquid hydrogen fuel comprises 83%. This assumes hydrogen derived from electrolysis of water however hydrogen derived from steam reforming of hydrocarbons would be about a third of the cost which would roughly halve the annual operating cost.

### 3.1.2 Kerosene Mach4.5 Cruiser

A parallel study carried out by DLR-Sart [14] focused kerosene as a fuel in order to explore the performance of this fuel in preference to hydrogen since its supply infrastructure is well established. In order to keep the wing loading in an acceptable range, the new supersonic cruise airplane has a wing size of 1600m$^2$. The total length reached to 103m. The LAPCAT-M4 employs a blended wing-body with a modified nose, a highly swept in-board wing panel, and a moderately swept outboard wing panel. The four advanced turbo-RAM-jet Variable Cycle Engines (VCE) are mounted in two nacelles on the wing lower surface adjacent to the fuselage. The location of the engine and nacelles is still open for adaptation if required by trim as long as they remain under the wing. The total take-off mass of the supersonic cruise airplane has been iterated in the first loop to the huge value of 720ton, which is well beyond any supersonic passenger aircraft built to date. The dry mass is estimated at 184.5ton and the structural index (dry weight to GTOW) is at a for airplanes low 26%. The HSCT would be able to transport about 200 passengers with their luggage over a distance of 16,700 km within 4 hours.

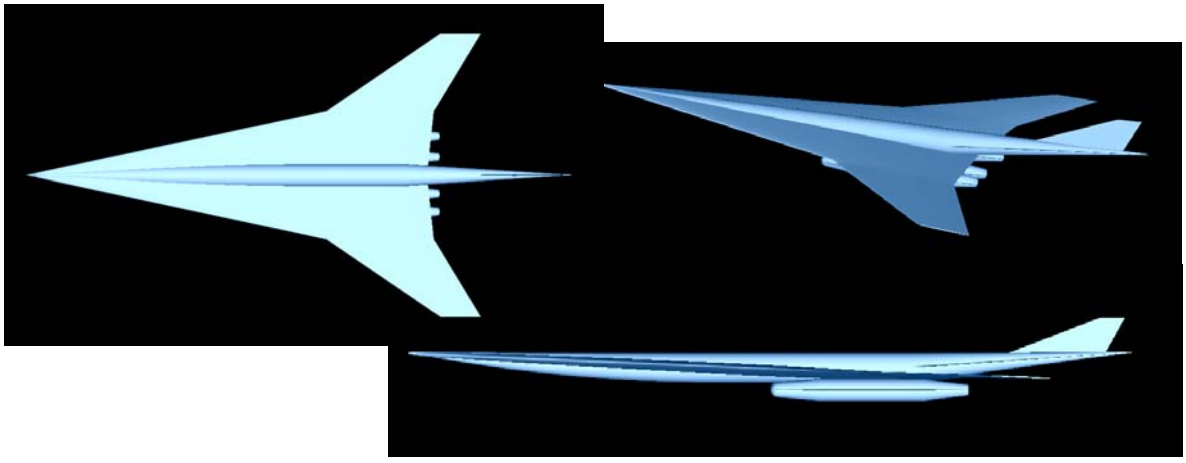

**Figure 17 Preliminary Mach 4.5 kerosene fuelled aircraft for 200 passengers with a MTOW of 720t**

## 3.2 Rocket Based Combined Cycles

In parallel to TBCC propelled vehicles, Rocket Based Combined Cycles was evaluated for two vehicle concepts. As the thrust to weight ratios for rockets are far higher (~60-100) than turbojets (~3), they might be a good alter-native for the acceleration phase despite their higher sfc. The preliminary design and

dimensioning of RBCC engines coupled with vehicle and a reference trajectory was addressed after the first vehicle designs for M4 (kerosene) and M8 (hydrogen) became available. For each of the vehicles, a basic RBCC concept was derived, and tools and rules for dimensioning the RBCC were developed. The evaluation showed that for the given mission kerosene as a fuel was out of scope, but that the mission could theoretically stand a chance using a hydrogen-fuelled RBCC.

The hydrogen-fuelled RBCC for Mach 8.0 is a planar design with a sophisticated intake system, and rockets integrated into struts. The nozzle consists of a single expansion ramp nozzle of the Sänger type and was tentatively demonstrated to be efficient for the proposed vehicle type. The RBCC engine model for the M8 vehicle was extended to include ramjet combustion and thermal choking to enable the examination of a mixed ramjet-scramjet configuration with different fuel injection positions and side wall struts in the remainder of the system.

From practical gas dynamic and manufacturing considerations, the scramjet combustion chamber should not exceed a maximum length allowing for a slight divergence to give margin for design issues other than the mixing process. By cooperation with specialized CFD analyses, the assumed model input parameters could be refined in a series of parametric studies to represent more realistic values.

The dimensioning of the propulsion system components allowed DLR-Sart to define the lower part of the latest generic LAPCAT-M8 air-plane geometry as illustrated in Figure 18. The upper section of the vehicle is dependent on the necessary volume for fuel tanks and the SERN expansion ratio intended to be as far adapted as possible. LAPCAT-M8 as a generic airplane is designed as a lifting body with a simple 2D-geometry in the central air-intake part, easing not only the conceptual lay-out but also CFD and experimental investigations.

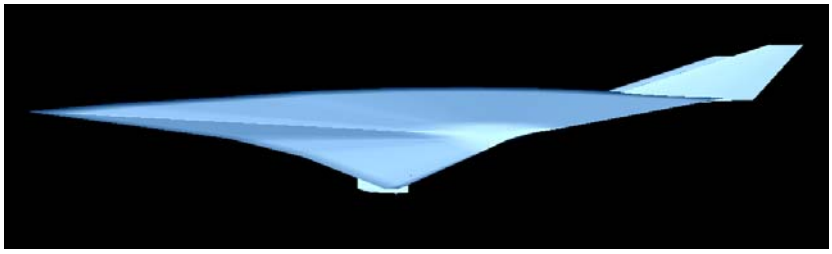

**Figure 18: Preliminary design of the LAPCAT-M8-3 cruiser based on a H2 RBCC**

The total length is 101.2m with a total span of 41.6m. Its height mounts up to 19.5m. The outboard region converges rapidly to the "wingtips", so that the leading edge sweep angle is about 82°. The stabilizer located in the tail part of the lifting body and two vertical fins, slightly inclined outboards, are to be used for aero-dynamic trim and control. Though using ultra light-weight structural design in high load and very high temperature environment, its empty weight mounted still to 370ton with an incredibly large take-off mass of 944ton.

As the RBCC requires a rocket ejector operation at low Mach number flight, its low performance along with the non-availability of reliable data, results in a very high fuel consumption during the acceleration phase. Its performance is highly critical to overall feasibility. This version of a Mach 8 hypersonic RBCC airliner could reach a limited range of up to 5800km.

One of the reasons for the less than impressive performance of LAPCAT-M8-3 is its disappointing aerodynamic performance in terms of lift over drag ratio. Whereas a slim design would result in a better aerodynamic performance, the need to integrate large hydrogen volume tanks resulted in a bulky vehicle. The analyses further revealed that an RBCC without an enormous thrust excess operates too long in an unfavourable fuel consumption regime, depleting about two-thirds of the totally available fuel. The mission is flown in the ejector mode up to a Mach number of 2.5 when switching to a pure airbreathing RAM-SCRAM-mode. After finishing the third iteration loop of the LAPCAT-M8 preliminary design the concept could not be considered as converging.

The vehicle-propulsion integration proved to be a difficult exercise and a redesign of the vehicle was

suggested. The aim was to ensure a good aerodynamic performance for both subsonic and hypersonic speeds along with a large volume for hydrogen fuel, an alternative propulsion unit for the acceleration phase with enough thrust and finally, realistic dry and gross take-off weights. The dual mode ramjet propulsion unit was kept for the acceleration and cruising at Mach 8. The challenge was to ensure that each of the components, i.e. aerodynamics, propulsion performance, volume and weight would not degrade the other when combining them.
This optimization loop resulted in a dorsal placement of the propulsion unit, including the large intake ramp and nozzle [16]. The aerodynamic performance was realized by using a blend of a waverider and a delta wing previously developed by DLR-AS for a Mach 12 speed. The poor performance of an ejector rocket was addressed by replacing it with a gas-generator fed air turbo-rocket (ATR) which has a good and nearly constant specific fuel consumption over a wide Mach number range. Moreover, this choice also allows for efficient cruise over land in a subsonic mode, to loiter and to ensure the containment of jet noise. This turns the aircraft into a versatile and operationally flexible vehicle (Figure 19).

The achievable range is strongly sensitive to the allowable acceleration loads. Higher loads lead to lower fuel consumption during the acceleration phase. The maximum g-loads on the passengers were limited to 0.2 and 0.4g in all directions. The GTOW was fixed at 600tons which corresponds to the present achievement in classical aircraft, e.g. the Antonov-225 with a 600 to 640tons GTOW and a 170tons of empty mass. A 400km range with subsonic cruise was imposed prior to acceleration to supersonic speeds along with a controlled and powered deceleration phase. This first leg ensures that the aircraft is flying subsonically over land and then supersonically once over sea. Depending on the flying strategy, the vehicle turned out to have a range varying from 14000km to 18000km with a touch-down weight of 240tons. The corresponding structural index (dry weight to GTOW) for these weights is fixed at 0.3, or 180 tons. A total of 60 tons for 300 passengers and accommodation, i.e. cabin, luggage, crew, galleys… is taken from the LAPCAT A2 vehicle estimates. The length, span and height are respectively 90m, 62.2m and 18.1m compared to 84m, 88.4m and 18.1m for the An-225. The internal volume of the concept can accommodate the 360tons of fuel needed with a reserve volume of about 1100m$^3$ or 80 tons of fuel weight. The vehicle control is not examined in detail but consists presently of two all-moving fins with dihedral and ailerons for roll and pitch.

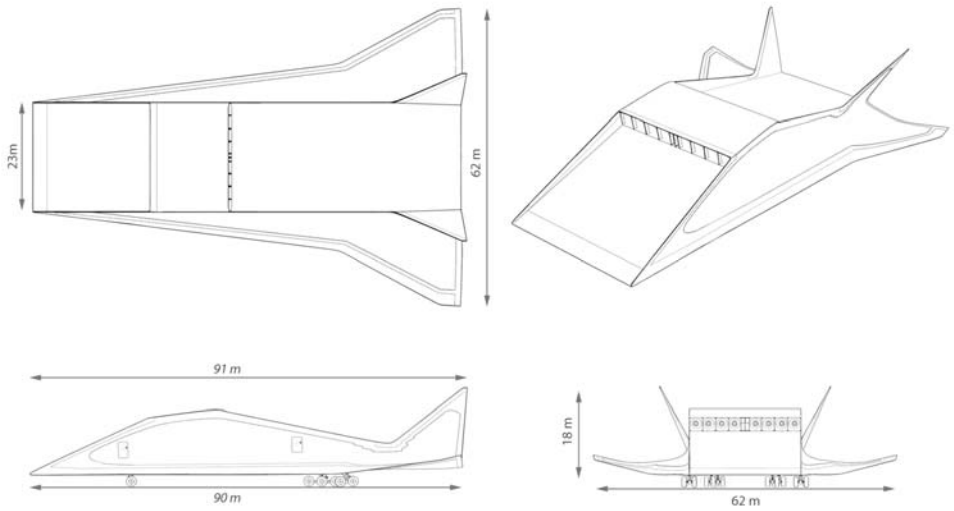


**Figure 19: LAPCAT-MR1: Conceptual Design of a Dorsal-Type Mach 8 vehicle.**

With this alternative design, the envisaged mission Brussels-Sydney is physically possible with part of

the trajectory at a cruise flight Mach number 8.0 using a hydrogen-fuelled scramjet and a tuned trajectory strategy. Due to its versatility, the vehicle can optimize its operation for different long haul trajectories with flight times varying between 3 to 5 hours. The three hours trajectory profile corresponds to a total of 30' of acceleration and a cruising at Mach 0.8 with a range of 400km ensuring flying subsonically over land. Once over sea, a 10' acceleration allows to reach Mach 8 (axial load of 0.4g with a covered range of 2,725km), followed by a 90' cruise at Mach 8 for 12,375km and a final descent and deceleration for 50' for 2,200km. This total journey amounts to 17,700km which can be extended by cruising for some time at Mach 4-4.5.

## 3.4 Combustion Experiments

Dedicated combustion experiments were clearly needed for both TBCC & RBCC concepts in order to evaluate and check the performance and characteristics at specific conditions for supersonic combustion and high-pressure combustion. Experimental data obtained in supersonic combustion experiments performed in the M11 connected tube facility at DLR Lampoldshausen have been evaluated for differently shaped strut injectors [23] (Fig. 10).

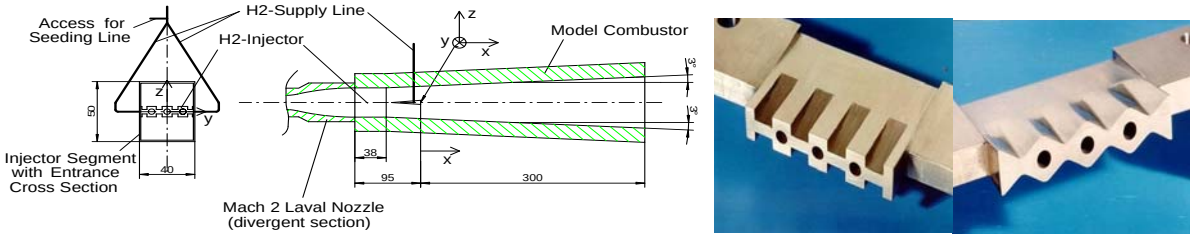


**Figure 20: Scramjet model combustion chamber with studied injectors: USCER (left); WAVE injector (right).**

The supersonic combustion experiments of a complete scramjet configuration consisting of intake, combustor and nozzle were performed in the DLR High Enthalpy Shock Tunnel Göttingen (HEG). The tests concentrated on the scramjet configurations used during the HyShot flight experiments (Fig. 11). Due to the involvement of DLR in the HyShot I and II flight experiments, wind tunnel data of WP5 and the numerical data from WP6 have be compared to flight data [18],[24] (Fig. 12).

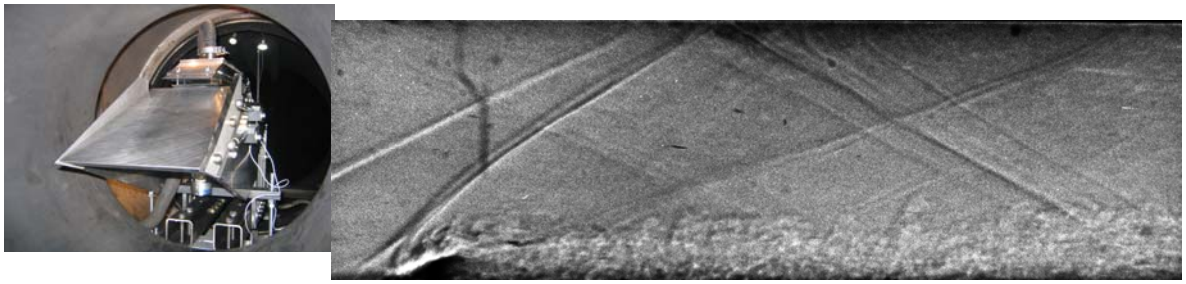

**Figure 21: Wind tunnel model installed in the HEG test section (left) and Schlieren visualisation of the wall normal gaseous hydrogen injection in the HyShot II combustor (right).**

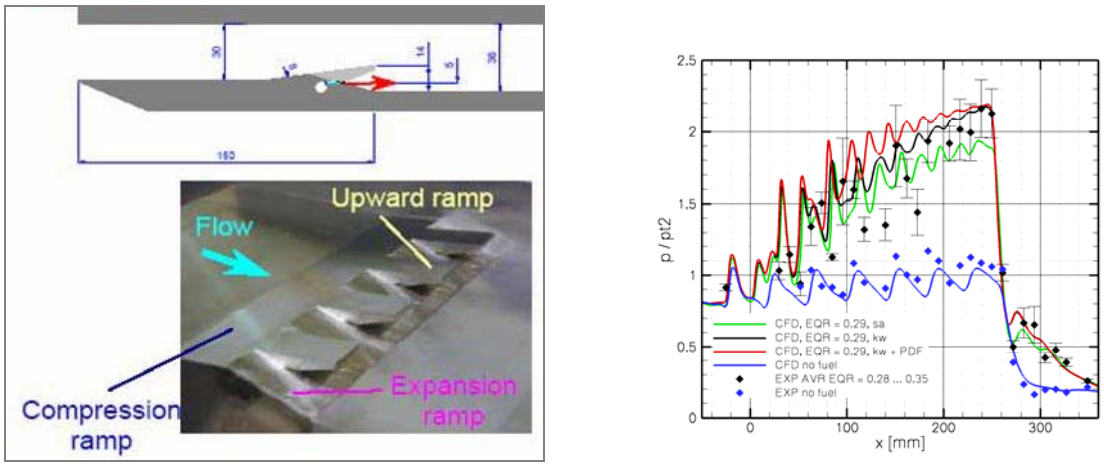


**Figure 22: Left: Hypermixer fuel injector configuration. Right: Pressure distribution for porthole injection; (S-A: Spalart-Allmaras turbulence model, k-ω: Wilcox k-ω turbulence model, PDF: assumed PDF for turbulence-chemistry interaction).**

In the framework of high pressure combustion experiments with focus on the HC disintegration processes, the ITLR shock tube at the University of Stuttgart has been equipped with a fast-response fuel injector [17] [25]. Currently, fluid disintegration experiments are being performed under supercritical and subcritical conditions, employing dodecane (as exemplary hydrocarbon fuel) and hexane in argon.

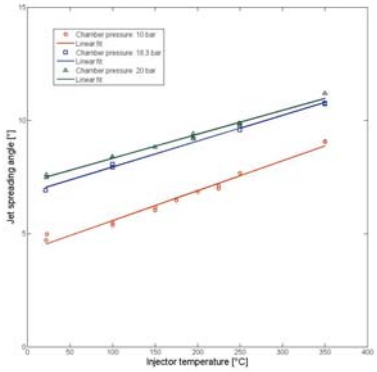


**Figure 23: Jet spreading angle as function of the fuel injection temperature for different ambient pressures: $T_5$ = 950K; Δp = 200 bar.**

The M3 test facility at the German Aerospace Centre, DLR in Lampoldshausen, has been refurbished to allow the use of hydrocarbon fuel such as methane (Figure 24). Quantitative thermometry of the hot gases using CARS-spectroscopy has been performed for the CH4/O2-flames. For the characterization of the ignition transient and stationary spray combustion software tools are developed to analyze shadowgraphs and high speed recordings of the flame emission [26].

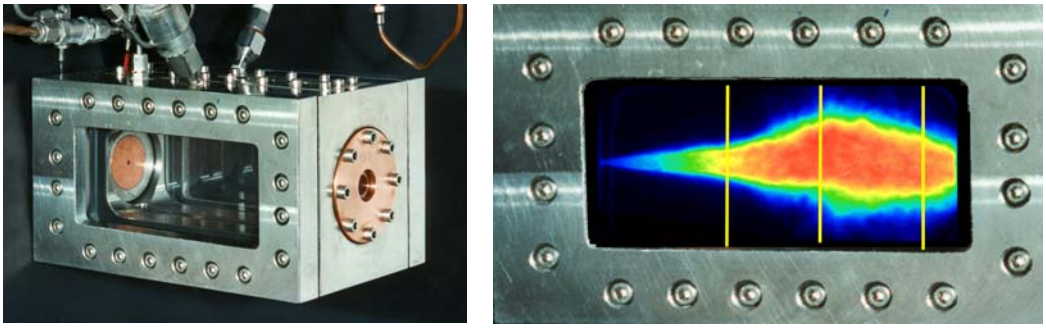

**Figure 24: left: Micro combustor M3 for the investigation of cryogenic spray combustion using methane and LOX; right: LOX/methane flame visualization**

## 3.5 Combustion Modelling and Validation

The goal was to investigate the physics of high-pressure and supersonic combustion requiring the development of new tools. In fact, numerical simulations performed on the basis of RANS (Reynolds Averaged Numerical Simulations) in combination with different models of combustion-turbulence coupling. Temptative LES (Large Eddy Simulations) have performed to explore their applicability and to improve RANS-based methods.

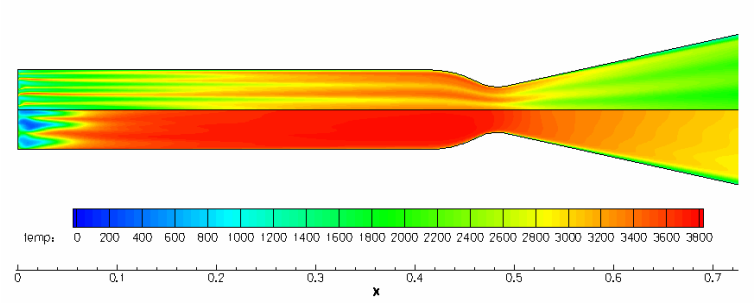


**Figure 25: RBCC configuration with HC/LOX combustion in rocket combustion chamber (top showing the non-premixed and bottom the remixed injection).**

The axisymmetrical EADS code Rocflam-II has been extended towards LOX/HC (Hydrocarbons, i.e. Kerosene and Methane) chemistries. The necessary fluid data and reaction schemes have been selected and implemented. The reaction model in Rocflam-II consisted of a tabulated equilibrium chemistry with a PPDF (*presumed probability density function*) approach to model turbulent combustion. Code validation has been carried out on available sub- and generic full-scale engines to the satisfaction of the involved EADS combustion modelling specialists (Figure 25). In the meanwhile the first company-internal spin-off of these LAPCAT achievements could be generated by employing the enhanced code in other preliminary development phases of engines prior to entering a regular development program.

For high-pressure combustion a compressibility factor formulation has been implemented and validated for typical rocket combined cycle operating conditions (super-critical in pressure, trans-critical in temperature). Extension and validation toward kerosene and methane consists of a tabulated equilibrium chemistry with a PPDF (*presumed probability density function*) approach to model turbulent combustion.

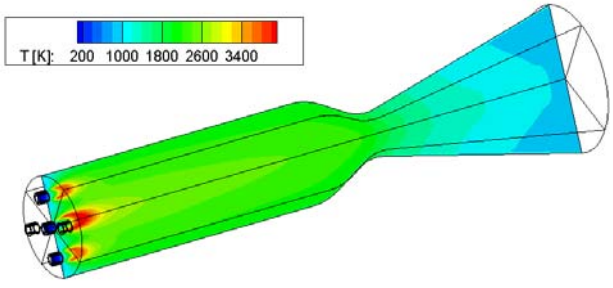


**Figure 26: Temperature contour for 3D simulation with realistic injection plate**

A thermodynamic model able to properly describe propellants injection in high pressure LOx/HC combustors has been developed and

implemented in the C3NS-PB flow solver. Two different approaches (compressibility factor formulation and analytical formulation) have been selected: the accuracy and robustness of both approaches have been preliminary assessed through comparison with experimental data available in literature. Furthermore, the compressibility factor formulation has been implemented in the flow solver and a suitable test case (RCM-1, "Nitrogen Cryogenic Injection", DLR Lampoldshausen, 2001) has been selected to test the capabilities of the model in typical rocket operating conditions (supercritical injection pressure, trans-critical injection temperature): the CFD simulations show a good agreement with experimental data Figure 26.

A turbulent combustion model (based on the Partially Stirred Reactor assumption) has been also implemented in the CIRA solver C3NS in combination with a reduced mechanism for oxygen/methane and oxygen/kerosene [27]. Three dimensional simulations of a rocket engine with a realistic injection plate configuration have been performed.

Using the ramjet of the RBCC configuration for the M4.5 kerosene airplane, the obtained combustion efficiencies and characteristic velocities for varying injection conditions allowed verifying the used values in the parametric study of the related propulsion system.

For supersonic combustion, finite rate combustion with appropriate turbulent mixing is used as a start extended further with an eddy-dissipation concept to account for turbulence dominated combustion [28]. A more complex extension towards turbulent combustion is based on an assumed PDF method to account for a wide range of applicability for premixed, non-premixed, partially premixed combustion and different Damköhler numbers. The numerical simulations of the complete flow-path including the wind tunnel nozzle and the HyShot Scramjet configuration show good agreement with the experiments [18], [33]. Wind tunnel results of performance characteristics (combustor) pressure rise and surface heat loads of the HyShot II scramjet configuration were reproduced by CFD. Uncertainties of numerical tools linked to different turbulence models were identified (Figure 22).

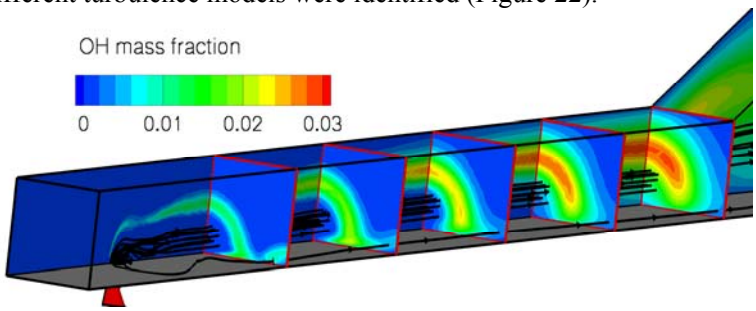


**Figure 28: CFD result of the flame structure (OH concentration) in the HyShot-II combustor with porthole injection**

Whereas the assumed PDF approach suffers from simplifications due to the chosen shape of the joint PDF, a transported PDF models require tremendous CPU times. Nevertheless a multi-variate-β-PDF for species distributions seems to be a good compromise between accuracy and CPU time, necessary for complex 3D simulations [29]. A major drawback of this approach is the required statistical independence of species and temperature fluctuations. The applicability of several hydrogen/air reaction mechanisms for scramjet applications has been performed. Seven detailed (9-species, 19- to 27-step), one reduced (7-step, 7-species) and one global kinetic scheme have been investigated. The basic result is that at critical conditions close to the ignition limit of hydrogen (this corresponds to low flight Mach numbers of a scramjet) only detailed mechanisms are able to accurately predict the ignition delay correctly. However, there are also significant differences between the detailed kinetic schemes and the best suited mechanisms for scramjet simulations are identified Figure

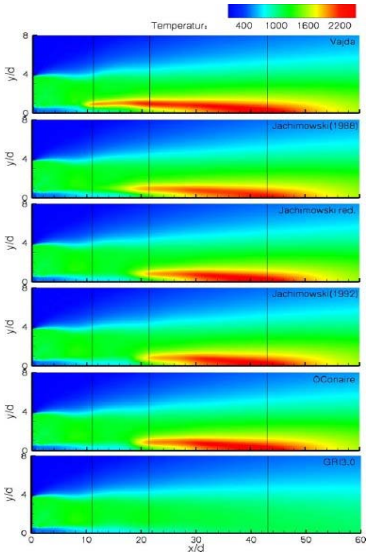


**Figure 27: 2D temperature fields of Cheng-experiment employing different reaction mechanisms**

27 shows the investigations of a lifted turbulent jet flame with supersonic inflow (Cheng et. al.) employing different reaction mechanisms.

Results obtained by LES simulation indicate combustion may be made to take place in a short distance by supersonic injection of hydrogen inside the supersonic airstream. The ISCM LES SGS is under validation [19] [30].

### 3.6 Design and Aerodynamics of Propulsion Components

To design a hypersonic vehicle using an air-breathing propulsion system with positive net thrust is a major technological challenge. The major difficulty lies in the determination of the pressure and skin friction drag. The accuracy to predict pressure drag depends upon the ability to characterize the complex system of shocks (i) acting at the inlet and (ii) due to the interaction of the nozzle flow with the external flow; the accuracy to predict skin friction drag, on the other side, depends upon the ability to determine the boundary layer state, i.e. laminar or turbulent and its behaviour with temperature. Such difficulties derive from the fact that in ground based facilities it is not possible to simulate complete real flight environments. Consequently, the successful design of a vehicle powered by an air-breathing engine would be based tomorrow purely on computational fluid dynamics (CFD), but today the numerical tools present strong limitations, in particular concerning turbulence modelling and shock-wave boundary layer interaction. Thus, the objective of the work-package has been the validation of design tools to determine the propulsive efficiency of air breathing hypersonic vehicles, i.e. not the intent to design an efficient inlet or nozzle but to improve the knowledge of the hypersonic flow physics, in particular intakes and nozzles with respect to transitional and turbulent flows and unsteady flows.

An air inlet representative of the LAPCAT Mach 8 vehicle has been designed by DLR-Cologne in accordance to geometric constraints driven by the vehicle and in accordance to requirements of the flow at the inlet exit stemming from the combustion chamber. A planar inlet, named LC01k, consisting of two external compression ramps and a cowl that causes two internal compression shocks has been designed. At the design point of Mach 8.034 and a flight altitude of 34.134 km the inlet performance fulfils (or exceeds) all flow requirements, i.e. mass flow, static temperature and static pressure. The windtunnel model (Figure 29) is equipped with pressure probes along the centreline of the inlet and the diffuser and with two Pitot pressure probes in the diffuser to measure the total pressure recovery. The mass flow through the inlet can be determined by a connected throttle, which is also used to vary the back-pressure. Further, it offers the capability to test different boundary layer bleed configurations and also to test different approaches to control the separation of the boundary layer at the inlets expansion corner. CFD rebuilding of the H2K-tests show that the RANS-based DLR-TAU code is able to capture almost all the dominant features, like the changes in flow features when the boundary-layer bleed-channel is open or close or due to varying Reynolds number. Due to the inherent limitation of classical RANS-codes, transitional intake flow has been assessed by LES and is very promising. In particular, for the first time a complete mixed-compression hypersonic inlet is studied using LES [31],[32].

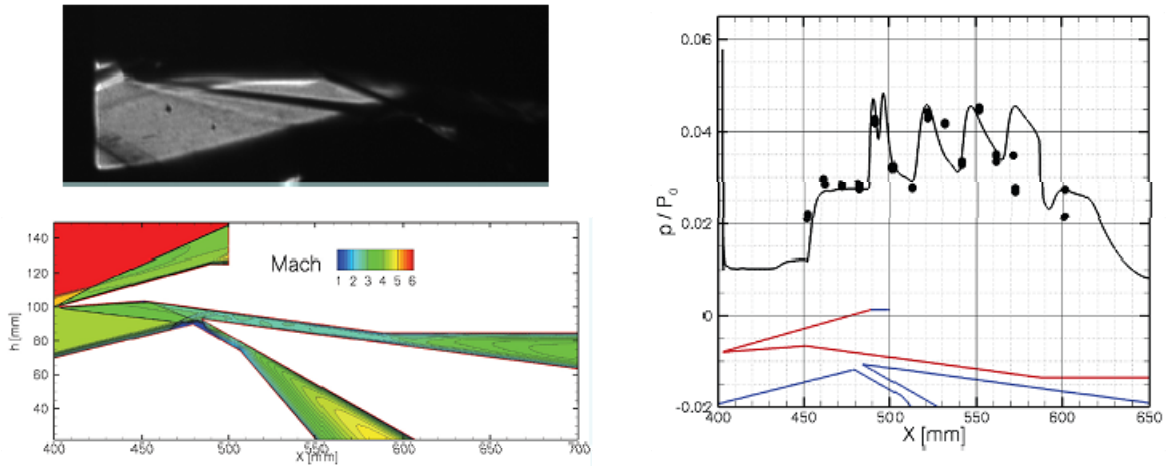


**Figure 29: LAPCAT Mach 8 Intake-LC01k assessment (top-down model position). Top left: Schlieren through the model window during the test in the H2K facility. Bottom left: CFD simulation with the TAU code. Right: comparison of normalized computed and measured pressure along the wall of the cowl.**

For the experimental study of the nozzle–base–external flow in the H2K facility a wind tunnel model of the SERN nozzle of the LAPCAT Mach 8 vehicle has been manufactured. The contour of the SERN nozzle has been designed by EADS-ST. The model has a modular structure and thus enables it to be used for nozzle experiments with various nozzle geometries. In contrast to common nozzle-base flow studies in the past, which were done with compressed cold air, here the isolated air supply chamber of the model allows supplying the model nozzle with a supersonic air flow with total temperatures up to 1000 K.

The experimental results reveal the shear layer separating the nozzle, the ambient flow and the inner and outer shock that adapt the pressure level of both flows to each other (Figure 30). The wall pressure measurements help to show the influence of the flow on the vehicle and therefore as a consequence on the nozzle thrust. The experiments showed that from all the variables the nozzle pressure ratio has the largest influence on the nozzle flow field. The extent of the exhaust plume and the displacement of the ambient flow clearly grow with increasing nozzle pressure ratio. CFD results for the complete SERN nozzle including Laval nozzle and base (also called nozzle-flap) are performed. The computations are in good agreement with the experimental results but indicate a higher under expanded flow leaving the SERN nozzle (Figure 30).

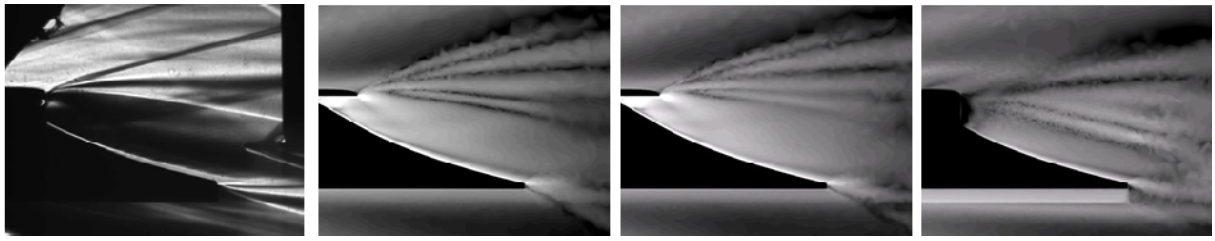

**Figure 30: left: Schlieren visualizations of the experiment (top-down model position) at nominal conditions. Following pictures: CFD simulations in 3 planes of different deep (outboard left to outboard right)**

Large eddy simulation (LES) of compressible flow with a mixed time-scale (MTS) subgrid model has been tested for three cases of turbulent and transitional flow: supersonic turbulent channel flow; propagation of localised transitional/turbulent spot in a supersonic boundary-layers and shock-induced separation bubble transition (Figure 31). The MTS model is found to perform well in the near-wall region without any ad-hoc near-wall damping functions. The subgrid-scale kinetic energy vanishes in the laminar regions, and it has been confirmed that this model perform well in predicting transitioning flows.

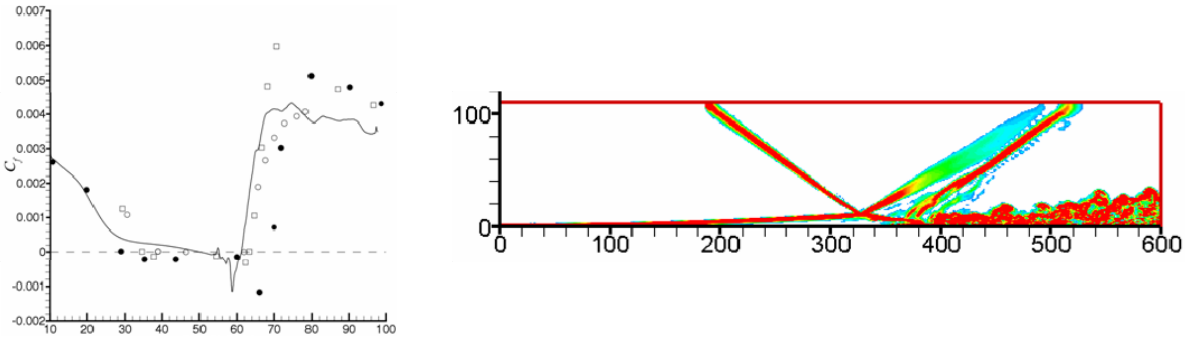


**Figure 31: LES simulation of a Ma=2 oblique shock-wave boundary-layer interaction (pressure ratio p3/p1=1.9) inducing a laminar separation bubble and transitional flow at re-attachment. Left: mean skin friction distribution along the flat plate: solid line present LES; filled circle and open square LES of Teramoto (2005); open circle Experiments of Hakkinen et al. (1959). Right: numerical Schlieren showing the instantaneous flowfield at time t = 1811 at a spanwise location z = 30.**

Decisive experimental data are provided on the set-up and propagation of turbulent spots embedded in a hypersonic boundary layer by means of thin film gauge signals. The transition-trip device model to be used in the gun tunnel of the University of Oxford is a flat plate with detachable leading edge that can be pivoted allowing testing in a Mach number range 2 to 7. Two sets of boundary layer "trips" have been fabricated on two additional leading edge pieces. Presently the experimental campaign is being carried out.

### 3.7 Conclusions

LAPCAT aimed for hypersonic speed transport by assessing advanced propulsion concepts and related technology for speeds up to 4 to 8 times the speed. Based on general trends in the evolution of aircraft performance and the possible aerodynamic and propulsive achievable efficiencies for high-speed vehicles, there's a potential to achieve antipodal range. Preliminary parametric studies within the project have shown so far that both a Mach 4-5 and a Mach 8 vehicle concepts based on hydrogen with a long-haul range are achievable. A kerosene based Mach 4.5 vehicle has also an interesting potential though more for a shorter range flight.

The vehicle systems defined during the project allowed the setting of working conditions of interest for detailed experimental and numerical work. Windtunnel models have revealed particular physical phenomena and enabled to justify the values for the different parameters used for the vehicle concepts. Also the simulation tools have been upgraded and were validated with the newly generated experimental database. The combustion processes and the related flow fields could be reproduced. However, ignition transients and ignition delays still remain critical for interesting flow conditions which are close to the ignition limits.

## 4.0 LAPCAT II PROJECT

LAPCAT II is a logical follow-up of the previous project whose objective is unchanged versus LAPCAT I. Among the several studied vehicles, only two novel concepts for a Mach 5 and 8 cruise flight were retained in the present program. The project, co-funded by the European Commission under the theme of air transportation kicked off in October 2008 and lasts for 4 years involving 16 partners out of 6 European member states. The consortium consists of 6 industries: Cenaero (B), EADS-Astrium (D), GDL (UK), MBDA (F), REL (UK) and Snecma (F); 5 research institutions: CIRA (I), DLR (D), ESA-ESTEC (NL),

Onera (F) and VKI (B); 5 universities: ULB (B), La Sapienza (I), Oxford (UK) , Southampton (UK), and Stuttgart (D).

Starting from the available Mach 5 vehicle (Figure 32) and its related pre-cooled turboramjet developed in LAPCAT I, assumed performance figures of different components are presently assessed in more detail:

- Intake design and performance
- Environment friendly design of combustor
- Nozzle design and performance
- Structural analysis

This will lead to an updated overall Mach 5 vehicle performance allowing the definition of a detailed development roadmap.

**Figure 32 : LAPCAT-A2: outcome of LAPCAT I project for civil Mach 5 transport (courtesy REL)**

Though the cruise flight of the Mach 8 vehicle based on a scramjet seems feasible, the fuel consumption during acceleration requires a large fuel fraction severely affecting gross take-off weight. Initial studies of a first stage rocket ejector concept gave poor range with large take-off mass. Integrated design of airframe and engine throughout the whole trajectory is now the prime focus to guarantee an optimal design in terms of range and flight time (Figure 33). Different concepts will be re-assessed and optimized to a final Mach 8 concept. Both turbo- and rocket-based engines will be investigated to assure better performance and fuel consumption during acceleration and cruise.

**Figure 33 LAPCAT-MR1: outcome of LAPCAT I project for civil Mach 8 transport**

The mission requirements of the follow-on project LAPCAT-II remain unchanged, as explained above, but focus will be now directed towards critical points which arose during the LAPCAT-I project. Two novel aircraft vehicles for high-speed flight are retained in the present proposal. The description of the objectives is split up along these selected concepts and finalized by a general environmental investigation goal.

## 4.1 Mach 5 Vehicle

Starting from the available conceptual vehicle design and the related precooled turboramjet named Scimitar, well-thought assumptions made for performance figures of different components during the iteration process within *LAPCAT-I* will be assessed in more detail. This includes the following items.

### 4.1.1 Intake Design and Performance

The intake (Figure 34) must operate over a wide Mach number range (0 to 5) whilst delivering the correct air mass flow and recovered pressure for the core engine and bypass system. This necessitates a mixed compression variable geometry intake with a number of external and internal shock waves and a final subsonic diffuser. The intake should be resistant to 'unstart' and 'buzz' to give carefree engine and vehicle handling, meet the engine life requirement at 1250 K operation, be resistant to panel flutter etc.

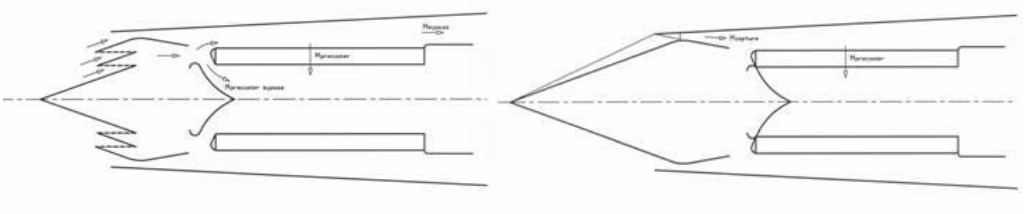

Figure 34: variable intake configuration: top retracted intake for Mach = 0÷1.647, bottom fully deployed intake for cruise Mach = 5.

### 4.1.2 Environment Friendly Design of Combustor

Though the most critical parts of the engine has been brought to a higher technological readiness level in *LAPCAT-I*, i.e. contra-rotating turbine and heat exchangers, the concern here is related to the too high thermal NOx production. As one of the FP7 goals is to cut the NOx emissions, special attention will be given towards different staged combustor lay-outs. This will most likely affect the engine's performance and requires special attention.

### 4.1.3 Nozzle Design and Performance

Identically as for the intake, the nozzle needs to operate over a wide operational range and requires a variable geometry. Throughout the acceleration phase, the bypass flow will interact with the core nozzle resulting into a larger base drag. Optimization should reduce potential loss in range followed by a structural design of the variable geometry.

### 4.1.4 Structural Analysis

An optimum design approach will be established minimizing mass whilst meeting the lifetime requirement. This exercise will result in estimates of the fuselage & wing stiffness and mass and volume distribution. The latter will serve as input for the aeroelastic studies in conjunction with control algorithms, allowing estimating flutter margins.

A requirements specification document for each of the above described components is already composed early in the project. The technical assessment of all components will be finished the latest one year prior to the end of the project, allowing the re-assessment of the vehicle and engine performance with the obtained figures of merits. The outcome of this re-evaluation will allow the definition of a detailed roadmap towards the production of the vehicle. This will include the detailed design and testing of subcomponents, subscale flight experiments up to the complete vehicle production.

## 4.2 Mach 8 Vehicle

Integrated design of airframe and engine throughout the whole trajectory is the prime focus here to guarantee a successful design. This means that both off- and on-design conditions for the different parts of a combined cycle need to be well understood, modelled and validated. A turbo-based engine will replace the former ejector rocket to assure better performance and fuel consumption during acceleration. Various cycles need to be evaluated and linked to the vehicle design. Important points to be addressed to realize these goals are:

### 4.2.1 Proper Development and Validation of Engine-Airframe Integration Tools and Methodology

Only a very limited number of beneficiaries do have tools for quick assessment of vehicle performance but they all differ in methodology, level of complexity (zero or one-dimensional) and mostly in application (e.g. launchers, space planes). The level of detail in aerodynamics and propulsion performance simulation is widely varying. It is of utmost importance to develop and re-orient these tools towards passenger aircraft for a fully integrated approach along the complete trajectory and for the combined propulsion cycles envisaged in this project. The complex interaction among the different components and disciplines (Figure 35) should be optimally addressed for a fast and efficient vehicle design and assessment. A key element in this approach is the proper definition of interfaces and control volumes of the different elements, in particular for the external and internal flow paths (
Figure 36). Proper validation and cross-comparison are needed on existing vehicles supported by properly chosen experiments within the project. Gradually the complexity of these tools will be increased and systematically validated and finally applied to the vehicle.

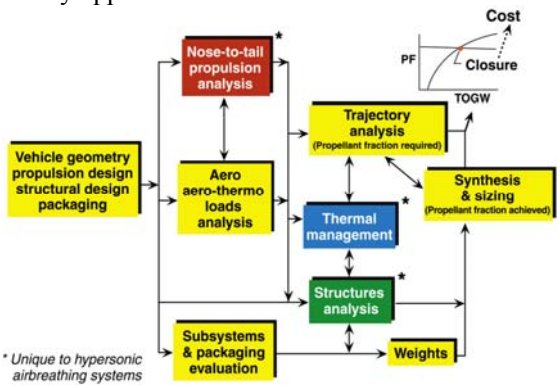


**Figure 35: Hypersonic Vehicle Design System [34]**

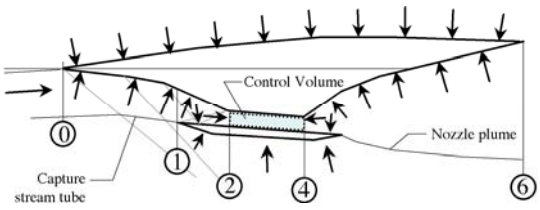


**Figure 36: Interface and control volume definition: (0) capture (1) inlet internal compression (2) combustion inlet (4) combustion outlet (6) nozzle exit. Arrows indicate the wall and interface pressure for the vehicle geometry and combustor control volume. [34]**

### 4.2.2 High-Speed Airbreathing Cycle Analysis

Closely linked to engine-airframe integration tools is the correct prediction of engine performance throughout its operational domain. Several new and particular cycles need to be implemented and investigated such as several variants on the air-turbo rocket/ramjet engine (Figure 37).

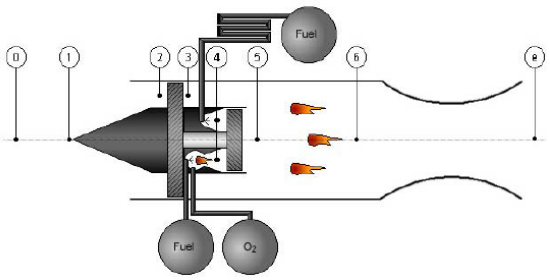


**Figure 37: Air Turbo Rocket/Ramjet: Expander cycle (top) and Gas Generator (bottom) [35]**

Though a dual mode ramjet cycle was investigated in *LAPCAT-I*, further level of detail on the chemistry, combustion efficiency etc… is needed, in particular for operation in off-design conditions. These cycle models will form a basic module into the above described engine-airframe integration tool.

### 4.2.3 Dedicated Experiments to Evaluate the Design in Various Operation Points

Validation of the integration tools will be based on experiments dedicated on both individual components such as intakes and combustors, but also on integrated models for the internal flowpath with and without combustion as well as a complete model with external and internal flow aerodynamics and interaction. This means that the wind tunnel models will be equipped with both detailed diagnostics as well as integrated force and/or moment balances. Also scaling issues will be addressed experimentally in order to extrapolate the validity of the tools to the design of larger vehicles, not able to be tested in available ground based facilities. This strong interaction among different tools towards the final design is nicely depicted in Figure 38.

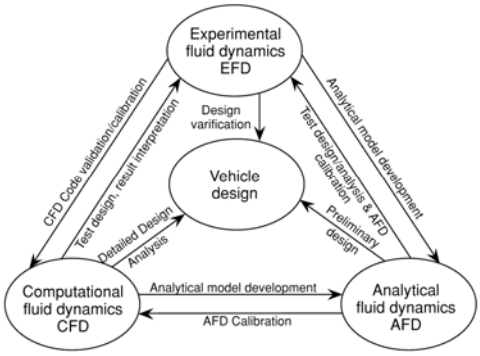


**Figure 38: Integral design approach [34]**

The availability of the integrated tool will allow the team also to assess previously investigated studies or configurations suggested in the literature. This extended assessment will increase the insight and know-how to move into a global multi-disciplinary optimization of high-speed vehicle designs. By this way lessons learnt form past studies will aid the current final vehicle design. This built-up experience and

validated tool development should give solid confidence to propose a fully integrated vehicle to comply with the mission goals. Once defined, a roadmap will be defined with a step-wise approach to future development, including one or more flight experiments to prove the maturity of the technology at different milestones.
As with any engine or vehicle design, its environmental impact is of importance. However, for vehicles flying at high speeds and high altitudes, limited know-how is available at present. The most important gaseous pollutants having an impact on the ozone concentration in the atmosphere are believed to be NO, $NO_2$, $H_2O$. Modelling studies showed that emissions of $NO_x$ by high-speed aircraft into the stratosphere may result in ozone depletion. In contrast, the $NO_x$ emissions into the troposphere lead to an increase of ozone concentration [3]. The quality of the effect of $NO_x$ emissions on the atmospheric ozone depends on the surface area of sulphate stratospheric aerosol layer and polar stratospheric clouds. However, these conclusions apply for hydrocarbon fuels and not for hydrogen as a fuel. Hence some of these conclusions need to be revisited to verify the influence of $NO_x$ and $H_2O$ onto the ozone layer and the formation of contrails with its direct and indirect effects.

### 4.3 Conclusions

LAPCAT-II started in October 2008 as a co-funded project of the European Commission within the 7th Framework Programme. Proceeding along the outcome of LAPCAT I, the project has now evaluated and cross-checked different configurations for the Mach 8 vehicle. More detailed results will become available publicly in the coming years.

## 5.0 ATLLAS PROJECT AND ITS ACHIEVEMENTS

The project ATLLAS (Aerodynamic and Thermal Load Interactions with Lightweight Advanced Materials for High Speed Flight) kicked off in October 2006. Its main objective is to evaluate and assess potential high-temperature resistant materials for sustained super- and hypersonic flight. This covers both materials for the external geometry as well as for the internal combustor geometries. The project, led by ESA-ESTEC, is co-funded by the European Commission under the 6th Framework Program and a consortium of 13 partners from industry, research institutions and universities.

The objective is to identify and assess lightweight advanced materials which can withstand ultra high temperatures and heat fluxes enabling high-speed flight above Mach 3. At these high speeds, classical materials used for airframes and propulsion units are not longer feasible and need to be replaced preferably by high-temperature, lightweight materials and if required, some parts with active cooling. Both metallic and non-metallic materials are tested extensively including Ni-based Hollow Sphere Packings, Ultra High Temperature Ceramics and several (non)-oxide Ceramic Matrix Composites. Envisaged cooling techniques for CMC based combustion liners are film, effusion, transpiration and regenerative cooling.

### 5.1 Introduction

For high-speed aircraft, material and cooling issues for both airframe and engine are one of the key elements which forces the designer to limit the flight Mach number. The expected benefits of economical, high-performance and high-speed civil-aircraft designs that are being considered for the future will be realized only through the development of light-weight, high-temperature composite materials for structure and engine applications enabling reduction of weight, fuel consumption, and direct operating costs.

When aircraft fly this fast for long periods of time, friction from the air passing over the aircraft heats up the outer surfaces of the fuselage and wings. For example, an aircraft flying at Mach 3 experiences a temperature increase of ~330ºC from this kinetic heating. The maximum temperature of the outer surface

would be at 350ºC. For Mach 6 the outer surface would be ~1200ºC. The extremely severe combination of component stress levels and high temperature operating conditions, as well as the requirement for an extended 25,000-cycle service-life, introduce the challenge of utilizing advanced materials without incurring excessive weight and cost penalties. Such materials' behaviour and related manufacturing processes are beyond current commercial experience and only little information is available.

Propulsion engineers are mainly confronted with increasing difficulties arising from high engine temperatures. The structural total-life requirements for the SST propulsion system are the same 30,000 hours as in subsonic commercial engines. Nevertheless, subsonic aircraft engines spend less than 10% of their mission time at the most severe engine conditions. On the contrary, SST engines spend about 60% of the mission time under the most severe combination of component stress levels and high temperature conditions. The challenge is to utilize advanced materials to cope with the high temperatures without incurring excessive weight and cost penalties.

It brings the engine designer new problems because of the higher operating temperatures required to produce the higher thrust. At Mach 2 air enters the intake at about -60°C, is compressed in the intake to about 130°C at the face of the engine and leaves the high-pressure compressor at 550°C. At Mach 3 this rises exponentially to respectively 325°C and 986°C.

Viable combustors concepts, having a long life goal of 18,000 hours, depend on the development and demonstration of a new class of high temperature ceramic matrix composites (CMC) for which no previous commercial practice exists. At the same time, lightweight, high strength and high stiffness metallic, intermetallic and ceramic composite materials are being examined for the exhaust nozzle design in order to meet engine noise and weight requirements.

The major challenge arises from the total airframe configuration. To meet it the aerodynamicist has to produce a satisfactory compromise between two inherently conflicting requirements: the need for minimum drag in supersonic flight and the need for controllability and ease of handling in subsonic flight. From a design point of view, the lift-to-drag (L/D) ratio is the most important aerodynamic parameter of airliners, affecting essential economic-related performance such as maximum range, payload and fuel consumption. The primary cause of SSTs' high specific fuel consumption (SFC) is the dramatic fall in airplane's L/D ratio at supersonic speeds. Concorde, for example, experiences an L/D reduction in the order of one-half that of subsonic jets.

The main goal, therefore, is to increase the lift-to-drag ratio throughout the speed regime of the next generation SST. Methods needs to be evaluated which include optimisation schemes coupled with state-of-the-art computational fluid dynamic (CFD) solvers, as well as non-linear design methods. The development and application of Multi-Disciplinary Optimisation tools involving aerodynamics, propulsion, structure and flight mechanism are in the end required to realize an optimum integrated airframe/propulsion aircraft. It is however not the intent to evaluate new and advanced propulsion concepts as is the case for a presently running EC-project LAPCAT[1]. Here we start from existing engines (turbojets) or engines which are within technical range (turbo-ramjets). Finally, a SST design should also consider the impact of the sonic boom impact and possible measures to reduce it.

## 5.2 Project Objectives

The ATLLAS project aims at providing a sound technological basis for the industrial introduction of lightweight advanced high-speed aircrafts on the long-term (15-20 years), defining the most critical RTD-building blocks to achieve this goal and finally to investigate in depth these critical technologies by developing and/or applying dedicated analytical, numerical and experimental tools.

Two supersonic aircrafts concepts are evaluated. The primary cause of the high specific fuel consumption for high-speed transportation is the dramatic fall in lift/drag ratio at supersonic speeds. The main goal is to find if the established empirical L/D barrier is fundamental or if it can be broken by careful design and in particular by close integration of the airframe and the engine. The study investigates an aircraft configuration suited to Mach 3 flight and another for Mach 6. Areas of critical aero-thermal loads are identified and evaluated.

Critical technologies for both the external airframe and the propulsion units are assessed. The major issues addressed are sonic boom and heat transfer reduction, high temperature resistant materials which are both lightweight and long-duration oxidation-resistant, novel cooling techniques, particular aerodynamic phenomena related to compressibility, and fuels that have both high energy content and good heat sink capability.

The concept of boom minimization is based on suppressing the coalescence of multiple secondary shock waves caused by the SST in supersonic flight, so that the overpressure (DP) at ground level is reduced. This can be achieved through the manipulation of aircraft's design characteristics, resulting in an optimised N-wave pressure signature with significant sonic boom loudness attenuation. In the proposed program eliminating the fuselage bow shock and the rear reattachment shock is investigated by careful integration with the propulsion system. Alternatively, creation of cold plasma in front of nose or leading edges allows the change of shock structure and its related strength.

Specific objectives for the envisaged concepts are related to materials and cooling. Lightweight airframe components are clearly needed for both concepts. The multi-functionality of hollow-sphere structures for aeronautical applications is evaluated for their low-density, thermal protection, acoustic absorption. Also Ultra-High Temperature Ceramics and oxidation resistant CMC materials for sharp leading edges and air intakes at sustained high heat fluxes typical for high-speed transport are investigated allowing the generation of a database for possible concepts and materials.

Also lightweight engine components are needed allowing the increase of the combustion liner and turbine vanes temperature resulting into lower NOx-emission and higher turbine inlet temperatures leading towards higher thermal and propulsion efficiency. Long-term oxidation and wear resistance of the combustion liner for lean combustion conditions are performed for the same reasons of setting up a database for possible concepts materials.

Despite the use of high-temperature protection systems, the imposed heat fluxes for airframe and engine still require the use of direct or indirect cooling to control material temperature. The initiation of high-temperature resistant materials automatically requires the (re)-investigation of novel cooling concepts by evaluation of various types of cooling processes (film, transpiration, effusion) within propulsion units with respect to cycle efficiency and controlling operational material temperatures. Also EHD cooling principles by altering the shock position and strength and hence the related stagnation heat flux are studied.

The emphasis in the area of loads definition is to develop and verify models to predict the combined effect of aero-thermal and material interaction on several lightweight high-temperature resistant materials. This is accomplished by integrating existing aerodynamic, heat-transfer, and structural codes. The results are then calibrated and verified with simplified experiments

The use of multi-disciplinary analysis and optimisation process (MDO) to model a sufficient complete flight mission by the inclusion of the disciplines aerodynamics, structure and flight mechanics allow to optimise the aircraft for maximal cruise range starting from a fixed maximal take-off weight and a given fuselage. As an appropriate balance between accuracy and numerical effort, high fidelity modelling based on an Euler flow solver and a finite element solver is intended for the high-speed cruise part of the mission using the disciplines aerodynamic and structure.

ATLLAS is carried out by a 13-member consortium. As major European manufacturers in the highly competitive high-tech field of aeronautical high-speed flight design and manufacturing, ASTRIUM (D), MBDA (F) and EADS-Innovation Works (D) provide the technical needs and application-specific expertise. One SME industrial partner, GDL (UK), has developed a design method particularly suited to highly integrated engine/airframes and is applying the method to the Mach 3 aircraft design. Another SME, ALTA (I), has developed renowned skills and expertise the field of high-speed experiments. The groups belonging to research centres (ESTEC (NL), DLR (D), ONERA (F), FOI(S)) and universities (Stuttgart(D), Munich (D), Southampton (UK) and UPMC at Paris (F)) are all working for long-time on specific issues of propulsion, combustion and aerodynamics with close contact to industry in bilateral, national and international collaborations. They provide basic knowledge, investigation means and testing facilities.

## 5.3 Novel Concepts for High-Speed Flight

Two aircraft configurations, suited to Mach 3 and Mach 6 flight are investigated. For both configurations, the major issues to be addressed from an aerodynamic point of view are sonic boom, aero-thermal loads, aerodynamic performance and fuels with good heat sink capability. The airplanes are being designed by two teams in parallel and integrated both almost by the same organizations, i.e. DLR, ESTEC, FOI, GDL, ONERA and UPMC. The selected design approach followed for each configuration has been completely different. The Mach 3 vehicle is the result of an inverse design strategy based on a method of characteristics where cruise efficiency and sonic boom mitigation have been the design variables. On the other side, the design of the Mach 6 vehicle is the result of applying a high-fidelity multi-disciplinary design optimization technique to an existing vehicle configuration. Here cruise range has been the optimization target. However, more than the configurations themselves the development and validation of the design-tools for both vehicles have required a major time and constitutes therefore one of the major achievements.

In support of the design of the Mach 3 vehicle, the theoretical limits to cruise efficiency have been determined and a global approach to aircraft cruise performance optimisation was set out. The strategy has been validated comparing predictions of cruise efficiency for Concorde and XB70. For the Mach 3 vehicle the analysis indicated that venting the exhaust in the lee of the wing and base of the fuselage will enable supersonic/hypersonic aircraft to have cruise efficiencies that are competitive with their subsonic rivals. A vehicle configuration has been developed featuring a circular fuselage with nose intake and an internal high bypass turbofan. A water tight CAD model of the outer mold line was developed, together with a general arrangement showing the locations of primary system, fuel storage, cabins and undercarriage (Figure 39).

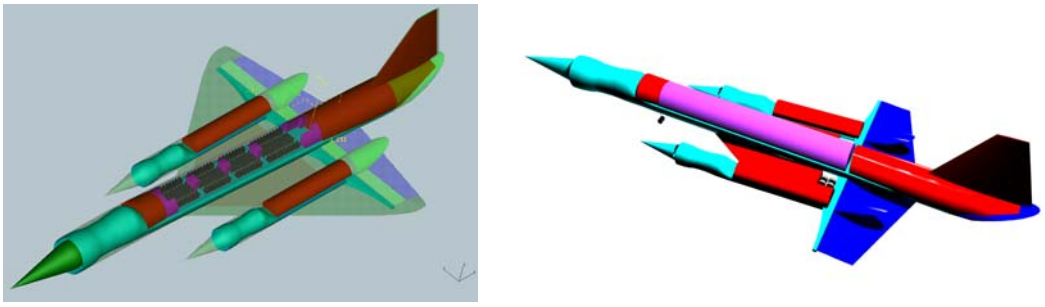

**Figure 39: Mach 3 vehicle CAD-model (left); configuration with fuselage and wing skins off (right). Cyan: air flow path; blue: wing nozzle and thrust surfaces; red: fuel tanks; magenta: cabin.**

The exhaust is ducted to the wing and fuselage bases. The wing has a high aspect ratio for good subsonic performance while drag due to thickness is eliminated by exhausting approximately two thirds of the propulsive stream from the wing trailing edge. Aerodynamic analyses for the Mach 3 configuration illustrated the feasibility of the propulsive-aerodynamic integration over a wide operational range. Particular attention is given to the expansion of the exhaust gases over the rear part of the wings in order to assess its impact on the overall vehicle performance over a wide range of flight Mach numbers (Figure 40).

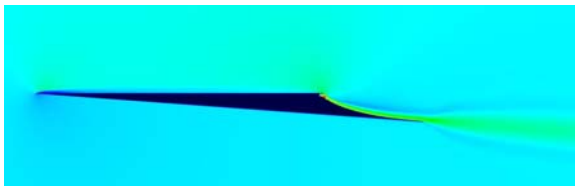

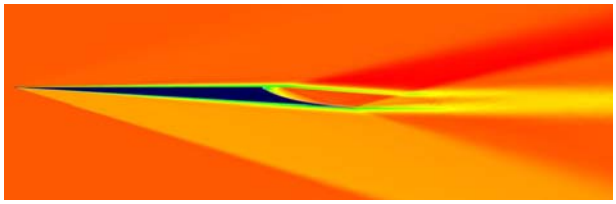

**Figure 40: Mach 3.5 configuration: Mach distribution including exhaust expansion in the aft part of the wing: top: M=0.4, Alpha=0; bottom: M=3.5, Alpha=0.**

Similarly, significant effort has been devoted to developing a propulsion model of the intake - ducted turbofan – air transfer duct and ramjet / afterburners (Figure 41). The models employs the compressor map scaling techniques of Kurzke and ensures that the work provided by the choked HP turbine meets the core compressor requirements, and similarly that the LP turbine drives the bypass fan. Compatibility between bypass and core streams requires that their static pressure be equal prior to mixing. Also, an initial mass budget has been developed and used to perform a trajectory flight-out simulation. The vehicle undertakes a cruise-climb profile, with cruise efficiency above to 3.8, indicating a fuel burn during cruise of 160tonnes over the designed range. Finally, CFD predictions of the vehicle at cruise have been performed. Lift, drag and pitching moments have been determined from the calculated momentum fluxes, together with integration of the surface pressure and viscous forces. The nose to tail CFD simulation has provided an important confirmation of the design premise, namely that exhausting in the lee improves cruise efficiency in comparison to a conventional design whilst resulting in a vehicle with acceptable aeronautical characteristics. But also the CFD simulations have shown an undesirable interaction of the wing nozzle flow field underneath the fuselage resulting in a reduction of lift of the overall concept; a relative high sonic boom signature (comparable to that of the Concorde) and a marginally negative thrust drag balance. Since parasitic drag from the fin was not included in the initial control volume analysis for the inverse design and also the real system has a greater ratio of wetted area to frontal area than originally assumed in the control volume optimisation, a future design should account for both effects.

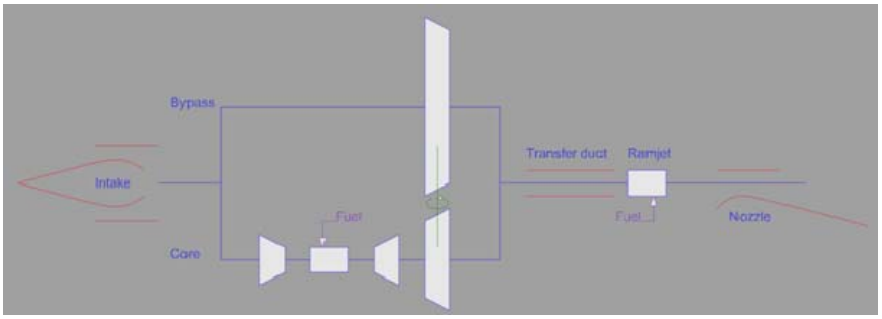


**Figure 41: M3T engine flow schematic**

For the Mach 6 vehicle, the departure configuration is based on the HYCAT 1A configuration designed by Lockheed in the late 70's. Parameters of different physical disciplines e.g. propulsion, structure and mission were provided by different ATLLAS partners and serve as input for the MDO process. Thus a complete mass budget, a propulsion table, mission database and geometry parameters are available. Within the ATLLAS project several MDO runs were performed whereas the last one includes all targeted disciplines. During the MDO process, for each configuration the following mass and structure analysis is performed:

i. determination of preliminary structural layout and structural masses;
ii. determination of maximum fuel mass;
iii. determination of a centre of gravity (COG) span depending on different fuel levels.

To reach these objectives the numerical method of finite elements (FEM) is used to increase result accuracy. During the ATLLAS project an initial FEM model was designed composed of shell and bar elements describing the basic structural layout. Furthermore element properties, material types and material groups were given to the model. Used materials are steel, aluminium, aluminium alloy and an aluminium-beryllium-alloy also known as Lockalloy or AlBeMet which is almost as stiff as steel but has a significantly lower density. The replacement of some parts of the fuselage cover by AlBeMet seriously improved the dynamic behaviour of the configuration. However the high costs of AlBeMet have to be mentioned which are not considered in the MDO process at the moment. The material properties were transformed to the MDO material library which was slightly extended by the C/C-SiC material for leading edges claimed by high temperatures. The material properties for C/C-SiC were provided by ATLLAS WP-3 and integrated to the structural process as anisotropic material. The arrangement of the several material groups is shown in Figure 42.

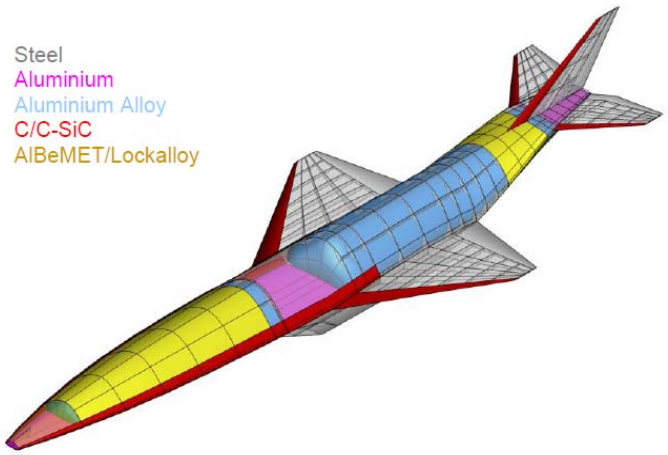


**Figure 42: FEM Materials group.**

The results of the final MDO are presented in Figure 43. The run was stopped after 520 iterations since based on former MDO runs no major improvements were expected beyond that. The time needed for a single iteration was between 3 and 5 hours while the overall time for one entire MDO process was 3 months.

At first the changes of the configuration seem less then expected. The most obvious changes are the enlarging of the forebody, modifications of the wing and the horizontal stabilizer geometry as well as the nozzle design. There are also changes in the wing span width and wing vertical position given by the forebody leading edge z-component. Additionally the double-trapezium wing profile is strongly modified by moving the middle edges to each other. It seems the profile shape is tending to a diamond profile. Additionally there are some marginal displacements of the nose and the wing tip position as well as a very small increase in tail thickness. During the MDO process for every configuration, a database is created containing more then 300 parameters to describe aerodynamic, propulsion, structural and mission performance. During the optimization the objective function is increased from 0.97 to 1.38. This means starting from a slightly penalized configuration the final configurations objective function is improved by almost 40%. The relative huge improvement is explained by the modification of the structural design and a better begin of cruise to end of cruise mass ratio and also by an improved interaction between propulsion system and aerodynamic. However, a final cruise range of 4250 km is still low. Respecting the considered reserve fuel and taking also the initial mission profile into account the maximum mission range of the final configuration can be roughly estimated to about 7400 km compared to 6200 km of the initial configuration. The estimation is based on 1200 km for the accelerated climb, 1500 km for the descent and 500 km due to reserve fuel. However the HYCAT 1A estimations of 9000 km mission range can not be confirmed within this work.

Manoeuvre loads are considered for the structural analysis of the Mach 6 configurations. The first case is the symmetric pull-up, which represents also a gust-load. For the fuselage, a similar bending-case also occurs at touch-down. The load-factor at limit-load is assumed to be $n_z$=2.7. A second test combines the simultaneous loading of the stabilizer and tail fin (Figure 44). It is concluded that some additional local resizing might be needed. Further optimization, includes shifting mass from stiffeners to the surrounding skin to improve bending stiffness

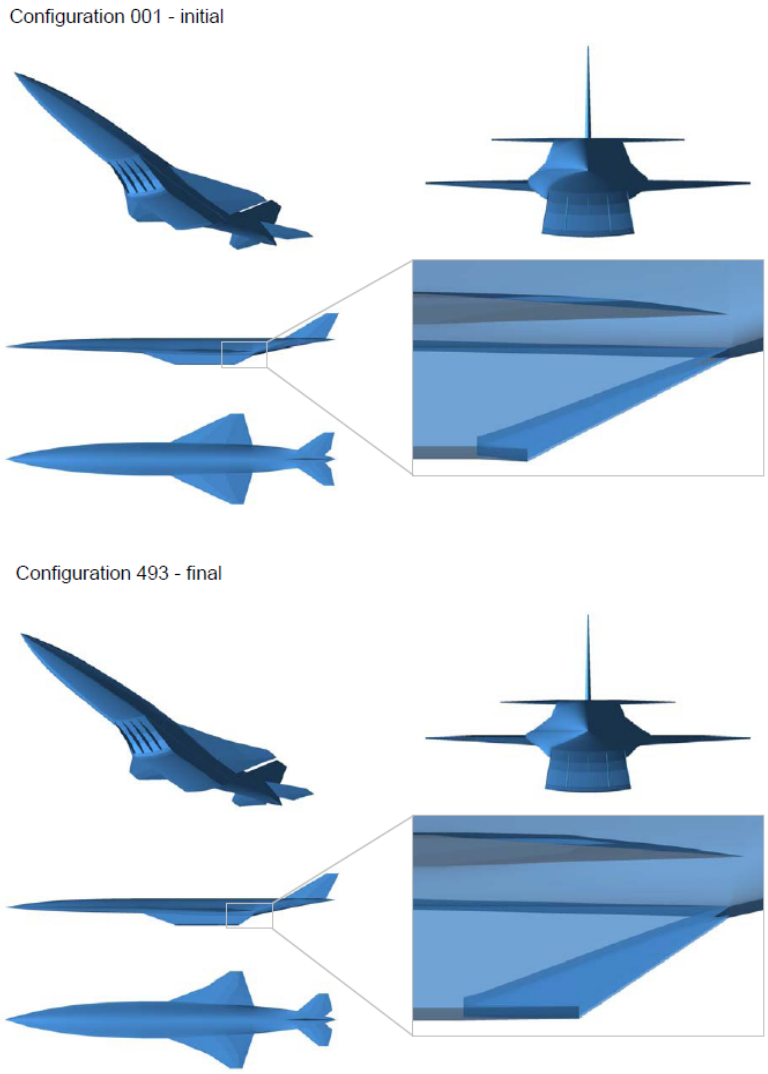


**Figure 43: MDO current results: top: initial configuration, bottom: current configuration.**

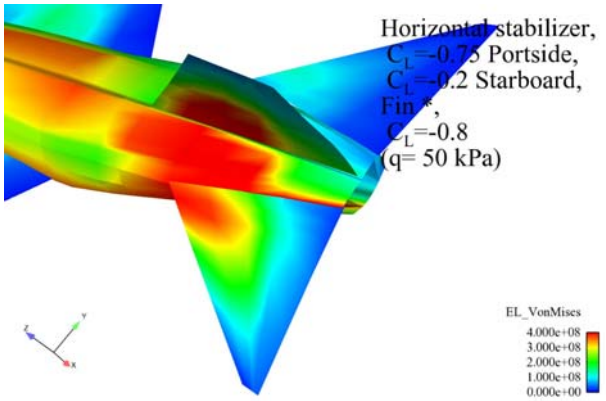


**Figure 44: Stress-levels (von Mises) for a tail load case.**

Further, a sensitivity analysis to the outer shape deformation has been carried out. The results show the most influent parameter being the first ramp deformation, with a visible effect on the intake aerodynamics as shown in Figure 45.

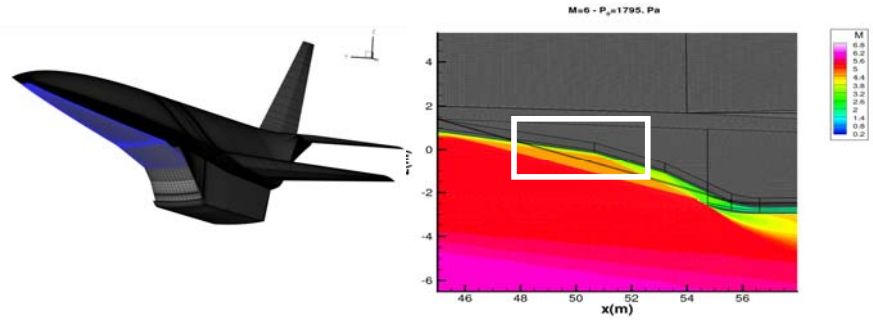


**Figure 45: Sensitivity to forebody and ramp deformations for the Mach 6 configuration.**

Due to the present results for future MDO processes the structural part of the MDO tool is one major point of interest. Indeed, here a fairly large and heavy aircraft has been analysed, which means that structural issues have a significant influence on the aircraft design (the structural weight is estimated to be about 30% of the gross-weight, whereas for instance the payload is about 6%). Large parts of the structure have their dimensions governed by stiffness requirements. The structural material chosen must of cause be compatible with the expected temperatures for the structure, which depending on insulation and cooling may still be high. The stress-levels calculated over significant regions of the tail and rear fuselage requires further attention. The specific strength at room temperature of titanium and extreme high strength steels are about 50% higher than that of aluminium. Not only the temperature limit for aluminium is much lower than steel and titanium, but its strength is also more drastically reduced at elevated temperatures. The choice made here to let stainless steel be representative for the specific stiffness seems appropriate during conceptual design and possibly during early stages of preliminary design. Beyond that a more detailed selection must be made due to different temperatures, thermal stress-levels and since dominant structural regions are designed for stiffness, but many parts will be designed under stress-constraints. The analysis performed here has indicated that a feasible design is likely to exist but a number of additional studies are needed (as for example the nozzle ramp displayed in Figure 46. More detailed design and analysis of a set of selected parts in different regions of the aircraft would improve data for the structural weight analysis. Such detailed design-work however requires more data about expected temperatures (cooling and insulation requirements). Within a more local design- and analysis study more attention can be given to design solutions to cope with thermal stresses and also maintenance issues.

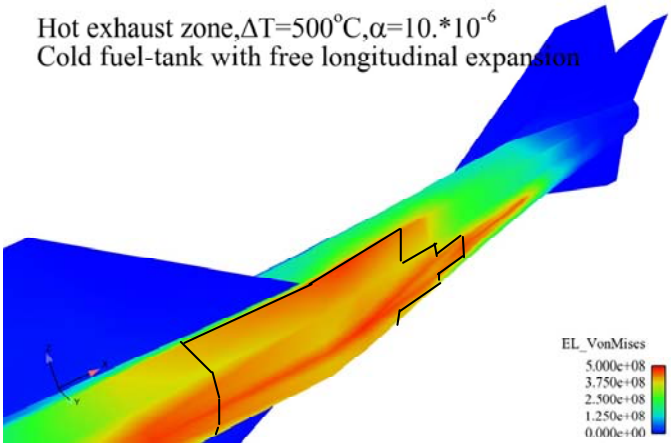


**Figure 46: Stress-levels for a temperature-case of □T = 500°C.**

The design of non-integral tanks for the Mach 6 reference configuration has been done using a new Multi-lobe Tank Extension Module, developed by DLR. This extension accounts for load factors, heat fluxes and fuel mass. The software is successfully used for a fast design of tanks that fit quite well inside the aircraft geometry.

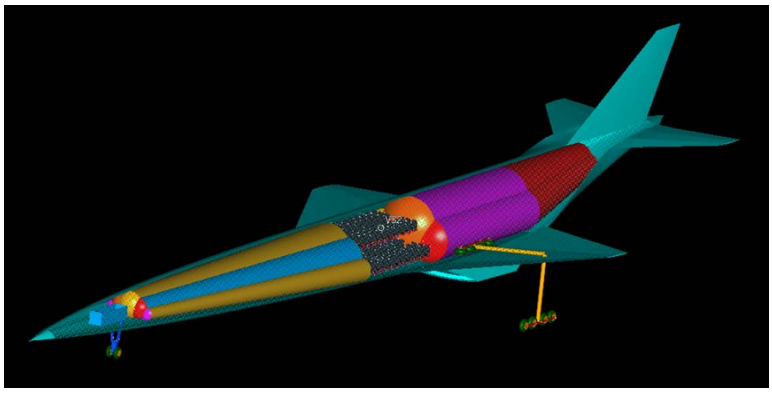

**Figure 47: Automatic multi-lobe tank generation with aircraft fuselage constraint.**

During ATLLAS, there have been advances in the area of Sonic Boom prediction. The work has demonstrated that gravity is directly responsible for the attenuation of sonic booms as they propagate towards the ground, while the gradient in acoustic impedance has no effect on the wave strength. Therefore current sonic boom theory, although giving satisfactory matches with ground pressure measurements at low supersonic Mach numbers may be inconsistent at high altitude high flight Mach numbers. More specifically, gravity is omitted from the acoustic propagation equations and artificial acoustic impedance effects are erroneously introduced. Since Whitham's theory for bow shock strength has been compared with a Method Of Characteristics (MOC) calculation in a uniform atmosphere (without gravity) and found to be very accurate, the theory has been extended to include the effect of gravity and ambient temperature and the results are in near perfect agreement with the numerical MOC solution for the same case. Finally the method has been also applied to predict signatures of the Northrop-Grumman Shaped Sonic Boom Demonstrator (SSBD) showing good agreement with the experimental ground signature as is demonstrated in Figure 48.

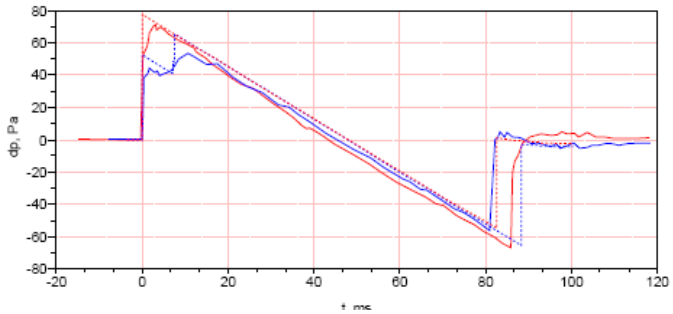


**Figure 48: Measured (solid) and MOC (dashed) signatures for the SSBD (blue) and F-5E (red), assuming a ground reflection factor of 1.8**

For the Mach 6 configuration, the atmospheric impact on sonic boom propagation has been quantified statistically by UPMC, based on numerical simulations and using meteorological data **[36]**. The atmospheric absorption and dispersion model has been integrated into an existing sonic boom code. Using CFD results provided by DLR and ONERA (Figure 49), the present study shows that the Mach 6 reference configuration produces a ground sonic boom with noise characteristics (shock overpressure and rise time) comparable to existing supersonic aircraft (like Concorde or military aircraft), but with a wider lateral extent which is due to a higher Mach speed and a higher altitude (Figure 49).

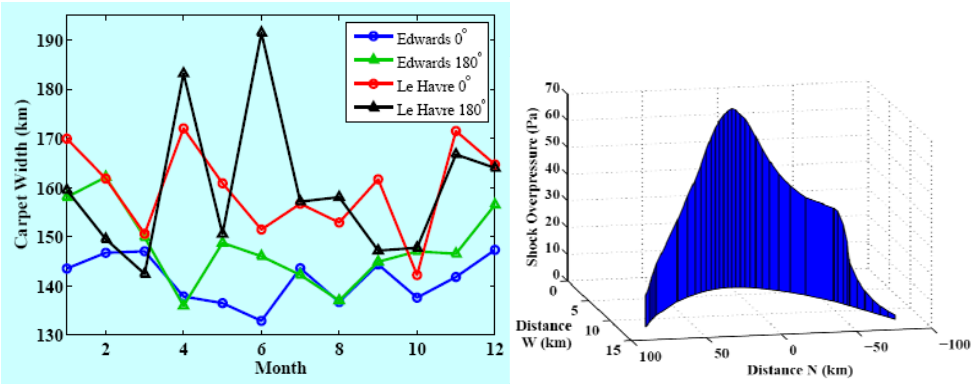


**Figure 49: Sonic boom prediction for the Mach 6 reference configuration. Left : Carpet width prediction for two locations (Edwards AFB, California, USA and Le Havre, France), two headings (West 0° and East 180°) and for the 1st of each month in year 1993. Right : One example of peak overpressure distribution.**

Further, as other authors had previously identified cruise conditions is by far the part of the mission least prone to cause sonic-boom annoyance. Analysis of the mission profile of a hypersonic transport aircraft remarkably similar to the HYCAT 1A and measured sonic boom data in a wind tunnel show that during descent the ground overpressure reached is two fold the cruise overpressure and during climb, even a four fold overpressure is reached. As the climb and descent phase of a mission are the legs most likely to pass over land, such very critical finding motivate to look for other type of measures to mitigate sonic boom like flow manipulation via magneto-hydrodynamic effects; via energy deposition (aero-jet or plasma spikes) or applying physical spikes. While none of them have had an important impact on the peak level of the overpressure, they affect the time-rise needed to reach the maximum. Here resides the potential of such measures since the time-rise is the primary source for the human-annoyance produced by sonic-boom. The study carried out for the Mach 6 vehicle shows that using energy deposition the time rise could be extended from 1ms to 30ms (!), but this comes at the cost of 100 MW which need to be deposited into the flow.

However, another application of energy deposition is the potential substitution of mechanical actuator

devices like ailerons, rudders, flaps, etc. (Figure 50). Indeed, a 0.56 MW/m thermal deposition is able to cause the same force as a 5deg mechanical flap deflection but requires less total power (i.e. thermal and finite thickness drag power combined) than the 5deg mechanical flap deflection (in terms of finite thickness drag power). Further, energy deposition could be used to substantially change the location of the centre of pressure, depending on the position of the energy deposition.

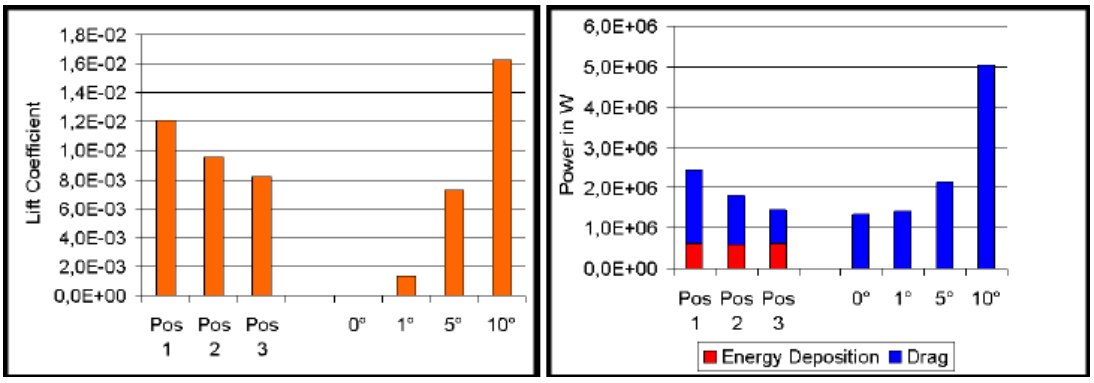


**Figure 50: Comparison of produced lift and required power for energy deposition and mechanical deflection.**

A logical follow-up of the study should now set up a more detailed materials requirement with respect to the vehicles thermal environment. Evolving from a more comprehensive study, the effects of the thermo-mechanics loads on vehicle aero-elasticity and structure dynamics can now be considered. From a pure thermal environment analysis, the materials investigated within ATLLAS satisfied both vehicles needs.

Further, for the ATLLAS Mach 3 vehicle, a power cycle employing cryogenic methane fuel has been developed to fulfil three roles within the vehicle: (i) provide cabin cooling from heat transfer through the external skin and internal air transfer duct; (ii) pre-condition the cabin ventilation air taken from the nose mounted intakes; and (iii) provide a source of auxiliary shaft power during cruise. Once the fuel has been used within the cycle, it is available for combustion, within the engines. Undertaking a typical flight over the design range (5,000Nm/9260km), 12t of methane fuel are required for the Mach 3 vehicle. The cabin insulation strategy has been carefully developed to ensure minimum weight of the insulation system, compatibility with the power cycle, and to retain the internal wall temperatures at 30deg C for thermal comfort. The preferred cabin wall is shown in *Figure 51*.

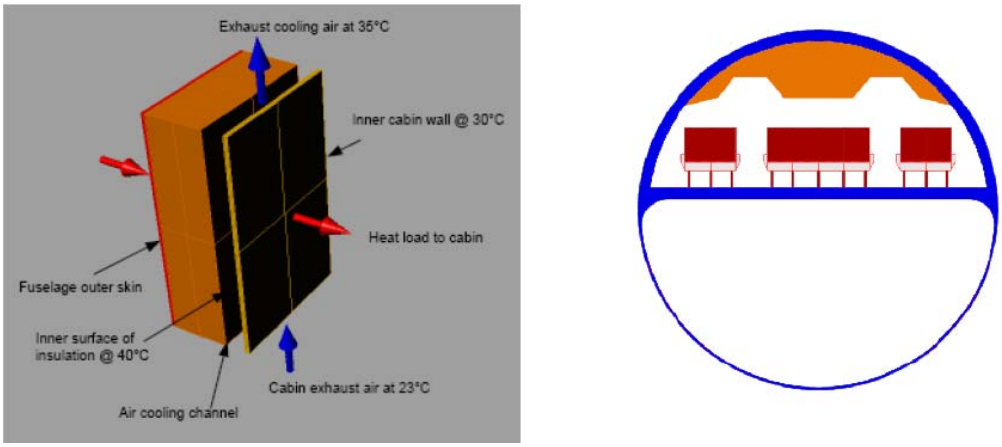


**Figure 51: Mach 3 vehicle cabin cross section and proposed wall make-up. Fuselage outer skin and structural zone (red), inner insulation zone, air gap, for cabin return air and inner skin.**

For the Mach 6 vehicle, fuelled by cryogenic hydrogen, it is observed that the latter provides nearly

10MW of latent heat sink capability in cruise. Environmental heat loads have been evaluated and an active cooling system is proposed for the cabin skin and a passive system for the fuel tanks. Even with modest amounts of insulation, cooling requirements remain small compared to the cooling availability in the fuel. Furthermore, bleed air is available at nearly 2bar, eliminating the need of additional compression and therefore with a helium loop operating over a relatively modest compression ratio, large amounts of power are available.
It is quite clear a lot of technologies need to be brought to a higher technology readiness level before one can even envisage kicking-off the manufacturing and operation of these types of vehicles. However, it is important that first the know-how and experience is put in place to assess whether or not any sort of high-speed concept has the required cruise performance. The study has shown that a cruise efficiency above three, i.e. L/D ratio times the propulsion efficiency, is recommendable for a long-haul cruiser. This can be achieved with the newly designed Mach 3 vehicle M3T (see Figure 6) which is also well above the Concorde's figure of merit. The Mach 6 vehicle is however rather disappointing even after a dedicated optimization process which brought it up with 10 to 20%. This doesn't mean a Mach 6 is basically not conceivable, but indicates rather that a 'classical' design as proposed by Lockheed is not recommendable. A different architectural design or an improved engine design, including intake and nozzle, is needed to make it attractive. As this perspective not out of scope, the Mach 5 A2 vehicle conceived during the LAPCAT project can achieve this critical cruise efficiency. The better performance for the latter is mainly due to a well designed engine concept.

## 5.4 Lightweight Airframe Materials for Sustained High-Speed Flight

High-speed aircraft are exposed to high thermal and mechanical loads. Especially the nose structure, wing leading edges, air intakes etc. reaches temperatures which require special heat resistant materials, structural concepts and optional cooling devices. As the requested aerodynamic performance for an aircraft focuses on a high aerodynamic lift to drag ratio requiring sharp leading edges and rather thin wing or stabilizer structures. The utilization and implementation of both of these requirements demands a detailed investigation of lightweight airframe materials including material design, coatings and determination of basic material properties withstanding high temperature requirements (Figure 52). This includes various tests on material samples to determine temperature stability, chemical resistance to the expected operational environment, mechanical stability and required additional physical properties. Three general classes of material investigation are considered: metallic hollow-sphere packings, Ultra High Temperature Ceramics (UHTC) and Ceramic Matrix Composites (CMC). Each of these is addressed below.

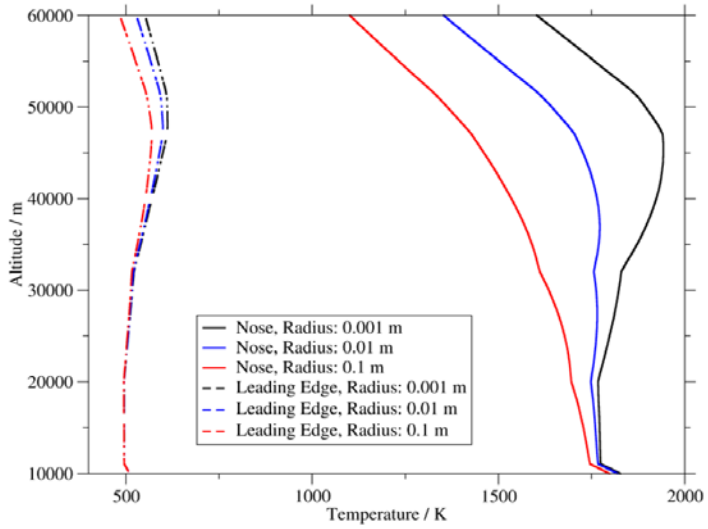


**Figure 52: Radiation equilibrium wall temperature at stagnation point, Mach 6, ε = 0.85, Λ = 65°.**

Various methods fabricating cellular solids, mostly foams have been investigated in the past. Most effort has been spent in the field of aluminium foaming processes. An entirely different concept to manufacture cellular solids is the approach via hollow spheres. Employing the hollow sphere technology, structures can be designed virtually to application needs. In contrast to classical foaming processes, there are no restrictions with regard to material selection (melt viscosity and stability). The powder metallurgical approach is applicable to any metal or even high performance alloys. The hollow sphere technology allows high degrees of porosities, reproducible properties and fair process control, structural regularity, excellent noise absorption and low weight.

The principal feasibility of metal hollow sphere based components for high-speed transport vehicle and propulsion systems are evaluated by ONERA on an engineering test sample level. The fabrication techniques for hollow sphere structures are adapted to the application requirements with regards to materials, densities and thermal properties [37]. In parallel, fabrication technologies for panels with hollow sphere cores are developed (Figure 53). This includes screening of suitable joining techniques (brazing, diffusion bonding) and relevant test methods thereof. Establishing suitable joining techniques for hollow sphere structures is a crucial step to supply components in sizes relevant for the envisaged application. A second axis aims at determining the mechanical and acoustic absorption properties of lightweight high strength structural panels for high temperature structures in nickel based microsphere panels.

In parallel a FE-based model is developed to characterise the mechanical behaviour under compression of hollow spheres packings (Figure 53). Accent is put on the influence of the architecture of the packing on its mechanical response. Calculations are conducted on infinite simple cubic (SC-), body centred cubic (BCC-) and face centred cubic (FCC-) packings by applying planar, uni-axial compressive loads [38]. It turned out that the behaviour of HSPs is mainly governed by the localised plasticity in the neighbourhood of meniscus ends for small strain levels; for higher strain levels, buckling of hollow spheres and self-contact between spheres occurred. Furthermore, the influence of the geometry and type of a HSP has been analysed. Like for other cellular materials, the effective mechanical behaviour of HSPs strongly depends on their compactness as well as on their relative density. For instance, the moduli increase with the compactness of the packings, which indicates that they are highest for FCC-like and lowest for SC-like packings. In order to estimate the sensitivity of the effective material behaviour of the packings, a calculus of variations for the constitutive material's behaviour is performed. It constituted, that a pure plastic behaviour for the packings does not exist, even for smaller strain levels causing a local plastic

contribution. Additionally, investigations on the effect of defects like e.g. a dispersion of the geometrical packing parameters and varying the solicitation rate were performed including an elasto-viscoplastic behaviour for the constitutive material.

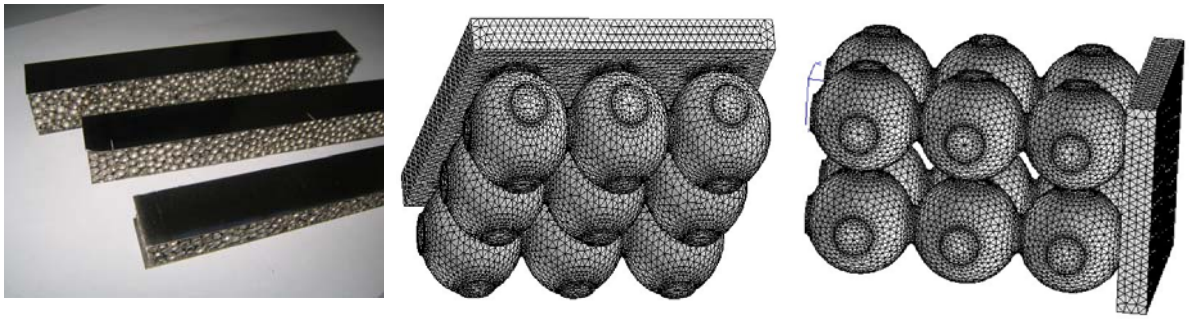

**Figure 53: Sandwich panels with a HSP core for structural testing and its mechanical modelling for its compressive behaviour. Left: 6x6x2 hollow spheres with t=0.56mm; right: 4x4x6 hollow spheres with t=0.56mm**

The interest in UHTCs has grown in the past years, especially in the US and in Italy. However, their application in aerospace is limited and demands for further exploration. Just two experiments under real flight conditions were undertaken with the Sharp Hypersonic Aero-thermodynamic Research Probe-Ballistic experiments 1 and 2 (SHARP-B1, 1997, and SHARP-B2, 2000). Oxide materials are, at best, intrinsically resistant to oxidation. The manufacturing and investigation of ultra high temperature ceramics within the project are based on a mixture between transition metals, borides and carbides. The interest of such associations is to promote the formation of dense refractory oxides like $ZrO_2$ and $HfO_2$. The most suitable way to produce sharp edges is to manufacture monolithic parts using hot pressure sintering of an appropriate mixture of powders. Monolithic UHTC inserts could be also applied in composite structures. Another challenge to succeed in this field is to achieve a sufficient level of toughness to overcome the brittleness of ceramic materials.

The work conducted by ONERA further developed the hot pressing sintering for three selected material compositions. In order to reduce contamination and to obtain the purest compounds possible, the attrition process and times was improved. Dimensions of the manufacturable flat samples could be enlarged up to 68x68 mm². Additionally discs and parallelepipeds were machined. In order to prove feasibility, very thin structures (thickness 1.9 mm) with minimal nose tips (radius app. 0.15 mm) are manufactured (Figure 54). Specific samples are being manufactured to investigate thermal and chemical characteristics at the arc-jet testing facility L2K of DLR Cologne [39].

**Figure 54: UHTC air intake prototype (40x40x1.9mm3); arc jet sample Ø 26,5; thermal and chemical tests t the L2K facility of DLR.**

Mechanical investigations determined the hardness indicating high values close to tungsten carbide. Measurements of toughness revealed that this parameter is very limited like common silicon carbide. Three point flexural tests showed that the flexural stress were equal or higher with increasing temperature, similarly for the flexural strain but nevertheless a significant decrease of modulus. Additionally, the thermal expansion of UHTC material was determined for a range between 20 °C and 1250 °C at argon atmosphere.

The application of ceramic matrix composites for leading edges and air intakes are investigated by three DLR institutes (BK, WF, AS-WK) and FOI. Its application demands a densified material with high thermal conductivity and emissivity. Hence, the fibre orientation and matrix composition should be well adapted along with adequate coating procedures to provide optimised surface properties. Chosen CMCs

are C/C-SiC and OXIPOL, manufactured by DLR-BK, and WHIPOX by DLR-WF. Structural tests at DLR-AS-WK focus on a generic but representative design and manufacturing of a sharp leading edge including an interface to an adjacent structure. This sample needed to consider structural and system aspects like joining technique to a cold substructure and sensor integration. One major objective is to fit this structural sample within an arc jet test facility for a test within high-speed gas flow conditions.

Though the application of C/C-SiC or C/SiC for re-entry vehicles is state of the art due to the material's excellent thermo-mechanical behaviour, their service-life is low in comparison to the requirements for hypersonic aircrafts, e.g. extended 25,000-cycle service-life. C/C-SiC and WHIPOX were already tested during SHEFEX as thermal protection system of a hypersonic experiment. In general, oxide ceramic based materials offer a wider framework to tune their material characteristics to the envisaged application. As WHIPOX has low emissivity characteristics, a dark coating based on spinel phase with high emissivity is developed and tested in the arc jet testing facility L3K. Different fibre orientations are investigated (1D = $\pm$3°, $\pm$15° and 0|90°) to determine Young's modulus, interlaminar shear strength, bending strength and notching sensitivity [43] below. Also creep tests are performed at 1100 °C. Unfortunately, for the non-oxide CMCs the measurements are limited to room temperature with respect to creep/fatigue. For optical characterisation, FOI measured the reflectance and transmittance at room and high temperatures [41] below.

Finally, a leading edge model is manufactured in order to study the thermal and chemical characteristics of a representative leading edge in an arc jet heated flow. Since the sharpness of the leading edges is limited by the material's manufacturing process, a leading edge nose radius of 2 mm was defined as baseline for all materials (C/C-SiC, OXIPOL, WHIPOX). Since there is no specific limitation for C/C-SiC, a very sharp leading edge is manufactured to study directly the effect of sharpness (Figure 55). FOI provided a numerical simulation for the comparison of the experimental tests. The structural part is modelled using a FE method. For the fluid-structure analysis, a modal representation of the structure is investigated in order to provide the model reduction needed to manage a large scale coupled analysis (Figure 56).

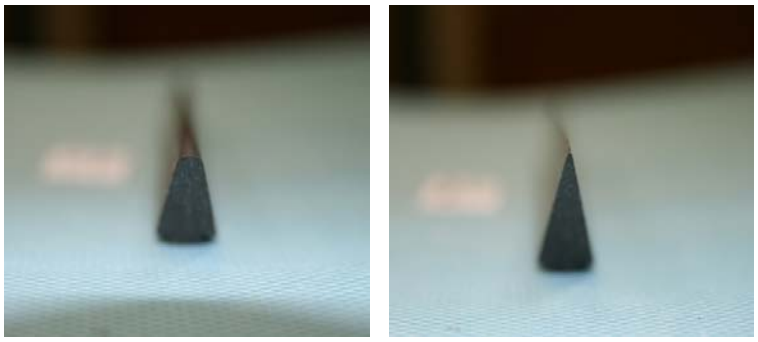

**Figure 55: C/C-SiC leading edge with radius 2 mm (left) and sharp-edged (right)**

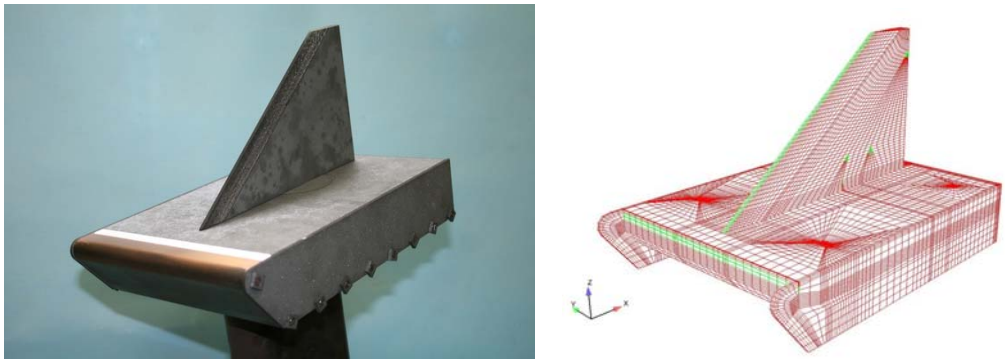

**Figure 56: Leading edge model and its mesh for numerical simulation at FOI**

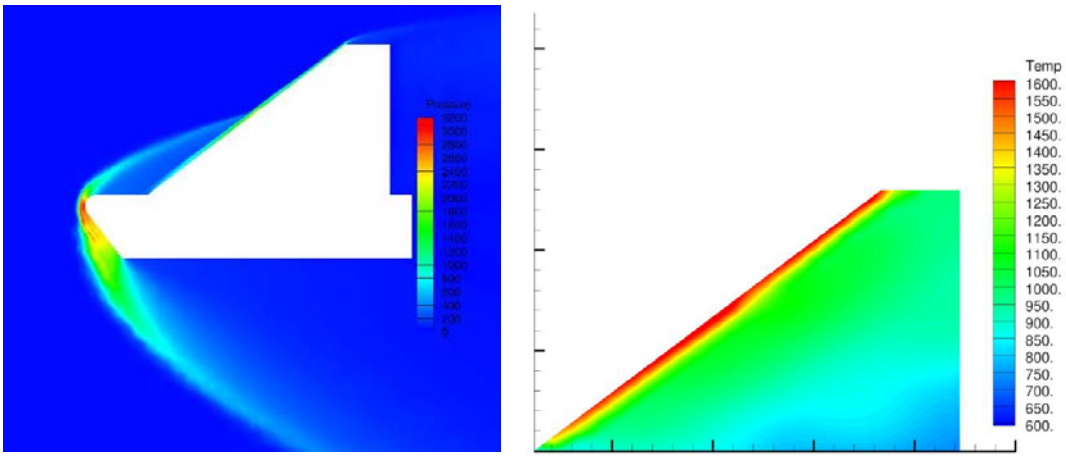


**Figure 57: Simulated pressure contour along the symmetry plane (left picture) and simulated wing temperature distribution for OXIPOL (in Kelvin) at α = 5°and δ = 0° (right picture).**

The overall outcome of the numerical validation is fairly good, despite some simplifications made, and the profile temperature dependence on the direction of the flow is well depicted by the simulation model. The surface temperature near the location of the bow shock is affected by the different angle of attack. The central part of the wing is relatively far away from the cover plate where the bow shock is weak for the considered angles of attack. Figure 57 shows the pressure contour along the symmetry plane of the model for $\alpha = 5°$*and* $\delta = 0°$.

## 5.5 Increased Engine Thermal Efficiency: Novel Cooling Concepts

The focus here is on increasing the combustion temperature by using lightweight materials and novel cooling concepts of the combustion chamber liners. Different fuels are investigated, which are required for the studied aircraft concepts: kerosene and cryogenic fuels. Both high-pressure (aerojets) and ramjets based combustion chambers are used as a test bed to deal with realistic operational gas flow conditions. Different cooling techniques are investigated under a wide parameter range, i.e. film, effusion, transpiration and regenerative cooling. The thermal performance is investigated and a comparison to the simulation results is performed. The cooling techniques are evaluated with respect to overall engine performance (e.g. specific impulse and thrust), and the production of NOx emissions. Detailed information is reported in [40].

Based on experience obtained from a transpiration cooled ceramic combustion chamber for rocket engines, it seems to be possible to use a similar cooling technology for high speed airbreathing engines.

With less air used for cooling, higher combustor liner temperatures are obtained in the order of 1500°C. With CMC turbine vanes able to cope with these higher combustor exit temperatures, the overall thermal efficiency increases.
Main focus is oxide ceramic based materials for combustion chambers. Besides their high temperature stability, the specific weight and their possibly oxidising stability offer a wide range of possible applications. In addition to the very high gas temperatures and pressure within the engine (combustion chamber, expansion nozzle etc.) the chemistry and gas composition (O2, H2O, CO2, H2, N, CH...) affects the structure of the material. Within this area, oxide based CMCs combined with active cooling are promising candidate materials.
The principle of this cooling technique is to create a gas flow from the cold substructure to the hot surface directly through the porous material itself. Thus, in addition to the direct cooling effect, the boundary layer at the surface is influenced reducing the convectional heat transfer and chemical reactions. In contrast to the above mentioned current development of the C/C based transpiration cooled burning chamber for a H2/O2 rocket engine with fuel rich burning conditions, engines for high-speed aircrafts are designed for optimised efficiency resulting in a lean, oxidiser rich burning condition. Thus, oxidation-resistant materials are of prime concern.

Regenerative cooling (PTAH-SOCAR existing cooled structure concept for example), transpiration cooling (for example through DLR porous materials) and film injection cooling are investigated. State of the art and existing models are used to define the configurations to be tested [44] below.

The design of the film cooling experiment is finalized and the first part of the experiments is finalized [45] below. The operating points are chosen in order to allow for a comparison of the different cooling techniques. Two film applicators have been designed and built in order to cover the envisaged operating envelope of the experiments. To improve the measurement accuracy by getting a direct heat flux measurement within the TUM facility, DLR Cologne develops a heat flux sensor concept (Figure 58). This is congruent with the constraints and requirements coming from the planned operational domain as well as from the test specimen. The probe is manufactured and calibrated at DLR Cologne, before it is tested at moderate heat loads in the oxidator rich combustion chamber at TUM. The development is aided by calculations of the transient and stationary temperature field of the sensor with ANSYS and by calculations of the heat fluxes during the calibration process of the sensor following the system identification approach.

**Figure 58: DLR Cologne heat flux sensor**

Different CMC materials are fabricated by DLR-BK in Stuttgart which is used for transpiration cooling tests in the TUM facility (Figure 59) [42].

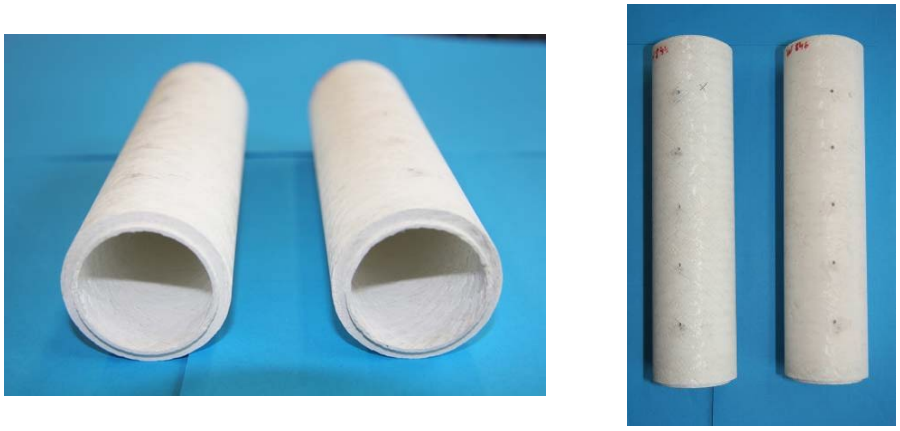

**Figure 59: WHIPOX liners manufactured by DLR for transpiration cooling tests at TUM**

Additionally Astrium designed two PTAH-SOCAR combustion chamber segments which are manufactured of CARBOTEX® material [46]. After the inner diameter of the liner has been braided, a spacer foam was applied in order to form the coolant passage before the outer diameter of the liner was manufactured. After the R-CVI process the hardware was checked in a CT scan as shown in Figure 60. The CMC liner is machined to the required dimensions (Figure 61) before the combustion chamber surface is coated via slurry siliconization and then machined to its final dimensions.

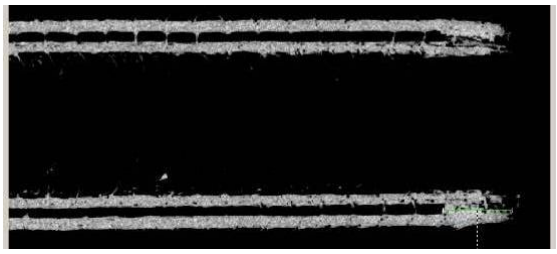

**Figure 60: PTAH-SOCAR CMC segment manufacturing process: CT scan after R.CVI process**

**Figure 61: PTAH-SOCAR CMC liner machined for joining with the microfibre shells**

Test results allowed characterizing the tested structures and headlined the possibilities and the limits of existing models, leading to enhance them afterwards. The axial distribution of the heat flux density as well

as the pressure drop in the cooling channels is recorded for the entire envisaged operating domain (Figure 62).

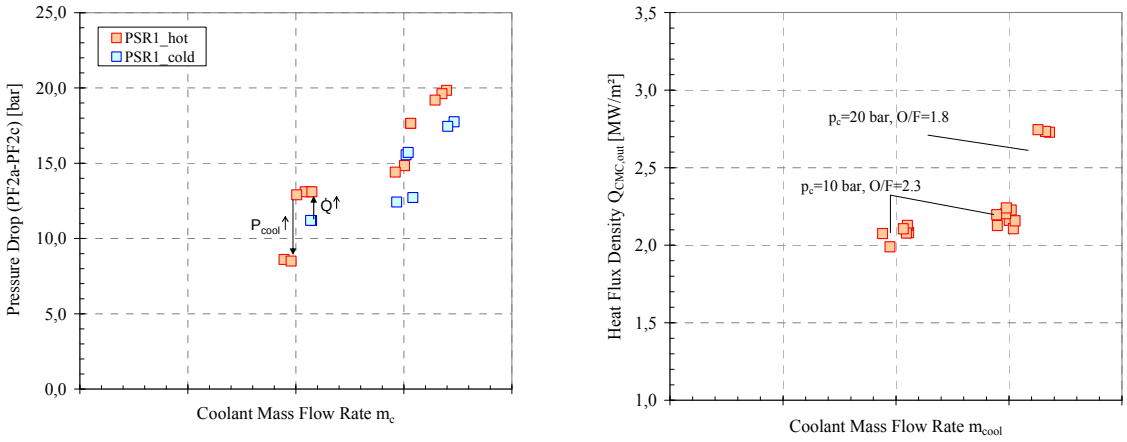


**Figure 62: Pressure Drop and Heat flux evolution for Carbotex$^{SI}$ PSR**

Despite the large effort on CMC materials for combustor, the behaviour of selected metallic materials are still of interest in a high-pressure oxidizing environment at high temperatures. After a material pre-selection by data / literature analysis was done, candidate materials for investigations are selected and a test plan for material property determination as well as material sample analysis was described. Physical property measurements (thermal conductivity, heat capacity, thermogravimetry under oxidative atmosphere) are performed. Different sets of samples were tested during an overall testing time of 300 s per sample (Figure 63).

**Figure 63: Inconel material samples during hot fire experiment and after test time of 300 s**

Post test analysis of several thermally loaded samples (visual, sample surface, oxide layer composition and thickness, microstructure, level of oxide layer formation / degradation / contamination, roughness, weight) are finished.
Also materials for dual mode ramjet combustors were investigated [47]. Several porous materials such as oxide/oxide materials (WHIPOX or OXIPOL), SiC-based material (C/C-Sic, SICTEX or CARBOTEX) and simple C/C are exposed to subsonic and supersonic (Ma=2) internal flow at total temperatures of up to

1450 K. With the use of infrared (IR) thermography and additional thermocouple instrumentation the transpiration cooling efficiency is investigated (Figure 64). The gas in the main-stream is an electrically heated air whilst as a coolant air and inert gases are used. The samples of CARBOTEX material in PTAH-SOCAR structure design were designed to be applied as a regeneratively cooled wall.

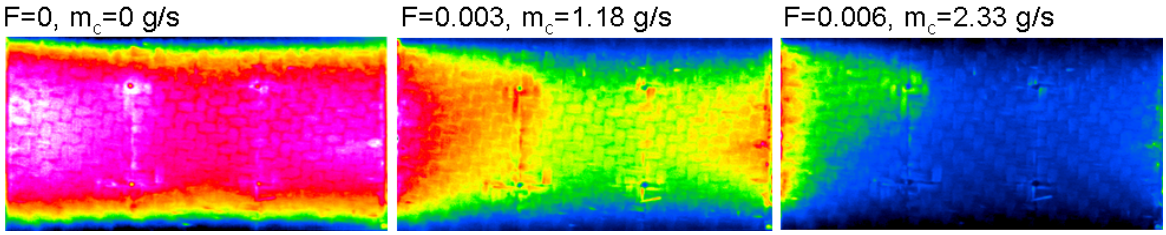


**Figure 64: Qualitative infrared-thermography images for 0/90-C/C sample with increasing blowing ratio F (main flow from left to right)**

Based on the vehicle performance and the outcome of the different cooling techniques and applicable materials, the design loop is closed by studying the performance of the engine concepts and evaluating the NOx emission. Therefore, FOI has established a basis for chemical equilibrium and chemical kinetics studies, including some different reaction sets for $H_2$ combustion. Initial results show relatively high NOx emission levels for the M6 concept.

## 5.6 Material-Aero-Thermal Interaction Modelling

In parallel to the above described experimental investigations, the modelling aims at enhancing and testing the coupled aero-thermal phenomena in the ATLLAS type high speed flows. The phenomena studied are shown in Figure 65 and described in more detail in [48] below, are addressed with different approaches (CFD, semi-empirical, commercial or in-house codes …). Comparisons have been performed with analytical and experimental results from literature, and some numerical cross-checks are planned.

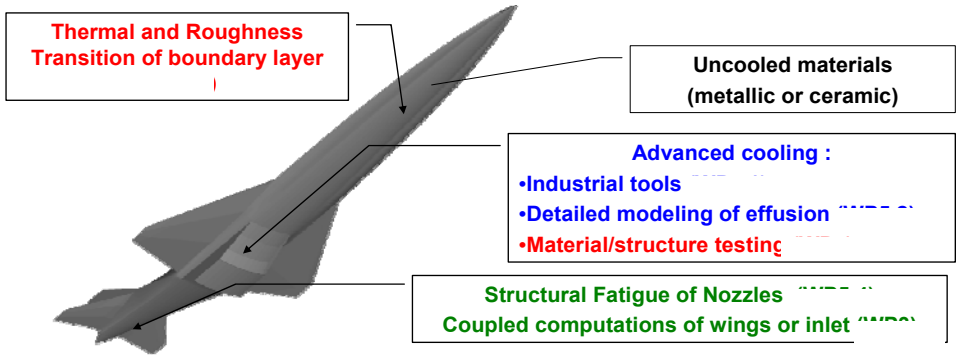


**Figure 65: Investigation of coupled phenomena on Mach 6 generic aircraft**

The emphasis in the area of loads definition is to develop and verify models to predict the combined effect of aero-thermal and material interaction on several lightweight high-temperature resistant materials. This is accomplished by integrating existing aerodynamic, heat-transfer, and structural codes. The results are then calibrated and verified with simplified experiments. The generic high speed aircraft is a support for the requirements of both the experimental work (TUM and ITLR high temperature flows with cooling techniques or advanced materials investigation) and coupled phenomenon computational tools.

ESTEC and MBDA focus on the modelling of multi-physics flow within porous media. On the basis of the commonly-stated computational plan, several porous medium and combustion test cases have been computed with different levels of refinement. As the test cases are completed, the software porous media flow-through model implementations are presently validated versus the different experimental campaigns.

The TUM combustion experiment was computed with different approaches. MBDA computed in 3D with CFD-ACE while ASTRIUM did some 2D with its empirically tuned code ROCFLAM (Figure 66). Comparison made on heat fluxes on the different segments of the water-cooled calibration chamber gives good agreement, except in the first segment, where mixing and ignition takes place.

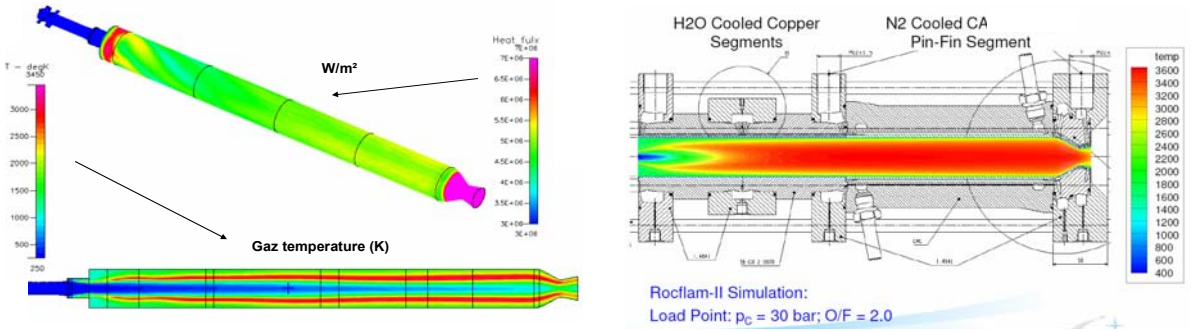


**Figure 66: NS computations of TUM experiment (left: 3D MBDA with CFD-ACE ; right : 2D ASTRIUM with ROCFLAM)**

For the heat transfer in porous media, a basic experiment was chosen in the published literature. The work of Provence University in Marseille consists of a porous medium (either glass or bronze), heated on two sides and fed with cold liquid pentane. The numerical sketch is given on Figure 67.

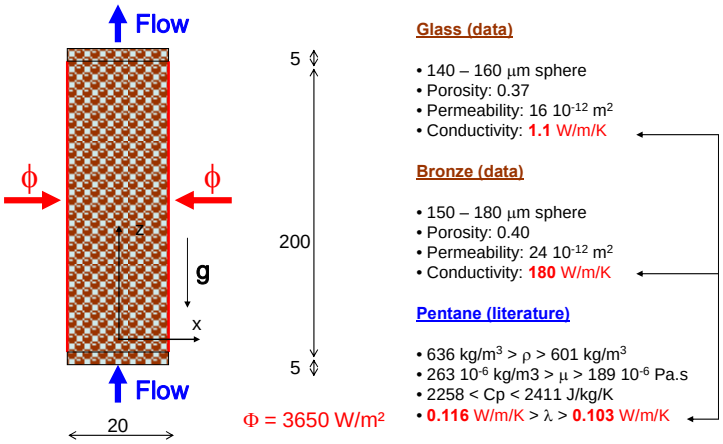


**Figure 67: Basic test case of heat transfer in porous media from Marseille laboratory (Rahli et alii)**

Different computations are performed by MBDA on the two experiments while varying the way of computation of the porous medium equivalent conductivity, from serial to parallel assumptions. The default formula used by CFD-ACE and the serial formulation give temperatures close to the measured ones.

The ITLR supersonic test case is the final check for the validation process done for air at three total temperatures: $T_{t,g}$ = 450 K, 600K and 1060 K [53],[54],[55],[49],[57] [58]. The wall temperature has been plotted versus the streamwise sample length for the lower value of $T_{t,g}$ = 450 K and the highest value of

1060 K (Figure 68). The thermocouple readings are shown as cross symbols in the plot. The numerical values have been extracted at the interface between the porous zone and the main-flow zone. The recovery temperature of the hot-gas is not reached in any data point of the plot, due to the non-adiabatic setup. A wall temperature profile was imposed down and upstream of the sample, obtained by a thermal analysis. The sensitivity of the temperature at the interface between the porous medium and the main flow is relatively high with respect to the thermal boundary conditions set at the side-walls of the sample.

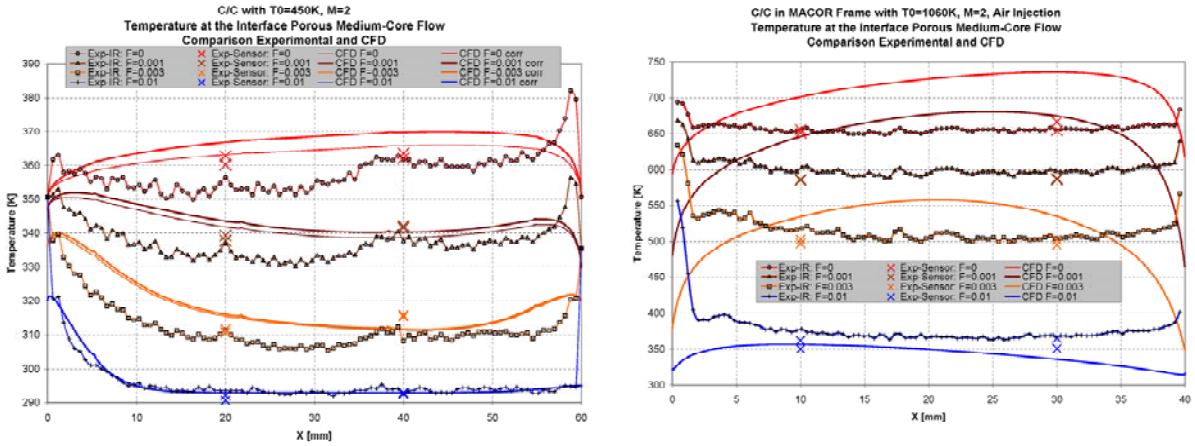


**Figure 68: Comparison between experimental and numerical results: temperature at the interface for different blowing ratios and core flow total temperatures: left: $T_{t,g}$ = 450 K; right $T_{t,g}$ = 1060 K.**

For $T_{t,g}$ = 450 K, the agreement between experimental and simulations is very good (Figure 68). For $T_{t,g}$ = 1060 K, the agreement between experimental and simulations is only good for the high blowing ratios. A discrepancy can be seen for the lower blowing ratio cases. This difference in computed and experimental interface temperatures increasing with freestream total temperatures was found to be due to thermal losses not taken into account in the CFD, i.e. radiation and translateral heat conduction. Based on a reduced heat balance model, the calculated extra heat losses are nearly 30% higher than the convective or the perpendicular conductive heat transfer for the test case at 1060K. Radiation is limited however and is only accountable for 10% of the additional heat losses. For higher blowing ratios, the agreement between the experimental data and the numerical temperature distribution is very good. The cooling effects, i.e. heat flux reduction and internal heat exchange, are dominating the thermal behaviour.
In Figure 69 the cooling efficiency is being plotted over the blowing ratio for $T_{t,g}$ = 450 K, 600K and 1060 K both for the experimental and numerical values. The general trend of the cooling efficiency, i.e. the relative surface temperature reduction with respect to the no blowing case can be reproduced very well by the numerical model.

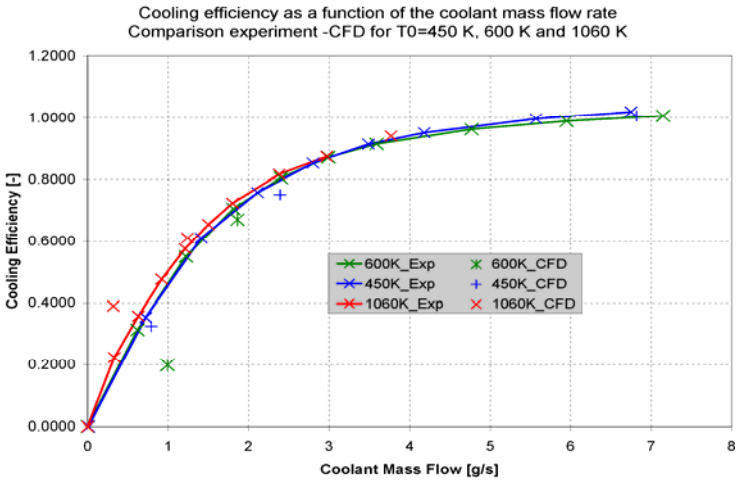


**Figure 69: Numerical and experimental cooling efficiency vs. blowing ratio for $T_{t,g}$ = 450 K, 600K and 1060 K.**

The final goal however is to use the hydrogen fuel rather than air as a coolant for the combustor walls. Therefore in a first step helium was used during experiments to get closer to the thermal capacities of hydrogen but yet avoiding interaction of combustion induced heat transfer. For the simulation, the extension towards hydrogen with and without combustion was performed to assess its global effect. In Figure 70, the density is plotted for the highest blowing ratio. Due to the helium transpiration, a shock wave is generated at the upstream side of the porous medium being reflected at the top wall.

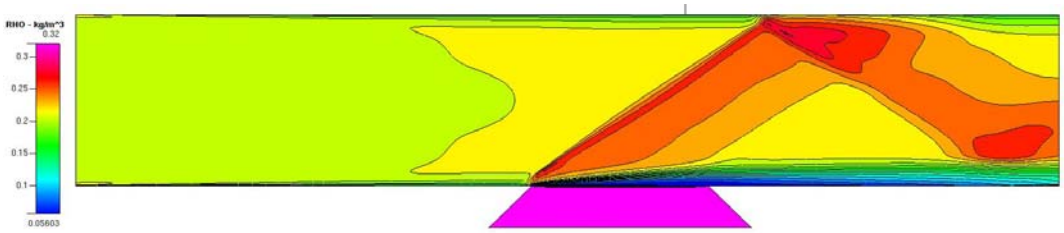

**Figure 70: Helium coolant injection: density contours.**

In Figure 71, the experimental results shows the cooling efficiency obtained with transpiration cooling with air (blue) and helium (green). The simulation results are added for the lowest, intermediate and highest mass flows of coolant. The results obtained for Helium are in very good agreement with the experimental results. Predictions of cooling efficiency obtained with hydrogen are represented in red. Due to the reduced mass flow, using the hydrogen fuel as transpiration coolant is of interest for high-speed engines. Plotting the cooling efficiency in function of a relative mass flow rate with respect to the heat capacities as shown in Figure 71, clearly demonstrates the similarity parameter to be used for design purposes.

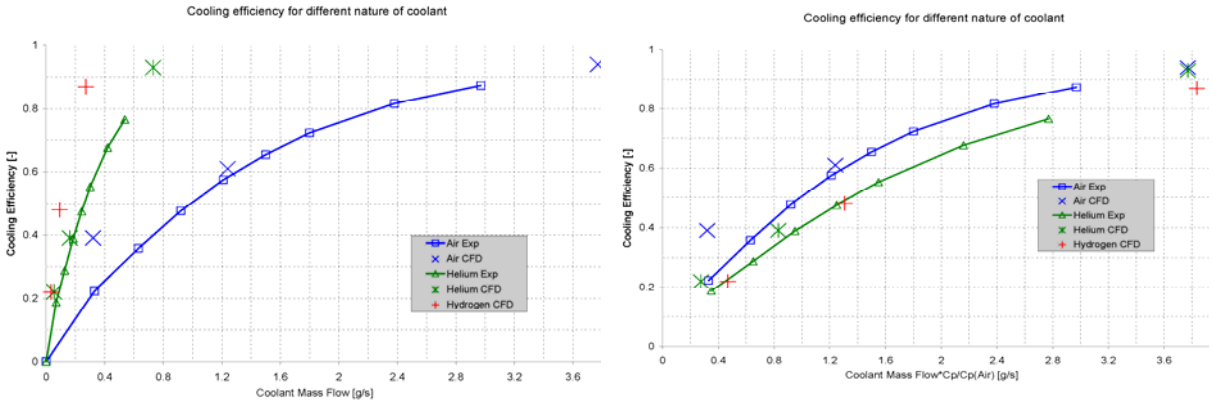


**Figure 71: Cooling efficiency as a function of coolant mass flow and coolant mass flow*$C_p$/ $C_p$(Air) for Air, Helium and Hydrogen.**

To examine how the hydrogen film reacts with the core flow, several combustion simulations have been performed where hydrogen is used as a coolant. An oblique shock induced by the transpiration cooling starts to become more prominent resulting in a higher core temperature above the porous sample (Figure 72). The location of the ignition can be identified by means of the OH-presence (Figure 73).

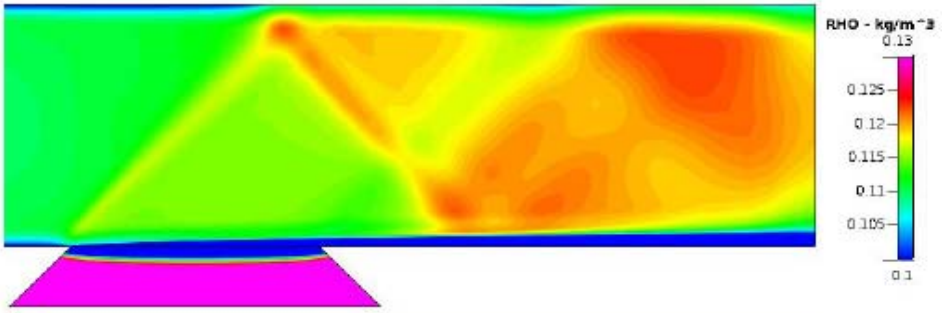


**Figure 72: Combustion ignition location related to reflected shock wave: case 6 (density contours).**

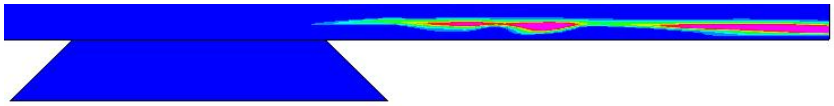

**Figure 73: Ignition location of H2 film by means of OH-contours.**

Whereas transpiration cooling clearly has a much better efficiency, due to the direct contact between the coolant and the solid wall to be cooled, this is less evident for effusion cooling. Detailed effusion cooling computations were performed at ONERA by means of an in-house CEDRE CFD tool on an experimental test case from Texas University. It entails a full geometry (10 half holes arranged in a staggered manner) with 2 blowing ratios (blowing ratio 0.25 and 0.65) and 2 main flow turbulence intensity levels (18% and 0.5%) After more deep investigation of the quasi periodic limits as well as the effect of refinement of the mesh, a new parametric study corresponding to an actual geometry tested at ITLR is made. The example of Figure 74 gives temperatures along the plate with an A310 (NS30) high temperature alloy extensively used by MBDA for hypersonic propulsion metallic structures. Agreement was good between experiments and computations.

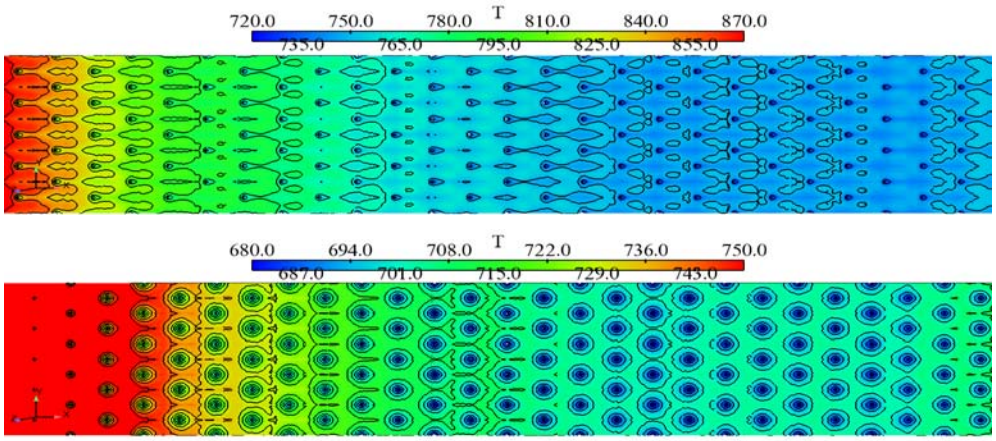


**Figure 74: Hot and cold temperature maps of the metallic multi-perforated plate in ITLR hot flow conditions**

A numeric aero-thermo-elastic analysis tool has been developed by FOI. It allows an accurate prediction of the coupling among the flow-field and structural components, highlighting the mutual interactions among heat transfer, aerodynamic loads and structural dynamic response. One of the main purposes of such investigation is the analysis of the structural integrity due to high temperatures and dynamic loads for the design of nozzles and thermal structures in high-speed flight applications. The proposed methodology is demonstrated on a typical panel in the nozzle part of the ATLLAS generic aircraft. This part of the aircraft is challenging, from an engineering point of view, as it is heavily loaded not only by local pressures and thermal loads but also by global forces acting on the rear part the aircraft. The panel is heavily heated on one side by the hot exhaust gases and at the same time cooled on the back side by the liquid hydrogen tanks inside the aircraft. This result in large temperature gradients through the thickness and creates potential problems with large thermal stresses and strains in the structure, that need to be accounted for in the thermal design. A coupled simulation performed for Mach 6 conditions of aerodynamic pressure, is shown in Figure 75. Different combinations of cooled or non-cooled lightweight sandwich structures with and without load carrying capability have been investigated.

The aero-thermal heat loads for intakes are somehow more difficult to assess than nozzles as they are prone to transition. Due to the compressibility and cold wall temperatures, the transition process is delayed and experiences a larger extent than what one would expect from incompressible theory. However, there is hardly any information available about the combined effects of compressibility, hot walls and roughness. Therefore a combined experimental and numerical effort is carried out to gain a thorough understanding of the physical processes taking place.

As an example, Figure 76 illustrates a breakdown process towards a turbulent spot induced by a roughness. Depending on the roughness height, the induced hairpin vortices can degenerate or amplify resulting finally into a classical breakdown process. The presence of turbulence is confirmed by the familiar hairpin structures that are to be found in the centre of the spot. This process can somehow be confirmed by experiments though the DNS results allows one to better understand the sequential physical processes taking place. The final results allow providing some correlations for transition onset and extent for the above application as shown in Figure 78. The cold wall reduces the spread angle of the turbulent spot by 20 to 30%. The lower wall temperature reduces the sound speed within the boundary layer (increasing the local Mach number), so it is perhaps not surprising that the reduced wall temperature has a similar effect to an increased Mach number on spot growth rate [51],[52].

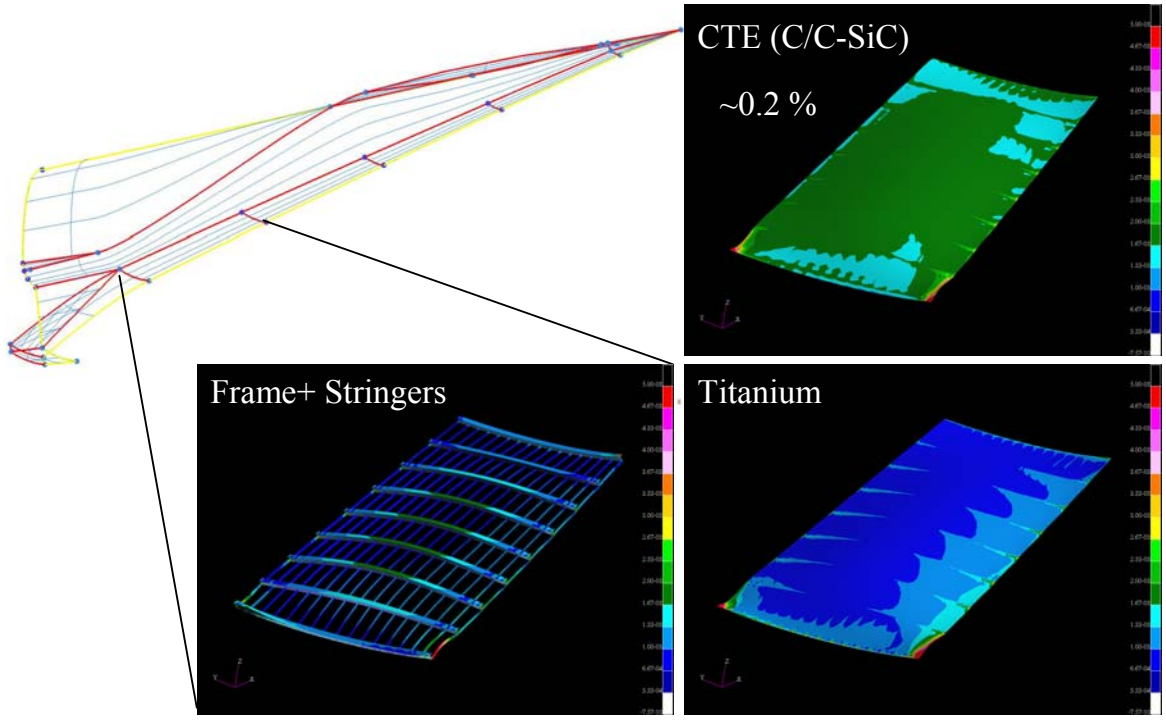


**Figure 75: Aerothermal loading of a nozzle sandwich panel with a Ti-sheet on the cold side and C/C-SiC on the hot side**

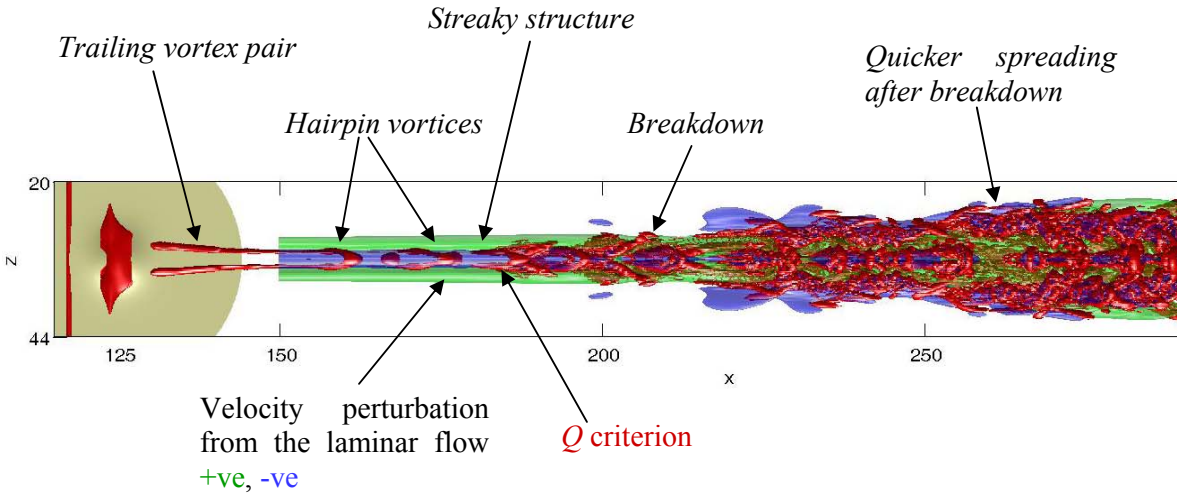


**Figure 76: Typical breakdown process within a compressible laminar boundary layer downstream of roughness.**

Performance of the transition experiment at Mach 3 and 6 with turbulent spot detection is investigated experimentally at ALTA (Figure 77) [59]. A variable roughness height allows deriving easily the critical Reynolds number at which the breakdown is triggered. A comparative analysis with the DNS data is indicated a good mutual correspondence as shown in Figure 78.

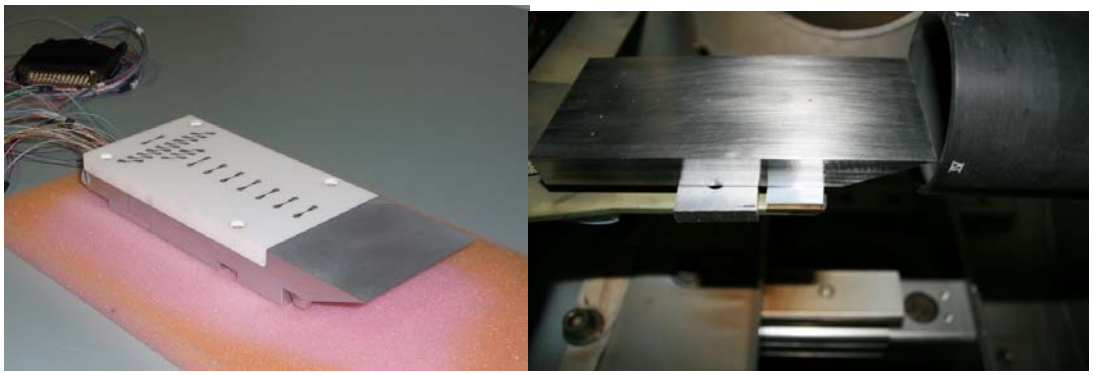

**Figure 77: Hot film gauged model with instrumentation detail (left) and thermocouple equipped flat plate in front of the HEAT Mach 6 nozzle (right)**

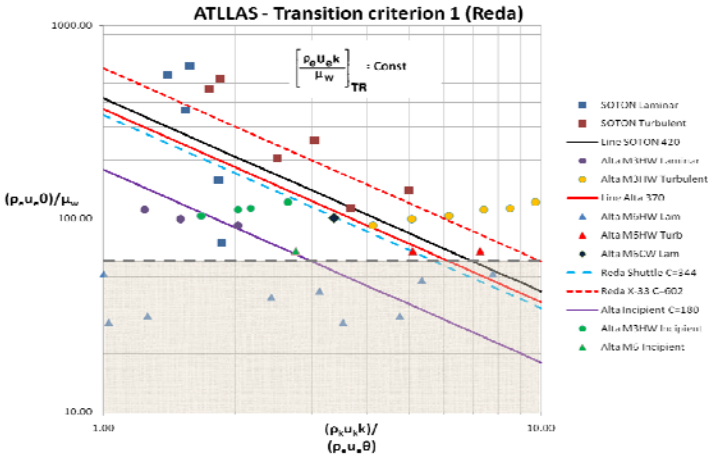


**Figure 78 : Effect of roughness on transition: ATLLAS experimental and numerical results compared with a proposed transition criterion compared to other available criteria.**

## 5.7 Conclusions

Overall design methods for high-speed transports at Mach 3 and 6 are revisited to increase the lift/drag ratio and volumetric efficiency through respectively a dedicated conceptual design methodology and a MDO-process. Within this MDO process, the need of lightweight and heat resistant materials is a prerequisite for a successful design.

Therefore, the prime focus of the ATLLAS project is on assessment of materials, cooling techniques and their interaction with the aero-thermal loads for both the airframe and propulsion components. The former focuses on sharp leading edges, intakes and skin materials coping with different aerothermal loads, the latter on combustion chamber liners. After material characterisation and shape definition at specific aero-thermal loadings, dedicated on-ground experiments are conducted. Both Ceramic Matrix Composites (CMC) and heat resistant metals are tested to evaluate their thermal and oxidiser resistance. In parallel novel cooling techniques based on transpiration and electro-aerodynamics principles are investigated.

Combined aero-thermal experiments test various materials specimens with a realistic shape at extreme aero-thermal conditions for elevated flight Mach numbers. Dedicated combustion experiments on CMC combustion chambers allow the reduction of combustion liner cooling resulting into overall thermal efficiency increase. Particular aero-thermal-material interaction influences strongly the aerothermal loadings. Therefore conjugate heat transfer, transpiration cooling and compressible transition phenomena are investigated and modelled. Similarly, the interaction of hot walls on high-speed transition is of utmost importance for intake efficiency and hence engine performance. This particular phenomenon is investigated experimentally and numerically for both flight Mach numbers.

## 6.0 ATLLAS II PROJECT

*ATLLAS-II* is a logical continuation project built upon the experience and technology development gained within *ATLLAS-I*. The focus will again be on advanced light-weight, high-temperature material development strongly linked to a high-speed vehicle design. The previous study revealed in the end that the optimal cruise Mach numbers is around Mach 5 to 6. In line with the reviewers' comments, a detailed design and feasibility study is proposed here which aim to a globally optimized vehicle with respect to aerodynamic, propulsive, structural and thermal layout but nevertheless allowing restrictions imposed by emissions regulations and sonic boom mitigation. The validated tools developed previously along with the lessons learnt will allow the consortium to further address and improve the multi-disciplinary design process.
In parallel, a lot of effort is still foreseen to extend the precious built-up material database with durability characterization both for the aero-frame and combustor related structures. Also new materials and compositions are addressed to cope with limitations previously encountered.

### 6.1 Design of a Mach 5-6 Vehicle

The driver to set the requirements for the material manufacturing, processing and testing is a Mach 5-6 vehicle. A fully integrated design taking into account several disciplines in the trade-off and optimization is foreseen, fully in line with the reviewers' comments. The points to be addressed are:

#### 6.1.1 Integrated Aerodynamic and Propulsive Flowpath Layout

The envisaged vehicle must operate over a wide Mach number range (0-5) and should still be efficient at cruise conditions. The wake analysis performed as part of *ATLLAS-I* suggests the cruise efficiency peaks at the cruise speed of Mach 5-6. However, the wake analysis takes no account of any material limitations and insulation weight at higher flight Mach numbers. The objective is to derive the optimum cruise Mach number by balancing thermal constraints (WP2.2) with the noted increase in cruise efficiency at higher speeds (WP2.1). The use of different fuel combinations will be assessed to maximize range, whilst recognising that the thermal management of the vehicle and/or the emission requirements will also require the use of cryogenic fuels such as liquid methane or a mixture of $CH_4$ with hydrogen. The challenging part is to design the vehicle that can create the flow-field described by the combined analysis. Also sonic boom constraints will have an impact on the global layout.

#### 6.1.2 Conceptual Structural and Thermal Design

Hypersonic vehicles are exposed to temperatures that are beyond the limits of classical airplane materials. In order to handle this problem the latest developments of new materials and composite structures suitable for high temperature application need to be taken into account. In this context, it is necessary to handle also the integration of heat-shield/heat-resistant materials and less heat-resistant load-carrying structural members including thermal management systems. One of the main objectives is to create inputs for virtual

testing and multi disciplinary optimisation (MDO) of realistic full-scale structures at operating conditions by the use of advanced numerical high fidelity methods. Besides the aero-thermal loads, also the unsteady loadings on the structure and control surfaces originating from shock-wave boundary layer interactions will be included. Their impact on control effectiveness and flutter will be first evaluated thoroughly as a separate topic, both experimentally as numerically, prior to the application onto the vehicle.

Despite the usage of high-temperature resistant structural materials, the passengers and cargo will require a stable thermal environment throughout the full vehicle's route. For subsonic aircraft, the cold ram air is used to thermally control the cabin air temperature which is drawn off the compressor. However, for high-speed vehicles, the ram air temperature needs rather to be cooled. The presence of onboard cryogenic fuels (e.g. $CH_4$) allows studying alternative designs to those used in subsonic aircraft. Open and closed cycles for the cabin air will be addressed.

### 6.1.3 Environmental Restrictions onto the Design Process

The major obstacles of introducing a supersonic aircraft have been the lack of solution to the sonic boom problem, emissions at high altitude and the risk of stratospheric ozone depletion. A first step has been performed in *ATLLAS-I* in terms of tool development and application. Sonic boom prediction for the studied vehicles in *ATLLAS-I* revealed similar levels as for Concorde but could eventually be alleviated by increasing the rise time, which transforms the boom rather into a puff. This encouraging path will be embedded into the design.
Apart from cruise induced sonic boom also acceleration from subsonic speed ($M < 1.0$) to cruise speed ($M = 5$ to 6) leads to the creation of a zone of sonic boom amplification due to ray convergence. This superboom may be especially annoying as it may be close to the coasts and very loud because resulting from the part of the flight path around Mach 1.2 – 1.3 for which the aircraft is at a much lower altitude than during cruise. It is known for Concorde type aircraft to be about 3 to 4 times larger than cruise sonic boom, with a major change in the waveform (from an "N"- to a "U"- wave) and with increased sensitivity with regard to local meteorology. To our knowledge, focused boom from hypersonic configuration has never been evaluated. Atmospheric turbulence is known to strongly modify the shock fronts of the sonic boom. In the mean it decreases the amplitude and increases the rise time, by means of scattering of the sonic boom by the largest structures of the planetary boundary layer. However, in a few percentages of cases, it may lead to its amplification, up to a factor 2, by means of random focusing. It is known for Concorde type booms to induce a variability of at least +/- 5 dBA (A-weighted Sound Exposure Level) in terms of usual noise metrics. Impact of turbulence on the sonic boom from a hypersonic configuration has never been evaluated.
Emission goals set by the EC could be achieved by the use of alternative fuels, such as methane or a $CH_4/H_2$-mix, having the potential to reduce carbon dioxide and particle emissions and thereby limiting the influence of supersonic aircraft on the atmosphere composition. The use of a more clean fuel will have the potential to eliminate the soot in the exhaust, something that has been lifted up lately as a concern in level with the $CO_2$ in the context of global heating. On the other hand required high combustion temperatures (regardless of fuel type) still make a reduction in NOx emission a challenge. Nevertheless, some guidelines formulated during *ATLLAS-I* will reduce it considerably if taken into account in the preliminary vehicle design. The global effect on the ozone at these cruise altitudes will be investigated as well.

### 6.1.4 Overall Vehicle Optimization and Final Assessment

The integration of the different subsystems, each optimized individually with preset restrictions, into a single vehicle system design does not necessarily ensure a globally optimized vehicle. Due to the complexity of interdisciplinary interaction, numerically steered improvement and optimization tools are applied here to ascertain a global optimum. Within the frame of the *ATLLAS-I* project a new modular MDO tool for the preliminary design of high speed vehicles was developed. The tool allows multiple-operational point analyses by means of aerodynamic and structural computations using CFD and FEM.

Also flight mechanics aspects and propulsion integration are taken into account. A key conclusion from the study is the dominating effect of structural dimensioning over aerodynamic improvements. Hence a stronger consideration of the structural modelling and analyses including aeroelastic and thermal effects are targeted in *ATLLAS-II*.
As a powerful precursor to the multi-disciplinary optimisation (MDO) a stochastic multidisciplinary improvement (SMDI) is proposed. SMDI makes use of techniques based on the Monte Carlo method. Its goal is to move the performance of a system towards a predefined target. The usage of Monte Carlo methods implies that a whole cloud of solutions is generated and moved through the design space towards the desired target.
As an ultimate verification, the optimized vehicle design will be tested for subsonic, transonic and supersonic speed to see how the design, mainly driven by cruise conditions, is able to cope with take-off and transonic acceleration. Variable settings of control surfaces to investigate trimming and stability will be part of the test campaign. The verification will be further backed-up and extended to other trajectory points, including cruise, with Nose-to-Tail computations which uses the windtunnel results also as a validation. The effect of boundary layer transition has a large effect on the vehicle drag and heat load. Therefore, dedicated experiments and LES simulations are also foreseen to assess the start and extent of the boundary layer transition taking important effects such as compressibility, wall temperature and roughness into account. All of this will further reduce the uncertainty margins when a final assessment will highlight the vehicle performance in terms of range, payload, fuel consumption, weight, emissions and sonic boom. These elements could serve as a first input to an economical assessment with respect to development and exploitation costs.

## 6.2 Advanced Material Development for Aero-Frame and Combustor Structures

As spelled out above, the highly loaded structure requires the implementation of advanced metallic and non-metallic materials which need to be light-weight and high temperature resistant. The large unknowns of these materials are their mechanical, thermal and optical (emissivity) characterizations at high temperatures as well as their durability capability. These information was completely lacking in the open literature at the start of *ATLLAS-I*. A first unique database is now available which lists these properties as useful engineering correlations as a function of temperature up to 1800 K. With respect to durability in real application environments, the samples have mostly been exposed to short duration tests. This lacking information will be a priority point in the material characterization. Nevertheless the database will be also expanded with new materials or compositions. This is needed to cope with shortcomings observed for certain materials in *ATLLAS-I* but which can be overcome by adapting their compositions or manufacturing process. This is mostly related to improve their oxidization behaviour or resistance to fatigue and fracture mechanisms.

### 6.2.1 Durability and Integration Technologies for Aero-Frame Materials

Both metallic and non-metallic materials are considered for the aeroframe-structure. The titanium matrix composites (TMC) and nickel based hollow sphere stackings (HSS) are investigated for use as (semi-)cold structure or as sandwich panel with good cooling and acoustic damping capabilities. The non-metallic class will focus on Ultra-high Temperature Ceramics (UHTC) and Ceramic Matrix Composites (CMC).

After the encouraging results on high-temperature Hollow Sphere Stacking (HSS) processing route obtained at the end of *ATLLAS-I* project, the objective of this second part is to carry on with the HSS materials characterization and testing in order to have several solutions dealing with components for structural hot areas of a high-speed aircraft, such as sharp leading edge, air intake or nozzles. In particular, the large challenge of extremely porous metallic materials such as cellular materials is their resistance to oxidation and to creep.

The development of high temperature Ni-based materials will be directed towards a protected-brazing route with sandwich materials that can be thermally characterized. This particular technique offers the advantage to be applied with every kind of elemental cells such as spheres, tubes or corrugated sheets. New high-temperature architectures obtained through brazing of tubes or relief-patterned sheets into a regular sandwich structure configuration will be investigated.

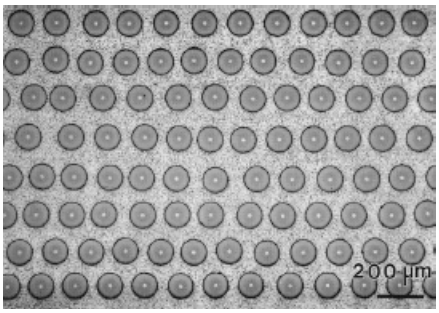


**TMC cross-cut (courtesy TiSiC)**

Titanium alloys and Ti-aluminides exhibit excellent mechanical properties for applications where high specific strength, high ductility and toughness, good corrosion resistance as well as high creep and fatigue resistance are required. Their useful service temperature range from room temperature to about 800K. New design concepts require however higher mechanical and thermal loading. Therefore new materials concepts must be developed beyond the classical monolithic titanium alloys towards titanium based composites. Such Titanium Matrix Composites (TMCs) combine high strength, stiffness and creep resistance of Silicon Carbide (SiC) monofilaments with the damage tolerance of Ti-alloys and Ti-aluminides while further reducing the materials density. The use of TMC on high-speed vehicles is related to shafts and hinges of control surfaces (ailerons, canards), different engine parts (compressor, turbines, shafts), structural and actuation struts, landing gears, brake systems. The intention is here to investigate and characterize the limits of TMC samples as well as the fabrication and testing process for compressor blades at high thermal and mechanical loading to evaluate the potential of titanium metal matrix composite (TMC) for high temperature material use in hypersonic applications. This will require characterization of the performance of TMC based on aerospace standard and alternative high temperature grade alloys. A down selection of the alloy type will allow for the fabrication of a full scale generic component part, scheduled for testing. Trial component designs and potential fabrication routes to achieve the required reinforcement architecture for an agreed performance specification will be developed.

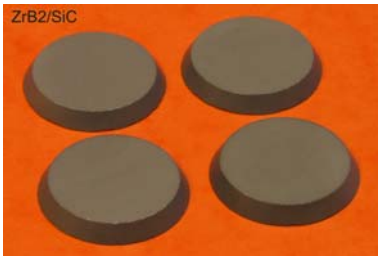


After the encouraging results on three selected Ultra High Temperatures Composites (UHTC) obtained during the *ATLLAS-I* project, the objective of this second part is to pursue the investigation of UHTC materials in order to have at our disposal several solutions for components working under severe thermal and structural loads e.g.: wing leading edge, nose, air intake etc. Their capability to be tailored to a sharp leading edge will improve the aerodynamic performance. The main objectives are firstly to select UHTC compositions able to sustain the requirements, secondly to acquire basic knowledge of these materials (manufacturing processes for example) and thirdly to thoroughly characterize the sintered ceramics.

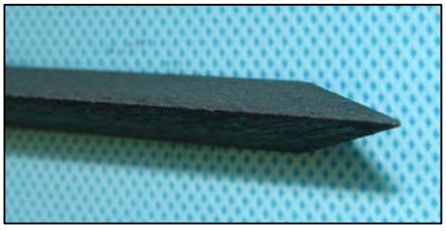

Works in *ATLLAS-I* clearly revealed the demand for experimental data concerning fatigue and creep behaviour of the investigated CMCs, especially at higher temperatures. For the integration of CMCs into the load bearing structures, the materials behaviour in the vicinity of stress intensifying elements like slots, notches and holes has to be determined, evaluated and taken into account for design. Test setups and procedures will be defined to test samples at operation relevant test conditions. Additionally, the investigation of test samples to check for material changes (caused by load changes) is foreseen.
For the CMCs, enhanced coatings will be applied; experiences on EBCs (environmental barrier coatings) with C/C-SiC are available and should be extended to other CMCs. Such a coating could be e.g. cordierite, which can be applied by means of vacuum plasma spraying. Coated CMCs are able to withstand high

temperature oxidation satisfying the demand of a long-term application.

As there will be a considerable temperature difference between the internal compartments and the aerodynamically heated outer skin of the hypersonic vehicle, different design possibilities of integrating the outer skin panels and the cold substructure needs to be explored. This temperature difference imposes a design constraint requiring an optimum fuselage structural concept very different from a conventional aircraft. Several different structural concepts exist for a primary cold load-carrying structure, which are explored at a first stage. Likewise the design and joining of the outer skin panels need to accommodate for the large thermal expansions in comparison to the substructure. Due to the finite panel size the influence of steps and gaps on airflow, and thus heating, but also on strength and stiffness will be analysed. An extensive know-how in joining a hot outer CMC structure to a cold, metallic substructure is proven for re-entry applications but not for hypersonic spacecraft demanding for long-life terms. It will be studied whether this technology can be adapted to civil hypersonic travel. Different aspects like e.g. inspection accessibility, exchangeability or fatigue considerations need to be treated here.

### 6.2.2 Durability and Integration Technologies for Combustor Materials

The high thermally loaded walls of the propulsion units require particular material development. Both metallic and non-metallic materials are considered for the different combustor components. CMC-based combustors with transpiration and/or regenerative cooled walls were shown to have a great potential as light-weight material combined with active cooling. However life-time and durability need to be proved to ensure their applicability for the defined goals. Nozzles parts or other heat loaded panels can be accommodated for by sandwich panels which have a high-temperature resistant core based on Ni-HSS. They have the additional possibility to act as cooled panel with good acoustic absorption. Finally, the most loaded parts are the injectors sticking out in the flow. Also here different materials are checked from the durability and integration point of view.

The measurement of erosion and damage of transpiration or convectively cooled walls is a critical issue for actively cooled propulsion systems. The long term behaviour and life-time characterization of different CMC (oxide or non-oxide) materials will be investigated using a small scale HVOF kerosene/oxygen burner. This investigation will focus on material compatibility with respect to combustion products ($H_2O$, $H_2$, CO etc.), changing of permeability, erosion resistance at high temperatures (< 3000 K), thermo-physical and porous-fluidic properties at both room and high temperature levels. Detailed local heat transfer data for regenerative internal cooling configuration will be addressed experimentally and numerically.

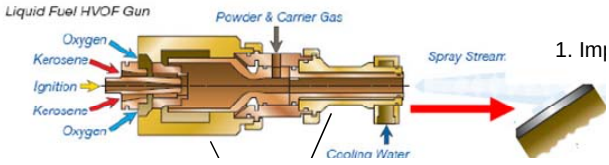


The high thermally loaded walls of the propulsion units require particular material development. A sandwich structure with HSS core combined with CMC panels was identified as a key technology in *ATLLAS-I* and appears to be an attractive component in the design of lightweight, high-temperature, actively cooled structures. In order to evaluate the thermal insulation performance of HSS, thermal characterisation of hybrid HSS-CMC structures need to be performed under realistic conditions. A HSS cooled or uncooled panel assembly

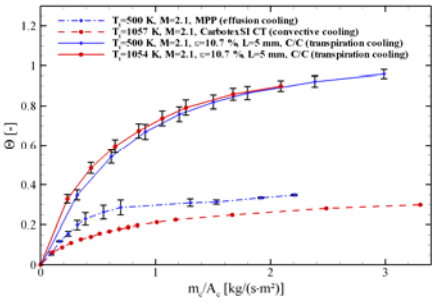

will be designed, manufactured and implemented at the exit of the existing SMR chamber for combustion test in METHYLE hypersonic test facility. These data will be used for a thorough inspection and feasibility assessment. To allow the assessment a dedicated coupled aero-thermal analysis will be performed. The numerical tools used were developed in *ATLLAS-I* and will be further developed for the present application.

### 6.2.3 Integration and Testing of (Un)Cooled Injectors

Injectors have to face a severe thermo-mechanical environment: aerodynamic loading due to the incoming air flow, very high temperature, high internal fuel pressure, etc. In addition, the final application requires very thin pieces to be efficient. UHTCs are very promising as uncooled fuel injectors used within airbreathing propulsion units. It was demonstrated in *ATLLAS-I* that these ceramics can quite easily be machined to obtain sharp leading edges or air-intakes e.g. by EDM or with diamond tools. Another approach is the use of porous CMC which is fuel-cooled by transpiration. Each type of injector will be experimentally exposed firstly in the ITLR supersonic subscale duct then to a really harsh combustion environment within the SMR dual-mode ramjet combustion chamber METHYLE.

## 7.0 CONCLUSIONS

Hypersonic technology developments within a European context have been revisited on the basis of the on-going projects LAPCAT and ATLLAS. Both projects are complementary addressing the required technology development allowing for hypersonic aircraft design and manufacturing i.e. aerothermodynamics, combustion, metallic and composite materials, conceptual vehicle design, numerical tool development and validation…

These projects allow acquiring the needed knowledge and technologies for a complete vehicle design and to test and evaluate them experimentally and numerically. The aim is to verify the feasibility of the concept to perform a complete mission including acceleration and cruise. In parallel, the environmental impact in terms of NOx generation, ozone depletion, sonic boom… are considered.

Preliminary concepts for Mach 3.5 and M4.5 demonstrated the possibility to cover a distance beyond 10,000km based on kerosene. Switching to hydrogen allows extending this distance provided careful attention is given to the propulsion cycle, the aerodynamics and the propulsion-airframe integration. The particular Scimitar cycle mounted onto the LAPCAT A2 makes an antipodal flight possible at Mach 5 flight speed. Going beyond this speed has shown so far that the integration aspect is of prime importance to achieve a decent range. A classical design of Lockheed, labelled as Hycat, could hardly get a 7,500km range at Mach 6 based on hydrogen even after an intensive MDO-process. Innovative designs paying attention to the integration aspects have a potential to get close to a 16,000km range at a Mach 8 flight speed.

The different tools to cross-check or predict the efficiencies of the vehicle, e.g. for propulsion or aerodynamics, are gradually put in place and verified to either dedicated basic or more applied experiments for these disciplines. In the meantime, advanced materials, cooling techniques and structural architectures are studied to cope with the high heat loads and temperatures encountered on particular spots on the fuselage and the combustion chamber.

Finally, these EC co-funded activities provide a unique opportunity to join researchers and industrialists from 22 different institutions beyond their national borders and to give access to each others unique facilities, methodologies, tools etc. related to hypersonic technologies. The opportunity to carry on with these projects within the 7$^{th}$ framework enhances even further this cooperation aiming at a clear definition of a European roadmap for a concrete high-speed vehicle development.

## Acknowledgements

The author strongly appreciates the inputs received from all partners involved in the ATLLAS and LAPCAT projects allowing composing this overview work on hypersonic technology developments with EU co-funded projects.

The work reported here was a combined effort resulting from the

'Long-Term Advanced Propulsion Concepts and Technologies' project investigating high- speed airbreathing propulsion. LAPCAT, coordinated by ESA-ESTEC, is supported by the EU within the 6th Framework Programme Priority 1.4, Aeronautic and Space, Contract no.: AST4-CT-2005-012282. Further info on LAPCAT can be found on the web-site http://www.esa.int/techresources/lapcat.

'Aerodynamic and Thermal Load Interactions with Lightweight Advanced Materials for High Speed Flight' project investigating high-speed transport. ATLLAS, coordinated by ESA-ESTEC, is supported by the EU within the 6th Framework Programme Priority 1.4, Aeronautic and Space, Contract no.: AST5-CT-2006-030729. Further information regarding ATLLAS can be found on http://www.esa.int/techresources/atllas.

'Long-Term Advanced Propulsion Concepts and Technologies II' project investigating high-speed transport. LAPCAT II, coordinated by ESA-ESTEC, is supported by the EU within the 7th Framework Programme Theme7 Transport, Contract no.: ACP7-GA-2008-211485. Further info on LAPCAT II can be found on http://www.esa.int/techresources/lapcat_II.

## References

[1] Routetracker, Based on Origin Destination and Route Area Statistics, Nov. 2006, IATA.
[2] Steelant J., `LAPCAT: propulsion technology', RTO / AVT / VKI Lecture Series on Advances on Propulsion Technology for High-Speed Aircraft, Von Karman Institute, St. Genesius-Rode, Belgium, 12-15/03/2007
[3] Steelant J., `Achievements Obtained for Sustained Hypersonic Flight within the LAPCAT project, 15th AIAA International Space Planes and Hypersonic Systems and Technologies Conference, 28/04 - 01/05-2008, Dayton, Ohio, USA, AIAA-2008-2578
[4] Steelant J., 'Achievements obtained on Aero-Thermal Loaded Materials for High-Speed Atmospheric Vehicles within ATLLAS', 16th AIAA/DLR/DGLR International Space Planes and Hypersonic Systems and Technologies Conference, October 19-22, 2009, Bremen, Germany, AIAA-2009-7225
[5] Steelant J., 'Sustained Hypersonic Flight in Europe: Technology Drivers for LAPCAT II', 16th AIAA/DLR/DGLR International Space Planes and Hypersonic Systems and Technologies Conference, October 19-22, 2009, Bremen, Germany, AIAA-2009-7206
[6] Küchemann D., The Aerodynamic Design of Aircraft, Pergamon Press, 1978.
[7] Anderson J., Introduction to Flight, 4th ed. McGraw-Hill, 2000.
[8] Penner J. E. et al., Aviation and the Global Atmosphere – A special report of IPCC Working Groups I and III, Cambridge University Press, 1999.
[9] Cain T., Zanchetta M. and Walton C.: *Aerodynamic Design of the ATLLAS Mach 3 Transport*, CEAS 2009 European Air and Space Conference, Manchester, UK, 2009.
[10] Cain T. and Walton C., The Sustained Hypersonic Flight Experiment, 12th AIAA Int. Space Planes and Hypersonic Systems and Technologies, 15-19 December 2003, Norfolk, Virginia.
[11] http://www.concordesst.com/concordeb.html
[12] Bond A., Turbine Based Combined Cycles, Advances on Propulsion Technology for High-Speed Aircraft, RTO-AVT-VKI Lecture series, March 12-15, 2007.
[13] Sippel M., Klevanski J. and Steelant J., Comparative Study on Options for High-Speed Intercontinental Passenger Transports: Air-Breathing- vs. Rocket-Propelled, IAC-05-D2.4.09, 2005.
[14] Sippel M., Research on TBCC Propulsion for a Mach 4.5 Supersonic Cruise Airliner, 14th AIAA Int. Space Planes and Hypersonic Systems and Technologies, AIAA 2006-7976, 06-09 November 2006, Canberra, Australia.

[15] Sippel, M.; Klevanski, J.: Definition of the LAPCAT Reference Vehicles LAPCAT-M4 and LAPCAT-M8, Issue:1, Rev. 0, LAPCAT Del. No. D.2.2.1, SART TN-005-2005, DLR-IB 647-2005/11, February 2006
[16] Murray N. and Steelant J., 'Methodologies involved in the Design of LAPCAT-MR1: a Hypersonic Cruise Passenger Vehicle', 16th AIAA/DLR/DGLR International Space Planes and Hypersonic Systems and Technologies Conference, October 19-22, 2009, Bremen, Germany, AIAA-2009-7399.
[17] Stotz I., Lamanna G., Weigand B. and Steelant J., 'Double-Diaphragm Shock Tube (DDST) for Hydrocarbon Disintegration Studies', 14th AIAA/AHI Space Planes and Hypersonic Systems and Technologies Conference, AIAA-2006-8109, 06-09/11 2006, Canberra, Australia.
[18] Karl S., Hannemann K., Steelant J. and Mack A., 'CFD Analysis of the HyShot Supersonic Combustion Flight Experiment Configuration', 14th AIAA/AHI Space Planes and Hypersonic Systems and Technologies Conference, AIAA-2006-8041, 06-09/11 2006, Canberra, Australia.
[19] Ingenito A., Bruno C., Giacomazzi E. and Steelant J., 'Supersonic Combustion: Modelling and Simulation', 14th AIAA/AHI Space Planes and Hypersonic Systems and Technologies Conference, AIAA-2006-8035, 06-09/11 2006, Canberra, Australia.
[20] Drummond J. P., Diskin G. S. and Cutler A. D., "Fuel-Air Mixing and Combustion in Scramjets", Technologies for Propelled Hypersonic Flight, NATO Research and Technology Organization, Working Group AVT 10, Final Report, January 2001.
[21] Jivraj F., Varvill R., Bond, A., and Paniagua, G., The scimitar precooled Mach 5 engine, EUCASS 2007, Brussels, Belgium, July 2007.
[22] Sippel, M., Research on TBCC Propulsion for a Mach 4.5 Supersonic Cruise Airliner, *14th AIAA Int. Space Planes and Hypersonic Systems and Technologies*, AIAA 2006-7976, 06-09 November 2006, Canberra, Australia.
[23] Haidn, O., Ciezki, H., Hannemann, K. and Karl., S., Selected Supersonic Combustion Activities at DLR within the European LAPCAT Project, *2nd European Conference for Aerospace Sciences (EUCASS)*, July 2007, Brussels, Belgium.
[24] Martinez-Schram J. , Karl S., Hannemann K. and Steelant J., Ground Testing of the HyShot II Scramjet in HEG, 15th AIAA International Space Planes and Hypersonic Systems and Technologies Conference, AIAA-2008-2538, Dayton, Ohio, USA, AIAA, 2008.
[25] Stotz I., Lamanna G., Weigand B. and Steelant J., 'Shock Tube Study on Hydrocarbon Free Jets at Elevated Pressures and Temperatures', 15th AIAA International Space Planes and Hypersonic Systems and Technologies Conference, AIAA-2008-2538, Dayton, Ohio, USA, AIAA, 2008.
[26] Pauly C., Sender J. and Oschwald M., Ignition of a Gaseous Methane/Oxygen Coaxial Jet, *2nd European Conference for Aerospace Sciences (EUCASS)*, July 2007, Brussels, Belgium.
[27] Cutrone L., Battista F., Ranuzzi G. and Bonifacio S., 'Simulation of Supercritical High Pressure Combustion for Advanced Propulsion System', 15th AIAA International Space Planes and Hypersonic Systems and Technologies Conference, AIAA-2008-2537, Dayton, Ohio, USA, 2008.
[28] Battista F., Ranuzzi G., Bonifacio S., 'Supersonic Combustion Models Development for Advanced propulsion Concepts', 15th AIAA International Space Planes and Hypersonic Systems and Technologies Conference, AIAA-2008-2553, Dayton, Ohio, USA, AIAA, 2008.
[29] P. Gerlinger, F. Schneider, M. Aigner, Multi-Variate Assumed PDF Modeling of Turbulent Sub- and Supersonic Combustion
[30] Ingenito A. and Bruno C., 'effect of the Turbulent Schmidt Number on Supersonic Regime', 46th AIAA Aerospace Sciences meeting and Exhibit, 07-11/01 2008, Reno (NV), USA.
[31] L. Krishnan, N. Sandham and J. Steelant , LES of Shock-wave/Boundary Layer Interactions in Hypersonic Inlet Compression Ramps, ISABE 2007, Beijing, China, 2-7/09 2007.
[32] Krishnan L., Sandham N.D. and Steelant J., `Shock-Wave/Boundary-Layer Interactions in a Model Scramjet Intake', AIAA J., Vol. 47, No. 7, July 2009, pp 1680-1691.
[33] Karl S., Hannemann K., Mack A. and Steelant J., 'CFD Analysis of the HyShot II Scramjet Experiments in the HEG Shock Tunnel', 15th AIAA International Space Planes and Hypersonic Systems and Technologies Conference, AIAA-2008-2538, Dayton, Ohio, USA, AIAA, 2008.
[34] C. R. McClinton, `High Speed/Hypersonic Aircraft propulsion Technology Development',

RTO/AVT/VKI Lecture Series on Advances on Propulsion Technology for High-Speed Aircraft, Von Karman Institute, St. Genesius-Rode, Belgium, 12-15/03/2007.

[35] J. Clough, 'Modelling and Optimization of Turbine-Based-Combined-Cycle Engine Performance', MSc-thesis, University of Maryland, 2004.

[36] A. Loubeau, F. Coulouvrat, "Effects of meteorological variability on sonic boom propagation from hypersonic aircraft", AIAA J., in press

[37] C. Davoine, A. Götzfried, S. Mercier, F. Popoff, A. Rafray, M. Thomas and V. Marcadon: „Metallic hollow sphere structures manufacturing process", Material Research Society Spring meeting, San Fransisco, USA, 13-17 April 2009

[38] Marcadon V., Roques E. and Feyel F., 'Modelling of Mechanical Behaviours of Metal Hollow Sphere Regular Packing under Compression Loadings', 11th Euromech-Mecamat, Turing Italy, March 2008.

[39] J.-F. Justin: „Investigations of High Temperature Ceramics for Sharp Leading Edges or Air Intakes of Hypersonic Vehicles", EUCASS 2009-511, European conference of Aerospace Sciences, Versailles, France, 6-9 July 2009.

[40] S. Soller, C. Kirchberger, M. Kuhn, T. Langener, M. Bouchez and J. Steelant, *Experimental Investigation of Cooling Techniques and Materials for Highspeed Flight Propulsion Systems*, AIAA-2009-7374, 16th AIAA/DLR/DGLR International Space Planes and Hypersonic Systems and Technologies Conference, Bremen, Germany, October 19th – 22nd, 2009

[41] M. Kuhn, T. Hallberg, 'Emissivity measurements of CMC materials', Material Science and Engineering, Elsevier, planned 2010

[42] M. Kuhn, H. Hald, M. Ortelt, C. Kirchberger, G. Schlieben, H.-P. Kau: *CMC Materials for Combustion Chamber Applications*, EUCASS2009-224, 3rd European Conference for Aero-Space Sciences, Versailles, France, 05-09 July 2009.

[43] M. Kuhn, S. Hackemann, E. Klatt, 'Material characterisation of CMC materials', Material Science and Engineering, Elsevier, planned 2010

[44] Kirchberger C., Wagner R., Kau H.-P., Soller S., Martin P., Bouchez M. and Bonzom C., `Prediction and Analysis of Heat Transfer in Small Rocket Chambers', 46th AIAA Aerospace Sciences meeting and Exhibit, AIAA-2008-1260, Reno (NV), USA, 07-11/01 2008.

[45] C. Kirchberger, G. Schlieben, A. Hupfer, H.-P. Kau, P. Martin, S. Soller: *Investigation on Film Cooling in a Kerosene/ GOX Combustion Chamber*, AIAA-2009-5406, 45th AIAA/ASME/ SAE/ASEE Joint Propulsion Conference & Exhibit, Denver, CO, USA, August 2nd-5th 2009

[46] Bouchez M. and Beyer S., 'PTAH-SOCAR Fuel-Cooled Composite Material Structure', 15th AIAA International Space Planes and Hypersonic Systems and Technologies Conference, AIAA-2008-2626, Dayton, Ohio, USA, AIAA, 28/04-01/05/2008.

[47] T. Langener, J. von Wolfersdorf, F. Cheuret and J. Steelant: *Experimental And Numerical Study on Transpiration Cooling With Supersonic Flow*, 19th Int. Symp. on Air Breathing Engines, ISABE, Montreal, Canada, 2009

[48] M. Bouchez, E. Dufour, L Benezech, F. Cheuret, J. Steelant, P. Grenard, J.A. Redford, N.D. Sandham, G.T. Roberts, A. Passro. D. Baccarella, M. Dalenbring, J. Smith, L. Cavagna: *Multi-level Coupled Simulations of Cooled Structures in the ATLLAS European Programme*, AIAA-2009-7374, 16th AIAA/DLR/DGLR International Space Planes and Hypersonic Systems and Technologies Conference, Bremen, Germany, 19-22 October, 2009

[49] F. Cheuret, J. Steelant, T. Langener, J. von Wolfersdorf: *Simulations on Transpiration Cooling for Supersonic Flow*, CEAS 2009 European Air and Space Conference, Manchester, UK, 2009.

[50] Krishnan L, Sandham ND, 'Effect of Mach Number on the Structure of Turbulent Spots', Journal of Fluid Mechanics, Vol. 566, pp 225-234, 2006.

[51] J.A. Redford, N.D., Sandham, G.T. Roberts, 'Roughness-induced transition of compressible laminar boundary layers', Seventh IUTAM Symposium on Laminar-Turbulent Transition, KTH, Stockholm, Sweden, June 23-26, 2009.

[52] J.A. Redford, N.D., Sandham, G.T. Roberts, 'Roughness-Induced Transition of Compressible Laminar Boundary Layers', AIAA Journal, accepted, 2010.

[53] F. Cheuret, J. Steelant, M. Bouchez and E. Dufour, 'Performance of Existing Models for Transpiration Cooling', Space Propulsion 2008, Heraklion, Crete, May 2008.
[54] T. Langener, J. von Wolfersdorf, T. Laux and J. Steelant, 'Experimental Investigation of Transpiration Cooling with Subsonic and Supersonic Flows at Moderate Temperature Levels', 44th AIAA/ASME/SAE/ASEE Joint Propulsion Conference & Exhibit, AIAA 2008-5174, Hartford, CT, USA, July 2008.
[55] T. Langener, J. von Wolfersdorf, F. Cheuret and J. Steelant: 'Experimental And Numerical Study on Transpiration Cooling With Supersonic Flow', 19th Int. Symp. on Air Breathing Engines, ISABE, Montreal, Canada, 2009.
[56] M. Bouchez, E. Dufour, L Benezech, F. Cheuret, J. Steelant, P. Grenard, J.A. Redford, N.D. Sandham, G.T. Roberts, A. Passaro. D. Baccarella, M. Dalenbring, J. Smith and L. Cavagna: 'Multi-level Coupled Simulations of Cooled Structures in the ATLLAS European Programme', AIAA-2009-7374, 16th AIAA/DLR/DGLR International Space Planes and Hypersonic Systems and Technologies Conference, Bremen, Germany, 19-22 October, 2009
[57] F. Cheuret, J. Steelant, T. Langener and J. von Wolfersdorf, 'Simulations on Transpiration Cooling for Supersonic Flow', CEAS 2009 European Air and Space Conference, Manchester, UK, 2009.
[58] F. Cheuret and J. Steelant, 'Transpiration Cooling Modelling for Supersonic Flow', Space Propulsion 2010, San Sebastian, Spain, May 3-6, 2010.
[59] A. Passaro, D. Baccarella, P. Caredda, J. Redford and N. Sandham, 'Experimental characterization of turbulence spots on a flat plate at Mach 6', 6th European Symposium on Aerothermodynamics for Space Vehicles, Versailles, France, Nov. 2008.